Controlling the Master

Molecular mechanisms of mTOR regulation

Inauguraldissertation

zur

Erlangung der Würde eines Doktors der Philosophie

vorgelegt der

Philosophisch-Naturwissenschaftlichen Fakultät

der Universität Basel

von

Matthias Wälchli

Basel, 2024

Genehmigt von der Philosophisch-Naturwissenschaftlichen Fakultät
auf Antrag von

Erstbetreuer: Prof. Dr. Maier, Timm
Zweitbetreuer: Prof. Dr. Hall, Michael N.
Externe Expertin: Dr. Jacob, Sandra

Basel, den 22.03.2022

Prof. Dr. Marcel Mayor
Dekan

I Abstract

Proteins are the functional units of life. Regulation of protein function and activity is a key cellular mechanism to respond and adapt to changing extra- and intracellular conditions. Evolution of complex signaling networks based on multidomain proteins and multiprotein complexes enables higher eukaryotes to sense and integrate signals and to communicate necessary responses by modulating the activity of target proteins.

An atypical kinase, the mammalian target of rapamycin (mTOR), is the master regulator of cellular growth and metabolism. Information about the current status of a cell is processed by a signaling network converging on mTOR, which integrates stimuli to respond by re-balancing anabolic and catabolic processes. mTOR acts as a component of two functionally and structurally distinct complexes, mTOR complex 1 (mTORC1) and mTORC2, and phosphorylates a large set of substrate proteins. More than 80 substrates are known, however the mechanism of their recruitment to mTOR complexes remains unknown for most of them. The activity of mTOR complexes is regulated by association with binding partners, translocation or posttranslational modifications. Dysregulation of mTOR signaling is associated with cancer, obesity and neurodegenerative diseases establishing mTOR as prime drug target. DEPTOR is an enigmatic regulator of mTOR that may act as tumor suppressor or oncogene. It is the only protein known to bind and inhibit both, mTORC1 and mTORC2.

The experimental part of this thesis reveals the mechanism of the regulatory interplay of DEPTOR with mTOR complexes based on structural and biochemical characterization. Using cryo electron microscopy I determined structures of DEPTOR bound to mTORC1 and mTORC2 at a resolution of 3.7Å and 3.2Å respectively. I obtained a detailed characterization of the mTOR-DEPTOR interaction by combining cryo-EM data with solving a crystal structure of the DEPTOR DEP domain tandem. Biochemical analysis of mTOR activity modulated by DEPTOR, and structure-guided mutants of DEPTOR allowed us to unravel a novel mode of mTOR regulation involving two distinct binding sites in the FAT domain of mTOR. Contrary to previous hypotheses, DEPTOR is not only an inhibitor of mTOR, but it allosterically activates or inhibits mTOR depending on cellular lipid signaling.

The second part of this thesis provides a review of mTOR substrates, their function and recruitment. We analyzed in particular phosphorylation motifs and recognition of substrates in the active site. The substrate recognition in the active site of mTOR is, in contrast to other PIKKs, only loosely defined.

In summary, the results presented in this thesis provide new structural and mechanistic insights into DEPTOR function and the regulation of mTOR, and may contribute to the development of novel therapeutic approaches.

II Table of Contents

III List of Figures

IV List of Tables

V Abbreviations

4E-BP1	Eukaryotic translation initiation factor 4E-binding protein
A-T	Ataxia telangiectasia
AGC	Protein kinase A, protein kinase G and protein kinase C
AKT	*RAC-alpha serine/threonine-protein kinase*
AMPK	AMP-activated protein kinase
AMPK	5' adenosine monophosphate-activated protein kinase
ARM	Armadillo
ATF4	Activating Transcription Factor 4
ATM	Ataxia telangiectasia mutated
ATP	Adenosine triphosphate
ATR	Ataxia telangiectasia and Rad3-related protein
ATRIP	ATR-interacting protein
CAD	carbamoyl-phosphate synthetase 2, aspartate transcarbamoylase, dihydroorotase
CASTOR	Cellular arginine sensor of mTORC1
ChK1	Checkpoint Kinase-1
CRIM	Conserved region in the middle
CTD	C-terminal domain
Cryo-EM	Cryo-electron microscopy
DDR	DNA damage response
DEP	Dishevelled, Egl-10, Pleckstrin
DEPDC5	DEP domain-containing protein 5
DEPDC6	DEP domain-containing protein 6
DEPTOR	DEP domain-containing mTOR interacting protein
DNA-PKcs	DNA-dependent protein kinase catalytic subunit
DSB	Double stranded break
E. coli	*Escherichia coli*
EF3	elongation factor 3
eIF4E	Eukaryotic translation initiation factor 4E
ER	Endoplasmic reticulum
ERK1/2	Extracellular-signal-regulated kinase ½
ESCC	Esophageal squamous cell carcinoma
ETAA1	Ewing's tumor-associated antigen 1

FAT	FRAP, ATM and TRRAP
FATC	FAT C-terminal
FKBP12	FK506-binding protein of 12 kDa
FLCN	Folliculin
FNIP1/2	Folliculin-interacting protein 1/2
FoxO1	Forkhead box protein O1
FoxO3a	Forkhead box protein O3a
FRAP	FKBP12-rapamycin associated protein
FRB	FKBP12-rapamycin binding domain
GAP	GTPase-activating protein
GATOR	GAP activity toward Rags
GTP	Guanosine-5'-triphosphate
GDP	Guanosine-5'-diphosphate
GEF	Guanosine nucleotide exchange factor
GTPase	Guanosine triphosphate hydrolase
HAT	Histone acetyltransferase
HDR	Homology directed repair
HEAT	Huntingtin, elongation factor 3, protein phosphatase 2A and yeast kinase Tor1
HM	Hydrophobic motif
IGF-1	Insulin-like growth factor 1
InsP6	Inositol hexakiphosphate
kDa	Kilo dalton
LFC	Lysosomal folliculin complex
LRS	Leucyl-tRNA synthetase
MAF1	Repressor of RNA polymerase III transcription MAF1 homolog
MAM	Mitochondria associated membranes
MAPK	Mitogen -activated protein kinase
MIOS	Missing oocyte meiosis regulator homolog
mLST8	mammalian lethal with sec-13 protein 8
MRN	Mre11-Rad50-Nbs1
MTHFD2	Mitochondrial tetrahydrofolate cycle enzyme methylene-tetrahydrofolate dehydrogenase 2
mTORC1/2	mammalian target of rapamycin complex 1/2
NHEJ	Nonhomologous end joining
NMD	Nonsense-mediated mRNA decay

NPC1	Niemann Pick C1
NPRL2/3	Nitrogen permease regulator 2/3-like protein1
NRPS	Non-ribosomal peptide synthetase
OTUB1	OTU domain containing ubiquitin aldehyde-binding protein
P-Rex 1/2	Phosphatidylinositol 3,4,5-trisphosphate-dependent Rac exchanger 1/2
PA	Phosphatidic acid
PDK1	Phosphoinositide-dependent kinase 1
PDZ	postsynaptic density 95, discs large, zonula occludens-1
PH	Pleckstrin homology
PI3K	Phosphoinositide 3-kinase
PIK	Phosphoinositide kinase
PIKK	Phosphatidylinositol 3-kinase-related kinase
PKA	cyclic AMP-dependent protein kinase
PKC	Protein kinase C
PKS	Polyketide synthase
PLD	Phospholipase D
PP2A	Protein phosphatase 2
PPARγ	Peroxisome proliferator-activated receptor-γ
PPIase	Peptidylprolyl isomerase
PR	Phosphorylation region
PRAS40	Proline-rich Akt substrate of 40 kDa
PRD	PIKK regulatory domain
PTEN	Phosphatase and TENsin homolog deleted on chromosome 10
PTM	Post transnational modification
Rac1	Ras-related C3 botulinum toxin substrate 1
Rab5a	Ras-related protein Rab-5A
RAFT1	Rapamycin and FKBP target
Rag	Ras-related GTP-binding protein
RAIP	Arg-Ala-Iso-Pro motif in 4E-BP
RAPT	Rapamycin target
Raptor	Regulatory-associated protein of mTOR
RBD	Ras binding domain
REDD1	Protein regulated in development and DNA damage response 1
Rheb	Ras-homolog enriched in brain
Rho	Ras homolog

Rictor	Rapamycin-insensitive companion of mTOR
RMSD	Root-mean-square deviation
RPA	Replication protein A
ROS	Reactive oxygen species
RSK	Ribosomal S6 kinase
RTKs	Receptor tyrosine kinases
S6K	S6 kinase
SAGA	Spt-Ada-Gcn5 acetyltransferase complex
SAM	S-adenosyl methionine
SAMTOR	S-adenosylmethionine sensor upstream of mTORC1
SAR1B	Secretion associated Ras related GTPase 1B
SAXS	Small angle x-ray scattering
SGK	Serum- and glucocorticoide-induced protein kinase
mSIN1	mammalian stress-activated map kinase-interacting protein 1
SLC38A9	Solute carrier family 38 member 9
SMG1	Suppressor with Morphological effect on Genitalia family member
SREBP	Sterol regulatory element-binding protein
TBC1D7	TBC1 domain family member 7
TFE3	Transcription factor E3
TFEB	Transcription factor EB
TIF-1A	Transcription initiation factor 1A
TM	Turn motif
TOR	Target of rapamycin
TOS	TOR signaling
TPRs	Tetratricopeptide repeats
TRD	Tetratricopeptide repeats domain
TRRAP	Transformation/transcription domain-associated protein
TSC	Tuberous sclerosis complex
TSC1	Tuberous sclerosis 1 protein
TSC2	Tuberous sclerosis 2 protein
UBF1	Upstream binding factor 1
ULK1	UNC-51-like kinase 1
UPF1	Up-frameshift suppressor 1 homolog
WAT	White adipose tissue
WT	Wild-type

1 Introduction

Life is not a static object. Life is a sum of processes like growth, development, sensing, reaction and energy consumption. Proteins, chains of amino acids coupled by peptide bonds, are the functional units of life. They transport molecules, catalyze chemical reactions, transmit signals, recognize other cells, stabilize and structure cells, synthesize or degrade proteins and regulate the function of other proteins or themselves by interacting with or modifying them. Proper protein function and regulation thereof is of utmost importance for a functional organism.

1.1 Regulating protein function

Proteins and their functions are controlled at different levels: their abundance can be adjusted by controlling transcription, translation or degradation. These mechanisms of regulations don't allow for fast adjustments to changing environmental conditions and are energy-expensive. However, they represent a long-term control instrument well suited to react to major changes and to adapt to new cellular roles. Immediate, short-term modulation of protein function is achieved by controlling localization, binding of small molecules, association with protein binding partners or post-translational modifications (PTMs). PTM describes the addition of modifying groups to one or more amino acids of a protein. The variety of PTMs ranges from small methylation, over glycosylation to covalent attachment of another protein like ubiquitin (ubiquitination).

The most prominent modification is the transfer of γ-phosphate of adenosine triphosphate (ATP) to a target amino acid, termed phosphorylation. Importantly, phosphorylation is a reversible process, where kinases catalyze the transfer of the phosphoryl group to the amino acid and phosphatases the reverse reaction (Figure 1.1 a). The human genome encodes for more than 500 different kinases which accounts for almost 2% of all genes[1]. The number of known phosphatases, which catalyze the reverse reaction is substantially lower (~190)[2]. According to the dbPTM[3] there are more than 1.5 million known phosphosites, while the most common phosphorylated amino acids are serine (86 %), threonine (12%) and tyrosine (2%)[4]. Phosphorylation of histidine and aspartic acid is less stable, therefore less studied and less observed. Phosphorylation can act like a molecular switch resulting in activation or inhibition of a protein function. Changing protein localization or regulation of protein interactions are other examples for processes induced or controlled by phosphorylation (Figure 1.1 b)[5].

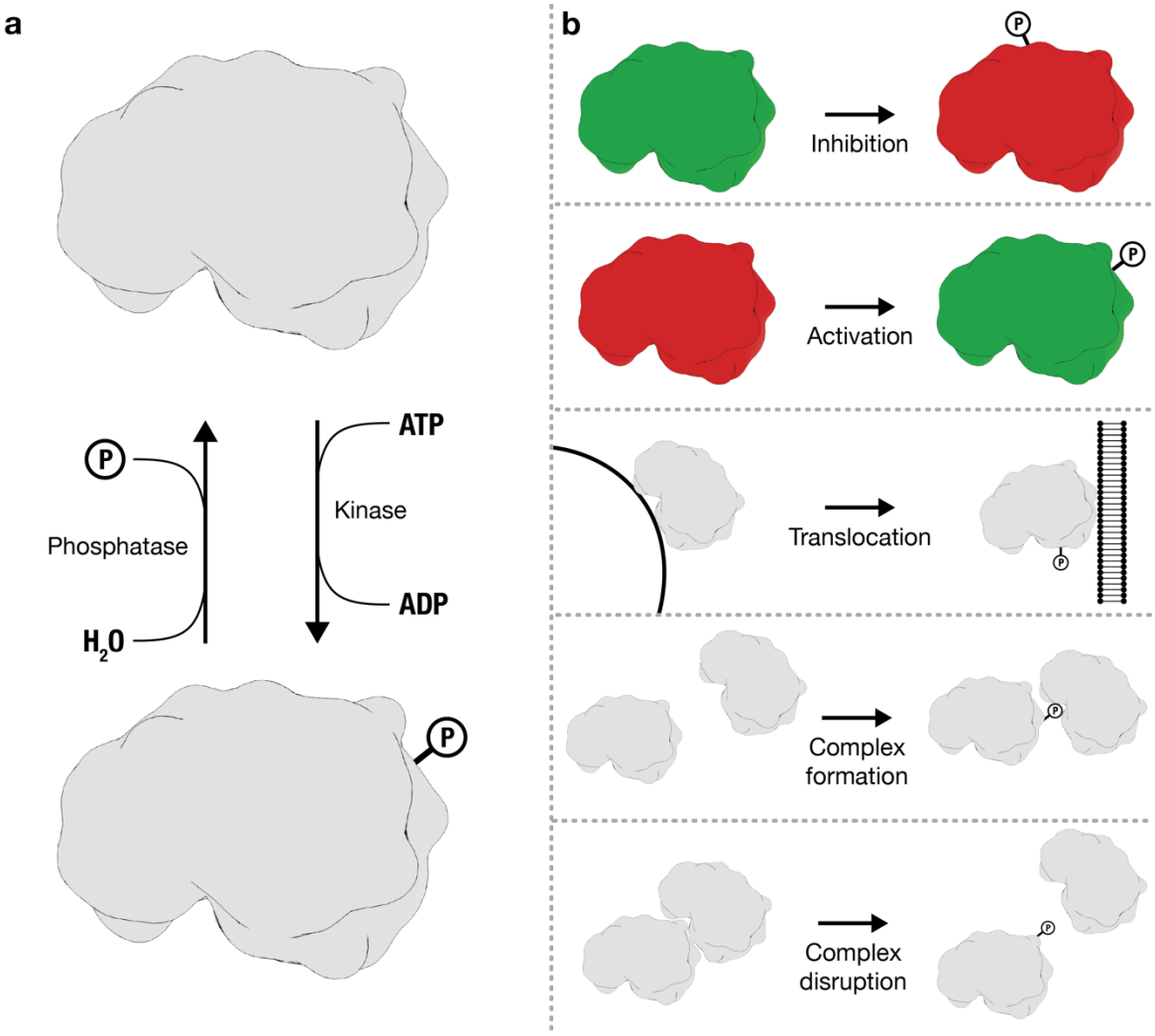

Figure 1.1 : Phosphorylation and associated mechanisms of protein regulation.
(a) Phosphorylation describes the transfer of a γ-phosphate group from ATP to an amino acid catalyzed by a kinase. The reverse reaction is executed by phosphatases. (b) Phosphorylation regulates protein function by a large variety of different mechanisms like activation, translocation or modulating protein interactions.

1.2 Rapamycin and its cellular target

In 1964 a medical expedition from Canada collected soil samples on Rapa Nui (Easter Island) to study the island's endemic microbial communities. 10 years later the team of Suren Seghal managed to isolate the Streptomycete strain AY B-994 belonging to the species *Streptomyces hygroscopicus* (Figure 1.2 a) from one of the soil samples which was found to inhibit *Candida albicans*. They isolated the principle active compound and named it rapamycin (Figure 1.2 b) in recognition of its source and antifungal properties[6,7]

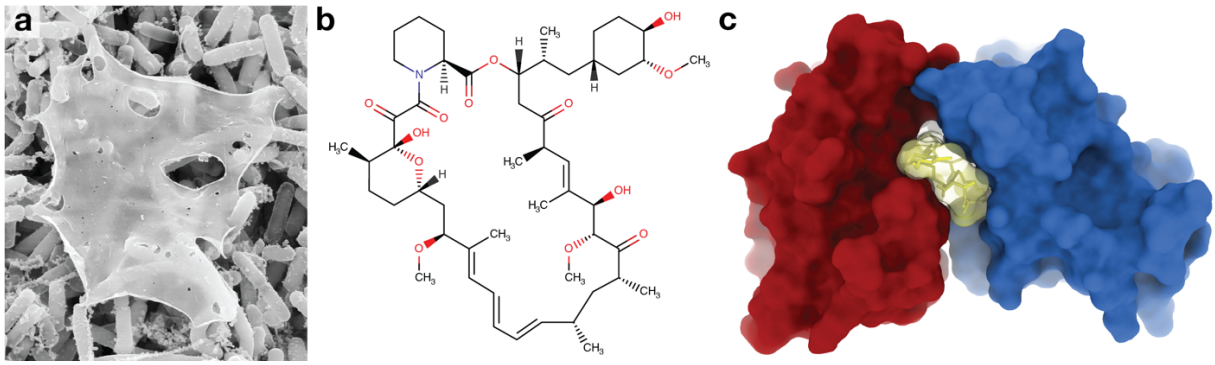

Figure 1.2 : The macrolide rapamycin binds to FKBP12.
(a) Scanning electron micrograph of *Streptomyces hygroscopicus* (Magnification: 2500x; Dennis Kunkel Microscopy/Science Photo Library) (b) chemical structure of rapamycin (c) Surface representation of the crystal structure of FKBP12 (red) -rapamycin (yellow) complex bound to the FKBP12-rapamycin-binding (FRB) domain of mTOR (blue) (PDB: 1FAP [8]).

Rapamycin is a macrolide[9] produced by a hybrid biosynthetic gene cluster consisting of modular type 1 polyketide synthase (PKS) and non-ribosomal peptide synthetase (NRPS)[10]. In the following years immunosuppressive and anti-proliferative effects besides the antifungal properties of rapamycin were described, leading to research on its cellular target[11-14]. Rapamycin and the structurally related FK506 both bind to and inhibit the *FK506-binding protein* (FKBP) cis-trans peptidyl-prolyl isomerase (PPIase)[14,15]. Inhibition of PPIase activity however cannot explain the observed effect of immunosuppression. Genetic mutational studies in yeast led to the discovery of the *targets of rapamycin 1 and 2* (TOR1/TOR2), homologs to phosphoinositide kinases[16-19]. TOR1/2 was found to be essential for cell cycle progression. Shortly after, by using a Rapamycin-FKBP12 complex as a bait, four groups independently identified the mammalian homolog of TOR1/2 and named it *rapamycin and FKBP target* (RAFT1), *rapamycin target* (RAPT), *FKBP-rapamycin associated protein* (FRAP), or *mammalian target of rapamycin* (mTOR)[20-23]. The field decided to use the name mTOR. The work of Barbet *et al.* in 1996 led to the conclusion that TOR is part of a novel signaling pathway which actively regulates cell growth[24]. This represented a paradigm shift in the way how cellular growth was perceived: It is an actively regulated process in response to environmental and developmental conditions and does not just happen when the necessary building blocks and nutrients are available.

1.3 Phosphatidylinositol kinase-related kinases

In the 1990s TOR and a number of other high-molecular weight protein kinases were identified as being more closely related to lipid-phosphorylating phosphatidylinositol kinases (PIKs) than to canonical protein kinases. They represent a novel class of atypical protein kinases termed PIK-related kinases (PIKK)[25]. Besides mTOR there are five more members of the PIKK family: *Ataxia*

telangiectasia mutated (ATM), *Ataxia telangiectasia and Rad3-related protein* (ATR), *Suppressor with Morphological effect on Genitalia family member* (SMG1), *DNA-dependent protein kinase catalytic subunit* (DNA-PKcs) and *Transformation/transcription domain-associated protein* (TRRAP).

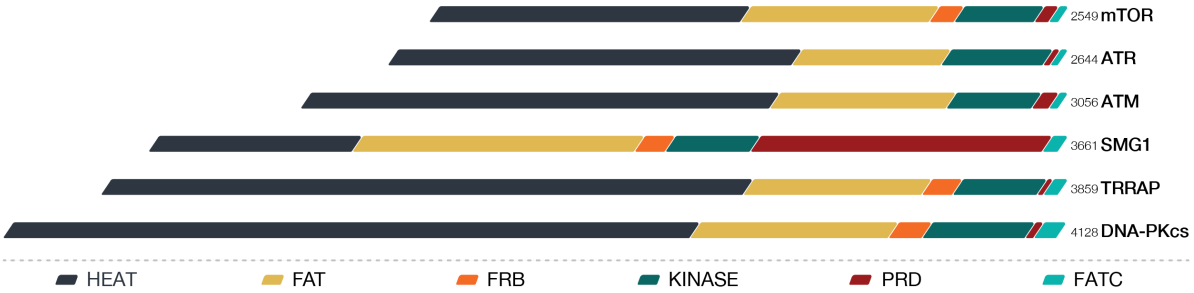

Figure 1.3 : Conserved domain architecture of PIKKs.
Characteristic domains are indicated schematically; length of domains is drawn to sequence scale. Name of domains and according color scheme at the bottom

All PIKKs share a common domain architecture (Figure 1.3). The N-terminal part of PIKKs consists of HEAT (Huntingtin, elongation factor 3 (EF3), protein phosphatase 2A (PP2A) and TOR1) repeats[26]. These repeats are followed by tetratricopeptide (TPR) repeats forming the FAT (FRAP, ATM and TRRAP) domain[27]. The C-terminal kinase domain includes two PIKK characteristic additions to the PIK-related kinase fold: the PIKK regulatory domain (PRD) and the FAT C-terminal (FATC)[25] motif, which initially led to the classification of the PIKKs into one distinct subfamily of kinases and is absent from canonical kinases. Four out of the six PIKK members harbor an additional 4-helix bundle located in sequence between the FAT and kinase domains. This bundle is termed FKBP12-rapamycin binding (FRB) domain based on the FRB domain in TOR, which has been identified first. The other FRB domains however are not known to bind the FKBP12-rapamycin complex.

PIKKs are essential checkpoint kinases reacting to cellular stresses. They exert their function by forming complexes with regulatory protein partners and by phosphorylating large sets of substrates, which will be discussed below. Structural characterization of PIKKs has been difficult due to their large size, structural flexibility and their functional requirement for binding partners. Advances in cryo-electron microscopy (cryo-EM) enabled the structural characterization of PIKKs in the last years, providing novel insights into their architecture, regulation and interplay with binding partners.

PIKKs coordinate signaling pathways in response to cellular stress. Genotoxic stress in form of DNA damage represents a major challenge for a cell[28]. The cell counteracts this threat by recognizing damage and activating signalling pathways to initiate and promote DNA repair.

Activation of this signaling cascade, the DNA damage response (DDR), is controlled by protein phosphorylation catalyzed by the PIKKs DNA-PKcs, ATM and ATR. At least one of them is encoded in every eukaryotic genome. DNA double strand breaks (DSBs) are repaired by non-homologous end joining (NHEJ) or homology-directed repair (HDR).

DNA-PKcs associates with a Ku70/Ku80 heterodimer at DSBs to form the DNA-dependent protein kinase holoenzyme (DNA-PK)-complex[29-31]. There DNA-PK serves as regulator and platform for the major pathway of DSB-repair, NHEJ. The N-terminal HEAT-repeat region of DNAK-PKcs adopts a circular cradle-like fold, whereas FAT and kinase domain form the HEAD domain (Figure 1.4 c). Kinase activity of DNA-PKcs is allosterically controlled by binding of DNA and the Ku70/Ku80 dimer to the HEAT repeat region[32-34].

Ataxia-telangiectasia (A-T) is a rare autosomal-recessive disorder leading to dilated or broken blood vessels (telangiectasia) and lack of muscle control (ataxia)[35]. In 1995, Savitsky *et al.* identified the gene mutated in A-T, which is ATM[36]. **ATM** functions in complex with the MRE11-RAD50-NBS1 (MRN) -complex[36]. The MRN complex associates with DSBs, recruits ATM to the site of damage and activates it. ATM in turn phosphorylates a large number of proteins, such as the cell cycle checkpoint kinase Chk2[37], p53[38,39] and H2AX[40] and activates HDR of DSBs. ATM adopts a butterfly-shaped symmetric dimer. Dimerization is directly mediated by the body, formed by FAT and kinase domain[41-43]. The N-terminal HEAT-repeat domains (Spiral and Pincer) are extending from this body and not involved in dimer formation (Figure 1.4 a). As for other PIKKs, the N-terminal regions are flexible and probably involved in the activation mechanism[43].

ATR, in contrast to ATM and DNA-PKcs, is activated by a large variety of genotoxic stresses, not only DSBs. ATR forms a complex with *ATR-interacting protein* (ATRIP), which recruits ATR to single-stranded DNA (ssDNA) coated by *replication protein A* (RPA)[44]. At these sites, ATR gets activated by a dimer of TopBP1 (Topoisomerase (DNA) II Binding Protein 1)[45] and ETAA1[46] to phosphorylate a large set of target proteins[47]. The *checkpoint kinase 1* (Chk1) is one of the best studied substrates of ATR[48]. ATR forms a heart-shaped dimer with a pseudo two-fold symmetry. The two ATR protomers dimerize in a head-to-head fashion involving the FAT- and kinase domain (FATKIN) region. An ATRIP dimer binds the N-terminal HEAT-repeat regions and forms the dimer interface there (Figure 1.4 b).

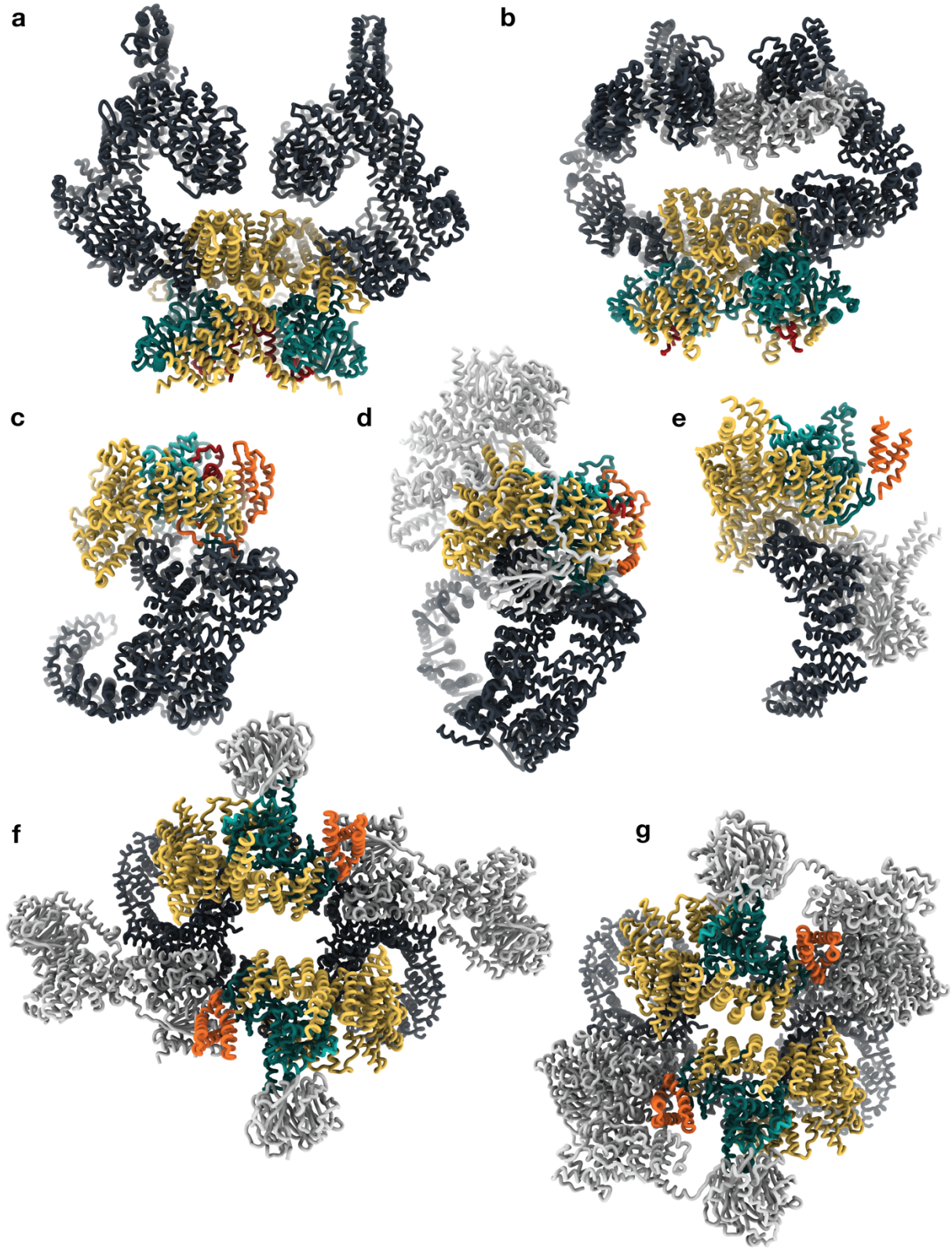

Figure 1.4 : Variability in structural architecture of PIKKs
Different modes of oligomerization and varying organization of HEAT repeats illustrate the architectural variability of PIKKs, color scheme according to Figure 1.3 binding partners shown in grey **(a)** ATM (PDB: 7NI5[42]) **(b)** ATR (PDB: 5YZ0[49]) **(c)** DNA-PKcs (PDB: 7OTP[50]) **(d)** TRRAP (PDB: 7KTR[51]) **(e)** SMG1 (PDB: 7PW4[52]) **(f)** mTORC1 (PDB: 6BCX[53]) **(g)** mTORC2 (PDB: 6ZWM[54])

TRRAP is the only member of the PIKK-family without kinase activity, caused by a lack of catalytic residues[55,56], but it still plays an important role in the regulation of gene transcription. TRRAP serves as a scaffold in Histone acetyltransferase (HAT)- complexes like the SAGA (Spt-Ada-Gcn5 acetyltransferase)-complex and TIP60 (nucleosome acetyltransferase of H4)-complex[57]. Recruitment of HAT and transcriptions factors (TFs) to chromatin by TRRAP leads to hyperacetylation of histones and subsequent transcription activation. Recent structural characterization of the human SAGA-complex shows that TRRAP is present as a monomer in this complex (Figure 1.4 d). The N-terminal HEAT-region forms a circular cradle-like structure comparable to the one found in DNA-PK[51].

SMG-1 controls nonsense-mediated mRNA decay (NMD), a surveillance pathway regulating mRNA stability[58,59]. SMG-1 functions in a complex with SMG-8 and SMG-9 to phosphorylate and activate the RNA helicase *up-frameshift protein 1* (UPF1)[60,61]. UPF1 represses translation initiation on mRNA targeted for NMD [62].

SMG-1-8-9 is, like DNA-PK, active in a monomeric complex[52,63-65]. The N-terminal repeats of SMG-1 form an "Arch" like structure, providing the binding sites for the complex subunits SMG-8-9. In contrast to other PIKKs the PRD-insertion of SMG-1 is large and spans around 1100 disordered residues (Figure 1.4 e). The cryo-EM reconstruction with a peptide from UPF1 bound represents until now the only structure of a substrate bound PIKK active site and allows important insights into substrate recognition[64]. All active PIKKs beside mTOR utilize an S/T-Q motif for substrate recognition in the active site. The glutamine reaches at +1 position into a hydrophobic cage and forms hydrogen bonds with the backbone. In agreement with utilization of the S/T-Q motif, this cage is conserved in ATM, ATR and DNA-PKcs. A detailed analysis of substrate recognition and associated motifs is provided in section 3.

The variability of structural architecture is high in the PIKK family, despite sharing a conserved domain organization. They differ in their oligomeric states and respective modes of oligomerization. Three PIKKs are monomeric (SMG-1, DNA-PKcs and TRRAP) while the other three are active as dimers (mTOR, ATM and ATR). ATM and ATR dimerize via the FAT domain, in contrast to mTOR, which dimerizes via α-solenoids formed by the HEAT repeat region. In general, the structural organization of the α-solenoids built up from HEAT repeats is highly diverse within the PIKK family. The structure of the C-terminal FATKIN, formed by FAT and kinase domain, however, is highly conserved within the PIKKs.

1.4 mTOR and its complexes

mTOR, like all other PIKKS, exerts its function in complex with binding partners. It forms two distinct complexes, *mTOR-complex 1* (mTORC1) and *mTOR-complex 2* (mTORC2). Both complexes share the subunits mTOR and *mammalian lethal with SEC13 protein 8* (mLST8), also known as GβL[66,67]. mLST8 is dispensable for activity of mTORC1, but was found to be essential for the function and integrity of mTORC2[68-70]. This was recently confirmed by the structural characterization of mTORC2[54] (see Figure 1.7). mTORC1 in addition contains the complex-defining subunit *regulatory associated protein of mTOR* (Raptor)[66,71,72]. Raptor mediates the substrate selectivity of mTORC1. It contains binding sites for short linear signaling motifs in mTORC1 substrates, the TOR signaling (TOS) motif and RAIP (Arg-Ala-Ile-Pro) motif[73-75]. *Proline-rich Akt substrate 40* (PRAS40) is an inhibitor of mTORC1 that acts by binding to the Raptor TOS site, where it competes with substrates to inhibit substrate recruitment[53,76-78]. Furthermore, Raptor represents an interaction hub for mTORC1 activation by amino acids (see 1.4.1. Amino acid sensing). mTORC2 is defined by the subunits *rapamycin-insensitive companion of mTOR* (Rictor), mLST8 and *mammalian stress-activated map kinase-interacting protein 1* (mSIN1)[66,79-82]. Protor-1 (protein observed with Rictor-1), also known as PRR5L (proline-rich repeat protein-5 like), interacts with Rictor, but its functional role remains unclear[78,83].

mTOR was, as mentioned before, discovered as the functional target of the FKBP12-rapamycin complex. Short-term rapamycin inhibits activity of mTORC1, but not mTORC2[66,79]. The binding site for the FKBP12-rapamycin complex at the FRB domain is in mTORC2 occupied by Rictor. Therefore, mTORC2 cannot be bound by rapamycin. However, long-term treatment with rapamycin affects mTORC2 function, likely by sequestering free mTOR and blocking assembly of mTORC2[84]. This fundamental difference had major influence on studying the role of both mTORCs: Availability of a specific inhibitor for mTORC1 and its application as tool for research facilitated understanding of the signaling network of mTORC1. Thus, the current understanding of mTOR signaling is still dominated by rapamycin-dependent observations and rapamycin-independent processes remain less understood[85-87]. The same is true for mTORC2, where the lack of a specific inhibitor hindered functional studies.

1.4.1 Signaling upstream of mTORC1

mTORC1 is a central regulator of cellular homeostasis. It integrates a variety of input signals like growth factors, amino acid availability, cellular energy state and stresses controlling cell growth and metabolism by phosphorylating target proteins.

A tight regulation network is necessary for mTORs ability to sense these input signals and adjust mTOR activity accordingly to react to changing cellular and environmental conditions.
The activation process of mTORC1 can be described in a simplified way by an "**AND**" gate logic where the small GTPases Ras-related GTP-binding protein (Rag) and Ras homolog enriched in brain (Rheb) represent these two gates (

Figure 1.5). mTOR activation requires (i) recruitment to the lysosome by Rag heterodimer and (ii) direct stimulation of mTOR by Rheb. These two gates are controlled by two central input signals: amino acid availability controls recruitment whereas growth factors regulate stimulation.

Amino acid sensing

Different mechanisms of sensing amino acids control the nucleotide state of RagA/B. The Rag GTPases are obligate heterodimers, of RagA or RagB binding to RagC or RagD. The Rag heterodimer is anchored to the lysosome by the Ragulator-complex, consisting of Lamtor1-5 (also known as p18, p14, MP1, C7orf59 and HBXIP)[88-91]. Recruitment of mTORC1 to the lysosome is achieved by binding of the Rag-dimer to Raptor[88]. Raptor reads out the nucleotide state by (i) interaction of the Raptor α-solenoids with RagA and (ii) a linker of Raptor termed Raptor-claw, which binds to the space between the Rag G-domains[91]. An interaction between Rag and Raptor is only possible if RagA/B is bound to GTP and RagC/D to GDP, which will be in the following the definition for the Rag-**ON** state. Regulation of mTOR localization is achieved by changing the nucleotide state of Rags by switching on and off proteins that act as GAP (GTPase-activating protein) or GEF (Guanine nucleotide exchange factor) for Rags.
The nucleotide state of RagA/B is controlled by *GAP activity towards the Rags 1* (GATOR1). GATOR 1 exerts, as the name indicates, GAP-activity towards RagA/B and thereby induces the Rag-**OFF** state[92]. GATOR2 counteracts the GAP activity of GATOR1 by a so far unknown mechanism[92]. GATOR1 is a trimeric complex consisting *of DEP domain-containing protein 5* (DEPDC5), *nitrogen permease regulator 2-like protein* (NPRL2) and NPRL3. GATOR2 is built up by the five subunits WDR59, WDR24, MIOS, SEH1L and SEC13. GATOR1 and GATOR2 form a higher-order complex with KICSTOR (KPTN, ITFG2, C12orf66 and SZT2). KICSTOR tethers GATOR1 to the lysosome and is therefore important for GATOR1s inhibitory function on Rags[93,94]. The KICTORS-GATOR1-GATOR2 serves as a platform for monitoring cellular amino acid levels; several sensing pathways converge on this mega-complex.
Availability of the amino acid leucine is sensed by Sestrins[95-99]. In absence of leucine, Sestrin2 binds to GATOR2 and releases its inhibitory activity towards GATOR1. SAR1B was recently described as another sensor for cellular leucine utilizing an analogous mechanism. However,

SAR1B binds the GATOR2 subunit MIOS, whereas Sestrin2 binds SEH1L. Due to a higher affinity for leucine than Sestrin2, SAR1B is able to sense lower leucine concentrations[100]. CASTOR (*Cellular Arginine Sensor for mTORC1*) senses cytosolic arginine by, like Sestrin2 and SAR1B, binding to GATOR2 and inhibiting its activity[101]. It functions as a homodimer of CASTOR1 or as heterodimer consisting of CASTOR1 and CASTOR2[102-104]. Interestingly, CASTOR binding to GATOR2 requires a conformational change CASTOR[105]. In contrast to the amino acid sensors mentioned before, SAMTOR (*S-adenosylmethionine sensor upstream of mTORC1*) acts with a different mode of action. SAMTOR monitors methionine levels through interaction with S-adenosylmethionine (SAM). In absence of SAM, SAMTOR interacts with GATOR 1 and KICSTOR and stimulates the GAP activity of GATOR1 in an unknown manner, which may include dissociation of GATOR2[106]. Binding of SAM to SAMTOR disrupts the interaction with KICSTOR and GATOR1 leading to inhibition of GATOR1 GAP activity.

The nucleotide state of RagC/D is regulated by a concerted interplay between FLCN (folliculin) and *Solute carrier family 38 member 9* (SLC38A9). FLCN possesses GAP-activity towards RagC/D. Together with *folliculin interaction protein* (FNIP), Ragulator and RagAC in an **OFF**-state, it forms the *lysosomal FLCN complex* (LFC). The **OFF**-state of the Rags is necessary to accommodate space for FLCN to bind in the cleft between the two Rags[107,108]. FLCN cannot exert its GAP activity in the LFC, because of an unfavorable conformation of RagC/D and FLCN. Therefore, disruption of this complex is necessary to allow mTORC1 activation. SLC38A9 serves as lysosomal arginine sensor[109-111]. At low arginine levels the N-terminal tail of SLC38A9 binds to the arginine binding site inside the transporter. When lysosomal arginine levels rise, arginine competes this tail out[112,113]. The N-terminal part of SLC38A9 is then available to bind to the cleft between the Rag G-domains, competing with and thereby destabilizing the LFC. Disruption of the complex allows then FLCN to adopt a conformation where it can exert its GAP activity. Dissociation of SLC38A9 then allows GDP to GTP exchange of RagA/C to form Rag-dimer in **ON**-state, able to recruit mTORC1 to the lysosome [114]. In addition to its role in arginine sensing, SLC38A9 may be also involved in sensing lysosomal cholesterol level together with the cholesterol transporter Nieman Pick C1 (NPC1) [115].

There are reports for additional amino acid sensing pathways, but their molecular mechanisms are unclear. Leucine and glutamine were described to be sensed through the metabolite α-ketoglutarate. During glutaminolysis, α-ketoglutarate is produced by glutamate dehydrogenase in dependence of leucine and glutamine levels. α-ketoglutarate in turn stimulates the nucleotide exchange from GDP to GTP in RagB[116]. *Leucyl-tRNA Synthetase* (LRS) senses leucine, associates with Raptor and RagD and serves as GAP for the latter[117].

Growth factor signaling

Rheb links growth factor signaling to mTORC1 activation. In a GTP-bound state, **ON**-state, Rheb stimulates mTORC1 activity at the lysosome[53,118]. The *tuberous sclerosis complex* (TSC) consists of the proteins TSC1, TSC2 and TBC1D7 (TBC1 domain family member 7) and has GAP-activity towards Rheb[119-121], thereby inhibiting its function towards mTORC1. If the TSC complex is inactive, the nucleotide binding state of Rheb reflects the cellular GTP/GDP ratio (100-200μM /10-20μM)[122]. Until today, no protein with GEF activity towards Rheb has been identified. Thus, mTORC1 stimulation by Rheb is solely dependent on the GAP activity of the TSC-complex[123,124]. The TSC-complex is regulated by inhibitory phosphorylation leading to dissociation of TSC from the lysosome and subsequent activation of Rheb/mTORC1[125,126].

Growth factors bind to receptor tyrosine kinases (RTKs) and thereby activate downstream kinases. Insulin binding stimulates the *insulin/insulin-like growth factor 1* (IGF-1) to activate the *RAC-alpha serine/threonine-protein kinase* (AKT), which phosphorylates TSC[121,125,127]. In addition to the PI3K/AKT pathway, the growth factor activated MAPK signaling cascade also inhibits TSC by phosphorylation mediated by *ribosomal protein S6 kinase alpha-1* (RSK1)[128] as well as *extracellular-signal-regulated kinase 1/2* (ERK1/2)[129].

Active AKT, besides targeting the TSC-complex, also regulates mTORC1 directly by phosphorylating the inhibitor PRAS40. Upon phosphorylation PRAS40 binds to 14-3-3 and is released from mTORC1[77,130]. In addition, AKT also provides a link to amino acid signaling by phosphorylating CASTOR1. Phosphorylation increases CASTOR1 affinity for E3 ubiquitin-ligase RNF167 leading to ubiquitination and degradation of CASTOR1[131].

Cellular stresses

Besides the two activating pathways of amino acids and growth factors, which work, as mentioned above in an AND-gate logic, mTOR has to be regulated in response to the cellular state respectively cellular stresses. This includes for example the energy state (level of ATP), oxidative stress and genotoxic stress. These input signals are integrated into the signaling network by modulating the two AND gate pathways or mTORC1 directly.

AMP-activated protein kinase (AMPK) serves as major counterplayer of mTOR activation. AMPK is allosterically activated by AMP (and less sensitive also ADP) and inhibited by ATP binding. Thereby AMPK is able to monitor small changes in cellular ATP, ADP and AMP concentrations. Active AMPK phosphorylates TSC2 to activate the TSC complex and thereby inhibits mTOR activation[132,133]. However AMPK also targets mTORC1 directly by phosphorylating RAPTOR at S792, which leads to 14-3-3 binding and inhibition[133].

Under oxidative stress REDD1 disrupts TSC:14-3-3 complex, which leads to activation of TSC and mTORC1 inhibition[134-136]. In contrast to stress-related regulation of mTORC1, which targets the TSC-Rheb axis, also mechanism targeting the amino acid sensing pathway have been described: Upregulation of Sestrins has been described under genotoxic stress (p53-regulated) and ER (endoplasmatic reticulum) stress[137,138].

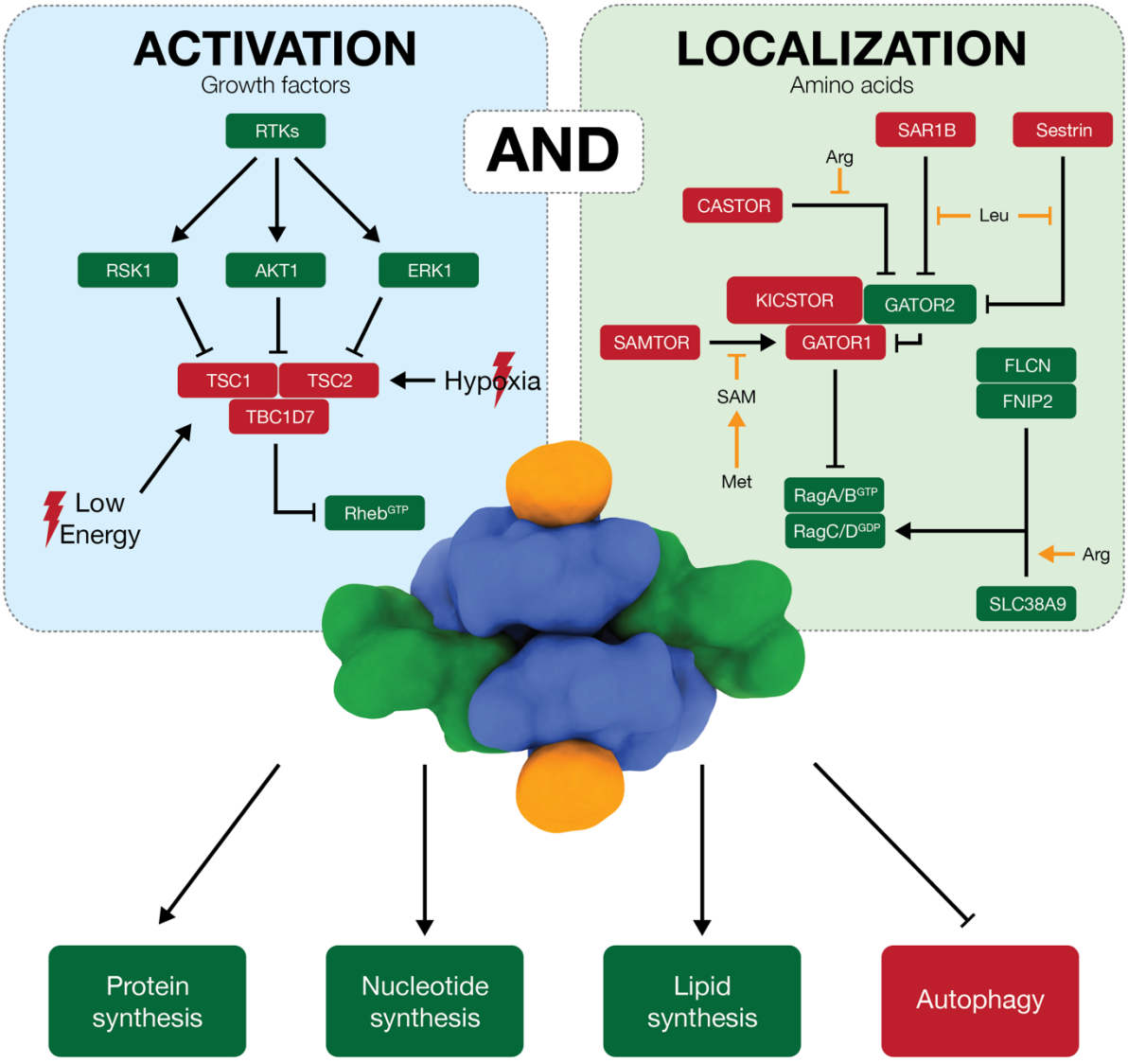

Figure 1.5 : mTORC1, activated by growth factor and amino acids, promotes anabolic processes. mTORC1 is activated by two different input pathways, namely growth factor and amino acid signaling, joined by an **AND**-gate logic: mTORC1 needs to be recruited to the lysosome via Rags and activated via Rheb. Input signals feeding into mTORC1 signaling are shown above the surface representation of mTORC1. Green colored protein (-complexes) indicate activating function on mTORC1signaling while red color indicates inhibiting function. Below the mTORC1 surface representation processes positively (green) and negatively (red) regulated by mTORC1 are shown.

1.4.2 The signaling output of mTORC1

The discussion above has focused on the regulation of mTOR activity. Active mTORC1 shifts the metabolic balance to anabolic processes: it increases the biosynthesis of proteins, nucleotides and lipids, and tunes down the catabolic autophagy (Figure 1.5).

Protein synthesis

Protein synthesis is the most expensive cellular process in terms of energy and ressources[139]. mTORC1 regulates proteins synthesis by phosphorylating eukaryotic initiation factor 4E-binding proteins (4E-BPs) and p70 S6 kinase 1 (S6K1). These two proteins are the best characterized mTOR substrates and they are used as standard read-out to observe mTORC1 activity.

4E-BP, existing in three different isoforms, binds to the translation initiation factor eIF4E and inhibits 5' cap-dependent translation[140-143]. Recruited to mTORC1 by binding of its TOS and RAIP motif, 4E-BP gets phosphorylated at four sites (Thr37, Thr46, Ser65, Thr70 Ser83). Phosphorylation induces formation of a β-fold in 4E-BP disrupting the 4EBP:eIF4E complex and activating 5' cap-dependent translation[144].

In a concerted phosphorylation-dependent mechanism S6K1 gets fully activated by mTORC1[145] and phosphoinositide-dependent kinase 1 (PDK1)[146]. S6K1 in turn phosphorylates its target, the ribosomal protein S6. The role of S6 phosphorylation is not yet fully understood. Alanine substitution of phosphosites do not affect translation effiency[147], however S6 is implicated in ribosome biogenesis[148]. S6K1 also phosphorylates the transcription factors UBF1[149], MAF1[150,151] and TIF-1A[152] to promote RNA biosynthesis.

Lipids

mTORC1 activation upregulates the transcription of rate-limiting proteins in fatty acid and lipid biosynthesis, which is essential for cellular homeostasis. SREBP1/2 (sterol regulatory element binding protein 1/2) are membrane-bound transcription factors which are cleaved in presence of sterols leading to translocation to the nucleus where they activate expression of genes for lipid biosynthesis[153,154]. mTORC1 phosphorylates and thereby expels the nuclear phosphatidic acid phosphatase lipin1, an inhibitor of SREBPs[155].

Peroxisome proliferator-activated receptor-γ (PPAR-γ) is a nuclear hormone receptor involved in regulation of lipid metabolism, especially adipogenesis[156]. PPAR-γ activation by mTORC1 during leads to initiation and maintenance of adipogenesis[157].

Nucleotides

Proliferating cells, like cancer and immune cells, have a high demand on nucleotides for DNA replication and RNA biosynthesis[158]. mTORC1 activates ATF4 (Activating transcription factor 4) which enhances expression of enzymes of the mitochondrial tetrahydrofolate cycle (mTHF), especially methylenetetrahydrofolate dehydrogenase 2 (MTHFD2) expression. Upregulation of these enzymes promotes *de novo* purine synthesis[159].

CAD (carbamoyl-phosphate synthetase 2, aspartate transcarbamoylase, dihydroorotase) catalyzes the first three reactions of *de novo* pyrimidine synthesis. CAD activity gets stimulated by phosphorylation at S1859 by S6K1[160,161].

Autophagy

Autophagy is the process of self-degradation in response to starvation or cellular stresses[162]. Thus, autophagy directly opposes cell growth. Autophagy is initiated by AMPK activated Unc-51-like kinase 1 (ULK1). mTORC1 phosphorylates ULK1 and thereby prevents ULK1 activation[163]. TFEB (transcription factor EB) fosters the expression of autophagy related genes. Phosphorylation-induced binding of 14-3-3 to and translocation of TFEB from the nucleus to the cytosol, is dependent on mTORC1 activity [164].

1.4.3 The signaling of mTORC2

Knowledge about the activation mechanism and downstream effectors of mTORC2 is scarce and literature is controversial. mTORC2 mainly phosphorylates and thereby activates kinases of the AGC kinase family, namely AKT, Protein kinase C (PKC), serum- and glucocorticoid-induced protein kinase 1 (SGK1).

mTORC2 promotes cell cycle progression and suppresses apoptosis via AKT and SGK1. Activated AKT and SKG1 inhibit the transcription factors forkhead box protein O1 (FoxO1) and FoxO3a by inhibitory phosphorylation. Target genes of these transcription factors promote cell cycle arrest, stress resistance and apoptosis[79,167].

There is evidence that mTORC2, in contrast to mTORC1 is primarily regulated by growth factors induced stimulation of phosphoinositide-3-kinase (PI3K) pathway. PI3K phosphorylates $PI(4,5)P_2$ resulting in phosphatidylinositol 3,4,5-triphosphate ($PI(3,4,5)P_3$), whereas PTEN (phosphatase and tension homolog) counteracts this reaction[168]. PIP_3 leads to localization of AKT to the plasma membrane and subsequent phosphorylation by PDK1 at Thr308. The role of PIP_3 in regards to mTORC2 activity and localization is not clear. It has been proposed that PIP_3 recruits mTORC2 to the membrane by binding of the PH (pleckstrin homology) of mSIN1[169]. Reports that this relieves the autoinhibitory role of mSIN1 towards the kinase domain are questionable, especially

in light of recent structural studies [54]. mTORC2 has been described to be active at different subcellular locations like the plasma membrane, mitochondria-associated ER membrane (MAM), early and late endosomes [170,171]. These different subpopulations appear to have varying dependence and sensitivity on PI3K signaling. mTORC2 localized at the plasma-membrane is constitutively active[171]. Interestingly, mTORC2 associates with the ribosome to phosphorylate nascent peptide chain of AKT to control its stability[172].

The small GTPases Rheb and RagABCD are central players of mTORC1 regulation, but Rheb does not activate mTORC2[173]. Recently several GTPases like Rab5[174], Rac1[175] and Ras alone or in complex with Rho[176,177] have been described to activate mTORC2. More - especially structural - studies are necessary to elucidate the precise functional relationship between these GTPases and mTORC2.

Activation of mTORC2 is directly controlled by the activity of mTORC1. Phosphorylation of insulin receptor substrate 1 (IRS-1) by mTORC1-activated S6K1 leads to a negative feedback loop affecting and downregulating PI3K/AKT/mTORC2 signaling[178]. This feedback loop serves as important signaling link to balance mTORC1 and PI3K/AKT/mTORC2 activity.

1.5 Structural characterization of mTOR complexes

Structural insights into mTOR architecture were for a long time limited to smaller fragments and subdomains. In 1996 a crystal structure of the mTOR FRB in complex with rapamycin and FKBP12 gave insights how the macrolide mediates binding of FKBP12[8]. Rapamycin is directly located in the interface and stabilizes the interaction (Figure 1.1 c).

A crystal structure of the FAT and kinase domain of mTOR bound to mLST8 was solved[179]. The FAT domain is formed by three TPR subdomains (TRD1-3) and wraps around one half of the kinase domain. The kinase consists, like the PI3K kinase domain, an N-terminal lobe (N-lobe) and C-terminal lobe (C-lobe), with a few important insertions: The FRB domain is inserted at the transition from FAT domain to the N-lobe. Another insertion forms the binding interface for mLST8, which sits on top of the C-lobe. Analysis of the active site revealed a constitutive active conformation.

The overall architecture of mTORC1 was first elucidated by a low resolution cryo-EM reconstruction at 5.9Å [180]. Interpretation of the density was facilitated by the previous published FATKIN crystal structure and a structure of Raptor from *Chaetomium thermophilum*. mTORC1 forms a dimer of heterotrimers consisting of mTOR, mLST8 and Raptor and adopts a lozenge-shape with a central cavity. The dimer is formed by interactions of the N-terminal HEAT repeats.

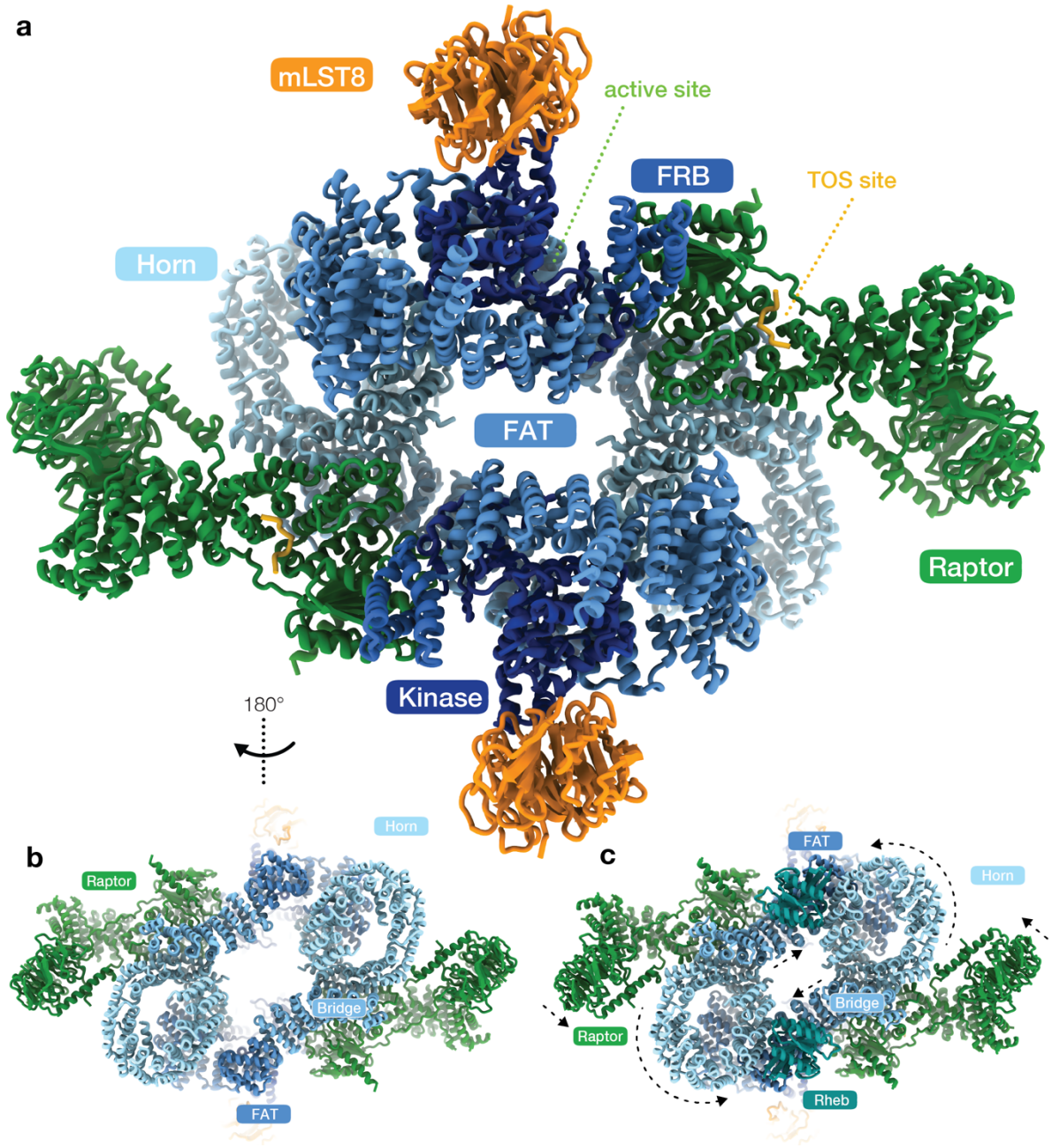

Figure 1.6 : Architecture of mTORC1 and its activation mechanism
(a) Front and (b) back view of the structure of mTORC1 (cartoon representation colored by protein chains; domains of mTOR are indicated by shades of blue) (PDB: 6BCX[53]) (c) Rheb binding induces conformational in the HEAT repeats which transmit allosteric activation to the active site (PDB: 6BCU[53])

These repeats are organized in two α-helical solenoids, the N-terminal Horn/N-HEAT(N-terminal) domain and the adjacent Bridge/M-HEAT(middle) domain. Due to the low resolution, it was not possible to unambiguously determine the topology of the repeats. A cryo-EM reconstruction of *Kluyveromyces marxianus* TOR (KmTor)-Lst8 at a resolution of 6.1Å with the help of red-fluorescent-protein (RFP) at several positions clarified the directionality of the HEAT-repeats. Since this complex formed stable dimers in absence of Raptor, dimer formation seems to be not dependent on Raptor[181]. However, as observed in the reconstruction of human mTORC1, Raptor

binds to the HEAT repeats in vicinity of the dimer mTOR interface and stabilizes the dimer[180]. For this structural study mTORC1 was expressed in *Spodoptera frugiperda* in the presence of rapamycin which allowed the authors to copurify FKBP from insect cells and visualize its binding in context of the entire complex. Binding of the FKBP-rapamycin complex narrows access to the active site and thereby exerts its inhibitory function[180].

High-resolution reconstructions of apo-mTORC1 and Rheb-stimulated mTORC1 provided important insights into activation of mTOR[53]. Rheb binds to an interface formed by Horn and Bridge and FAT domain, which requires rotation of the Horn towards this site. Movement of the Horn causes conformational change in the FAT domain. This includes rotation between TRD1 and TRD2 FAT subdomains. The movement is transduced towards the C-terminal portion of the FAT domain and the catalytic cleft. Movement of the kinase C- and N-lobe towards each other leads to realignment of active site residues increasing k_{cat} of mTOR[53].

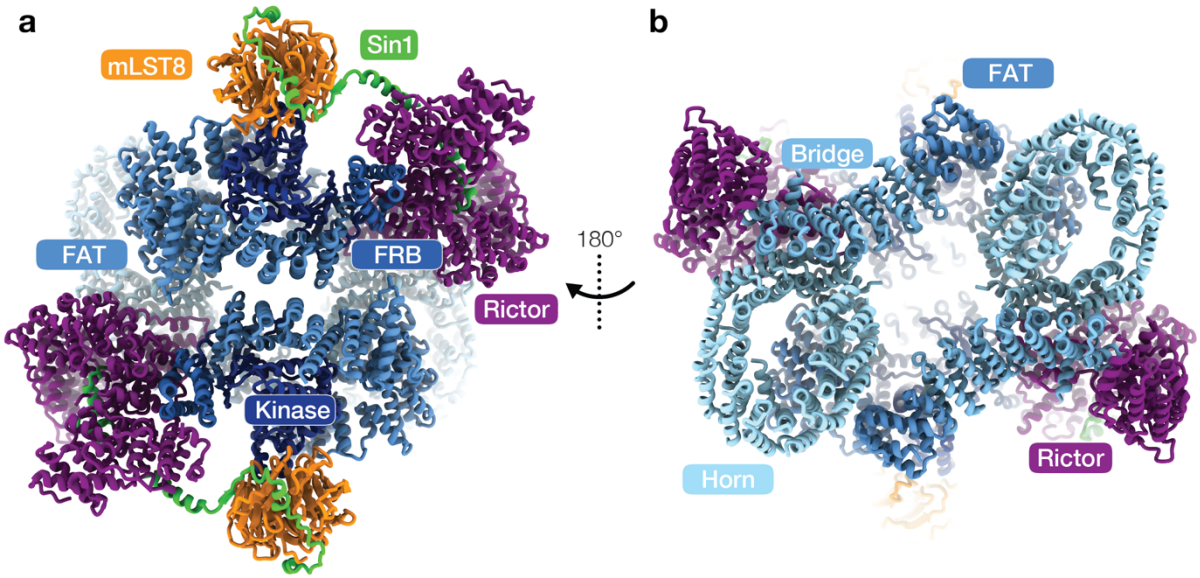

Figure 1.7 : Architecture of mTORC2
(a) Front and (b) back view of the structure of mTORC2 (cartoon representation colored by protein chains; domains of mTOR are indicated by shades of blue) (PDB: 6ZWM[54])

The structural organization of mTORC2 has recently been resolved at high resolution using cryo-EM. mTORC2 adopts the same overall architecture as mTORC1. Rictor takes over the position and role of Raptor in stabilizing the dimer. The CD-terminal domain of Rictor binds on top of the FRB domain, explaining the effects on mTORC2 observed due to rapamycin treatment[54]. The N-terminus of mSin-1 is deeply inserted into a pocket between Rictors AD- (Armadillo repeat domain) and HD (HEAT like repeat domain). mSIN1 extends towards mLST8 and provides a

structural link between Rictor and mLST8, highlighting the importance of mLST8 for mTORC2 complex assembly.

It is important to mention that for both human mTOR-complexes many disordered, unstructured or flexible regions could not be visualized. This includes the PRDs, PH and CRIM domain of mSIN1, a large 500 aa insertion of Rictor and many long loops with no assigned function.

1.6 DEPTOR is an inhibitor of mTOR complexes

DEP domain-containing 6 (DEPDC6) was discovered in 2009 to be an mTOR-interacting protein and therefor named DEP domain-containing mTOR interacting protein (DEPTOR). DEPTOR was co-purified with mTOR using low-salt purification designed for the isolation of PRAS40[77,182]. DEPTOR is a protein of 409 amino acids (46 kDa) consisting of two N-terminal DEPs (Dishevelled, Egl-10, Pleckstrin) and a C-terminal PDZ (postsynaptic density 95, discs large, zonula occludens-1) (Figure 1.8). The N- and C-terminal domains are connected by a roughly 120 amino acid long linker containing multiple phosphorylation sites.

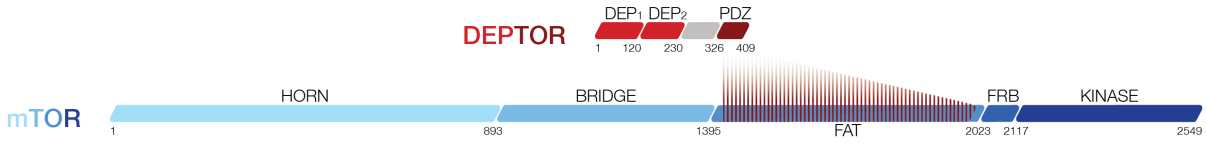

Figure 1.8 : DEPTOR interacts with the FAT domain and inhibits mTOR
The PDZ domain of mTOR binds to the FAT domain of mTOR and thereby inhibits both mTOR complexes

The tandem DEP (DEPt) arrangement present in DEPTOR is rare and just found in three other proteins: *phosphatidylinositol (3,5)-trisphosphate (PIP3)-dependent Rac exchanger 1* (P-Rex1*) and 2* (P-Rex2) and *supersensitivity to pheromone* (Sst2)[183]. Interestingly the P-Rex protein have been described to interact with mTOR as well[184]. Furthermore, besides sharing the tandem DEP domains, P-Rex1 and 2 also possess a PDZ domain. DEP domains are known to target proteins to membranes by interacting with lipids like phosphatidic acid (PA) or membrane receptors[185]. A helical core consisting of three α-helices and a β-hairpin protruding from this core are characteristic for these domains.

PDZs are around 90 aa in size and found in more than 600 human proteins[186,187]. The most prominent of PDZ domains is the formation of complexes by binding to 5-10 C-terminal residues of their target proteins.

DEPTOR was found to bind via its PDZ domain to the FAT domain of mTOR[182], while the DEP domains are dispensable for complex formation (Figure 1.8). Peterson *et al.* could show that DEPTOR interacts with both mTOR-complexes and is therefore a shared subunit. *In vitro* kinase assays showed that DEPTOR depletion increases activity of both mTOR-complexes towards

their main substrates (S6K1, 4E-BP1 and AKT). As for binding, also the inhibitory role of DEPTOR has been described to be dependent on the PDZ domain[182]. Thus, DEPTOR is the only know protein binding to and inhibiting both complexes. However, the role of DEPTOR in a cellular context is more complex. All published experiments investigating outcome of DEPTOR depletion or overexpression in cells have been reanalyzed in a recent review [183]. In cells, DEPTOR depletion leads to activation of mTORC1, but promotes mTORC2 activity. DEPTOR overexpression however results in inhibition of mTORC1 and activation of mTORC2. This unexpected behavior can be explained by a model where DEPTOR inhibits the feedback loop from mTORC1 to mTORC2 (discussed above) and PI3K/AKT signaling rules over mTORC2 inhibition by DEPTOR[183]. There are also exceptions to this "feedback model" which may depend on explored cell type or other details of the experimental setup. It is important to mention that DEPTOR inhibits activity of mTORC1 to a lesser extent than eg. Rapamycin and residual mTORC1 activity can be observed [183]. The exact roles of DEPTOR in cellular signaling need to be determined.
Besides being an inhibitor of mTOR, DEPTOR was found to be phosphorylated in the linker region in an mTOR-dependent manner, and thus can also be considered as an mTOR substrate.

1.6.1 Regulation of DEPTOR function

DEPTOR phosphorylation by mTOR play an important role in the regulation of DEPTOR. DEPTOR levels were found to decrease under mTOR-activating conditions[182,188-190]. Sequence analysis of DEPTORs linker region revealed presence of β-TrCP phosphodegron motif (pSpSGYFpS). Phosphorylation of DEPTOR by mTOR primes DEPTOR for other kinases like 1 (CK1), S6K1, RSK1 at the phosphodegron. Phosphorylation allows for binding of β-TrCP leading to ubiquitination by the $SCF^{\beta TrCP}$ E3 ubiquitin ligase and degradation of DEPTOR. Therefore, DEPTOR is regulated in a positive feedback loop by mTOR, where mTOR auto-amplifies its activation by DEPTOR degradation. Deubiquitination by OTU domain–containing ubiquitin aldehyde-binding protein 1 (OTUB1) counteracts this process [191].
Besides this degradation-based mechanism of regulating DEPTORs function on mTOR several other mechanisms have been described:
The lipid second messenger phosphatidic acid (PA), produced by phospholipase D 1 (PLD1), has been demonstrated to be a critical factor in mitogenic activation of mTOR[194,195]. Production of PA leads to displacement of DEPTOR from mTORC1 relieving its inhibition[196 ,197]. This regulatory mechanism describes a potential link of mitogenic signaling towards mTORC1 which is not dependent on the TSC-Rheb axis. In addition to regulation on protein level, DEPTOR is also controlled on the transcriptional level. mTORC1 and mTORC2, stimulated by growth factors,

directly suppress DEPTOR expression. This represents a feedforward loop in mTOR signaling, where the active mTOR-complexes downregulate expression of an inhibitor[182,198].

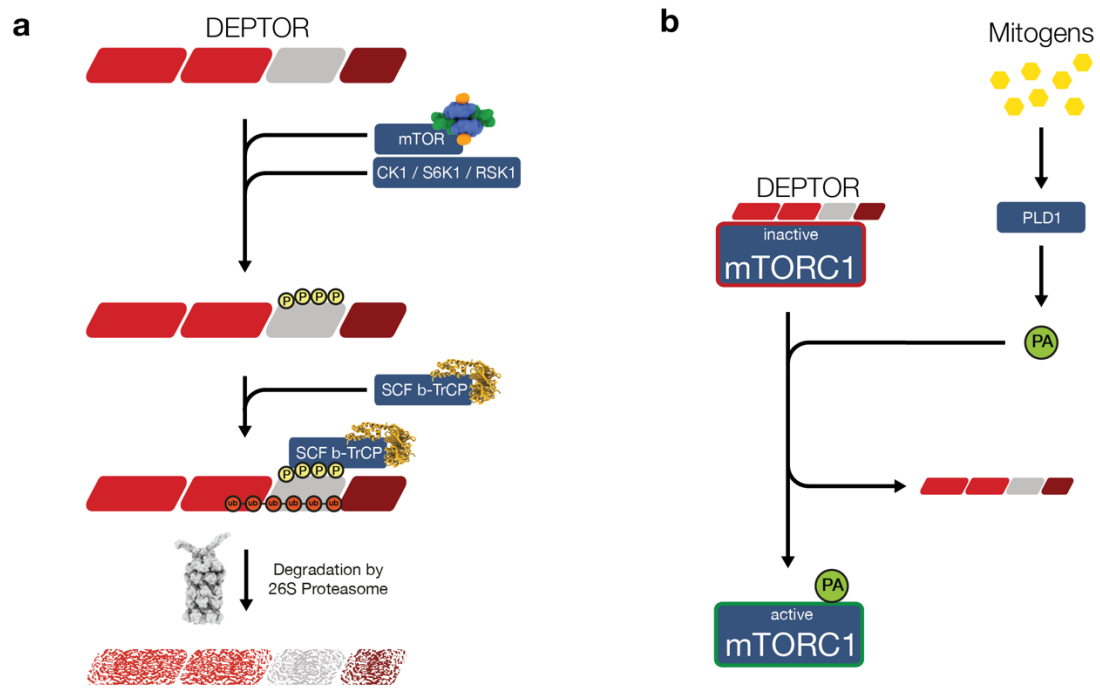

Figure 1.9 : DEPTOR is regulated by degradation and displacement from mTOR-complexes
(a) Sequential phosphorylation of DEPTOR by mTOR and other kinases targets DEPTOR for SCF β-TrCP mediated degradation by the 26S proteasome (mTORC1, PDB: 6BCX[53]; β-TrCP, PDB: 6M90[192]; 26S-Proteasome, PDB: 5L4G[193]) (b) Mitogen-stimulated production of phosphatidic acid leads to displacement of DEPTOR from and activation of mTORC1.

1.6.2 Role of DEPTOR in disease

Even though the exact function of DEPTOR in cellular signaling and molecular mechanisms thereof remain elusive, DEPTOR was found to modulate mTOR and PI3K signaling pathways. These two pathways are central in regulation of cell growth, survival and proliferation and found to be misregulated in the context of diseases such as cancer. Thus, it is important to also understand the function of DEPTOR in light of these clinical pictures.

DEPTORs dual role in cancer

mTOR signaling is elevated in most cancers. Therefore, one would expect that an mTOR inhibitor like DEPTOR can be considered as a tumor suppressor and would be downregulated in cancers. Indeed, DEPTOR mRNA levels were found to be low in most cancers[182]. This finding has been confirmed by several other groups which found that low DEPTOR levels in cancers like esophageal squamous cell carcinoma (ESCC), pancreatic or lung cancer[199,200,201] are necessary

for tumorigenesis in these cancers. DEPTOR has been also[201] described to be specifically downregulated at the invasive front of endometroid carcinoma[202] or in metastatic breast cancer cells[203], which supports that DEPTOR may counteract cell migration and invasion.

In stark contrast to these anti-proliferative characteristics of DEPTOR are observations in other cancer types. DEPTOR is massively overexpressed in multiple myeloma[182]. In combination with studies in osteosarcoma[204] or triple negative breast cancer[203], is has been suggested that DEPTOR is critical in promoting survival by targeting the mTORC1 feedback loop and activating AKT. In contrast to cancer progression, DEPTOR is not considered to be important for cancer initiation, since overexpression or deletion does not increase the rate of spontaneous tumor formation[205-207].

One could conclude a simplified model where DEPTOR acts as oncogene when it relieves the feedback loop inhibition on PI3K and in turn activates AKT. Vice versa, DEPTOR would represent a tumor suppressor role when DEPTOR loss leads to activation of the PI3K/mTORC2/AKT signaling[183]. The ground truth of DEPTORs role in cancer is certainly more complex and may be dependent on cancer type, cancer stage and many more factors. Extensive studies are required to gain a detailed understanding of the underlying molecular mechanisms.

DEPTOR promotes adipogenesis

Almost every second adult in the US is considered to be obese[208]. Obesity is cause or promotes many diseases like diabetes, cancer or cardiovascular diseases, representing a major challenge for health systems[209]. DEPTOR expression level in white adipose tissue (WAT) of obese humans has been found to correlate with the degree of obesity[206]. In agreement with this observation, DEPTOR overexpression in mice increases WAT mass. DEPTOR partially inhibits mTORC1 and impairs the feedback loop towards PI3K/mTORC2/AKT, by reducing phosphorylation of IRS1, while phosphorylation of 4E-BP1 or S6K1 was not affected[206]. Activated AKT signaling leads to expression of genes controlled by PPAR-γ, the regulator of adipogenesis[210], and FoxO1/3a phosphorylation[206]. DEPTOR may present a target for counteracting adipogenesis.

1.7 Aim of this thesis

mTOR complexes are central regulators of cell growth, proliferation, survival and death. Defective regulation of mTOR is a cause for or associated with many diseases including cancer, obesity, diabetes and neurodegeneration. Mechanistic understanding of this complex signaling network and its regulation on a structural and functional level is key for development of promising therapies. DEPTOR is the only known protein that binds and inhibits both mTOR complexes. Furthermore, DEPTOR has been attributed an enigmatic role in cancer, being oncogene and tumor suppressor. Despite its peculiar function and unique characteristic, structural and functional information on DEPTOR is not available and many question remained open. In this thesis I aim to gain mechanistic insights into the function of DEPTOR in controlling mTOR complexes by addressing the following questions:

What is the functional organization of DEPTOR?
How does DEPTOR bind to mTOR complexes?
Are DEPTORs role as mTORC1 substrate and inhibitor linked?
How does DEPTOR inhibit mTOR-complexes, by affecting substrate recruitment or turnover?
Is there any difference in the interaction of DEPTOR with mTORC1 and mTORC2?

Chapter 2 presents the structural and functional characterization of DEPTOR and its interaction with mTOR. A hybrid structural approach using single particle cryo-EM of DEPTOR bound to mTORC1 and mTORC2 in combination with crystallographic characterization of the DEPTOR tandem DEP domain provides insights into the DEPTOR interaction with mTOR-complexes. In combination with *in vitro* biochemical characterization this study revealed a novel allosteric inhibition mechanism of mTOR. It also paves the way for future studies on DEPTOR functions independent of mTOR. This chapter is reproduced from the publication “Regulation of human mTOR complexes by DEPTOR” (M. Wälchli, K. Berneiser, F. Mangia, S. Imseng, L.-M. Craigie, E. Stuttfeld, M. N. Hall, T. Maier; *eLife*; 2021).

Chapter 3 reviews current knowledge on mTOR substrate interactions. The review focuses on providing a detailed overview on substrates of mTORC1 and mTORC2, the function of these substrates and how they are recognized. Furthermore, phosphorylation motifs and recognition of substrates in the active site have been analyzed. This chapter is reproduced from the manuscript “mTOR substrate phosphorylation: mechanism, motifs, functions, and structures” (S. Battaglioni[1], D. Benjamin[1], M. Wälchli, T. Maier and M. N. Hall; submitted to *Cell; 2022*)

[1]Authors contributed equally

1.8 Declaration of own project contribution

For the structural and functional characterization of DEPTOR, I have produced mTORC1, mTORC2 and DEPTOR by producing virus, expressing the proteins in insect cells *Sf21*. I have cloned DEPTOR mutants and fragments based on own structural data, and produced them in insect cells or *E. coli*. I optimized existing and established new protocols for purification of the produced proteins. I optimized buffer conditions and grid preparation conditions and protocols for single particle cryo-EM analysis. I collected data on electron microscopes and processed single particle cryo-EM data. I optimized crystallization conditions for the DEPTOR tandem DEP domain, collected data at the synchrotron and processed X-ray data. I performed model building, structure validation and structure analysis for all structural analyses. I analyzed small angle X-ray scattering (SAXS) data for the DEPTOR DEP tandem domain. I performed *in-vitro* kinase activity assays and analyzed resulting data. I wrote the manuscript "Regulation of human mTOR complexes by DEPTOR, prepared figures and animations. A list of contribution for all authors is found at the end of the manuscript.

For the review "mTOR substrate phosphorylation: mechanisms, motifs, functions, and structures" I have analyzed published structural data on the active site of mTOR and other members of the PIKK family. I participated in manuscript writing and prepared figures for structural representations.

2 Regulation of human mTOR complexes by DEPTOR

Reproduced from:

Regulation of human mTOR complexes by DEPTOR

Matthias Wälchli, Karolin Berneiser, Francesca Mangia, Stefan Imseng, Louise-Marie Craigie, Edward Stuttfeld, Michael N Hall, Timm Maier

Available on eLife: https://elifesciences.org/articles/70871

2.1 Abstract

The vertebrate-specific DEP domain-containing mTOR interacting protein (DEPTOR), an oncoprotein or tumor suppressor, has important roles in metabolism, immunity and cancer. It is the only protein that binds and regulates both complexes of mammalian target of rapamycin (mTOR), a central regulator of cell growth. Biochemical analysis and cryo-EM reconstructions of DEPTOR bound to human mTOR complex 1 (mTORC1) and mTORC2 reveal that both structured regions of DEPTOR, the PDZ domain and the DEP domain tandem (DEPt), are involved in mTOR interaction. The PDZ domain binds tightly with mildly activating effect, but then acts as an anchor for DEPt association that allosterically suppresses mTOR activation. The binding interfaces of the PDZ and DEPt domains also support further regulation by other signaling pathways. A separate, substrate-like mode of interaction for DEPTOR phosphorylation by mTOR complexes rationalizes inhibition of non-stimulated mTOR activity at higher DEPTOR concentrations. The multifaceted interplay between DEPTOR and mTOR provides a basis for understanding the divergent roles of DEPTOR in physiology and opens new routes for targeting the mTOR-DEPTOR interaction in disease.

2.2 Summary

Structural and functional analysis reveals the mechanistic basis for mammalian target of rapamycin (mTOR)-dependent roles of DEP domain-containing mTOR interacting protein (DEPTOR) in cancer and metabolic regulation.

2.3 Introduction

DEP domain-containing mTOR interacting protein (DEPTOR), conserved in vertebrates, modulates the activity of the serine/threonine kinase mammalian target of rapamycin (mTOR), a master regulator of cell growth. mTOR acts in two functionally distinct multiprotein complexes, mTOR complex 1 (mTORC1) and mTORC2[21,66,79,167,211,212], and DEPTOR is the only protein reported to bind and inhibit both mTOR complexes[182].

DEPTOR is a 46 kDa protein comprising an N-terminal DEP (Dishevelled, Egl-10 and Pleckstrin) domain tandem, herein referred to as DEPt, and a C-terminal PDZ (Postsynaptic density 95, Disks large, Zonula occludens-1) domain. The PDZ domain has been suggested to interact with mTOR[182]and DEPt mediates phosphatidic acid binding[213]. The linker connecting DEPt and the PDZ domain contains a phosphodegron motif. mTOR phosphorylates this motif, leading to subsequent additional phosphorylation, ubiquitylation by the $SCF^{\beta TrCP}$ E3 ubiquitin ligase, and

DEPTOR degradation[188-190]. DEPTOR degradation, in turn, leads to activation of mTORC1 and inactivation of mTORC2 via the mTOR negative feedback loop. OTU domain-containing ubiquitin aldehyde-binding protein 1 (OTUB1) counteracts this process by deubiquitylating DEPTOR[191]. The interplay of mTOR and DEPTOR with the feedback loop from mTORC1 to mTORC2 and other signaling pathways leads to complex response patterns linked to variations in DEPTOR abundance depending on cell type and state[183,214].

DEPTOR plays central roles in cancer, obesity and immunodeficiency[183,205,206,215,216]. It can act as both an oncoprotein and tumor suppressor[183], and its effect in modulating PI3K-AKT signaling is variable depending on cancer type and cellular status. DEPTOR levels are low in most cancers due to active PI3K signaling[183]. In few cancers, including multiple myeloma[182], DEPTOR is overexpressed and promotes cancer cell survival. DEPTOR expression levels are increased in white adipose tissue in obesity and DEPTOR promotes adipogenesis by tuning down mTORC1 feedback control and thereby activating AKT signaling[206]. Despite its relevance to human health, DEPTOR is the only direct protein regulator of mTOR complexes whose molecular mechanism of action is unknown[53,91,217].

2.4 Results

To investigate the interplay of DEPTOR and mTOR in both human mTOR complexes, we combined cryo-EM analysis of recombinantly expressed and purified DEPTOR-mTORC2 and DEPTOR-mTORC1 complexes at resolutions of 3.2Å and 3.7Å (Fig. 2.1-S. 1, 2, 3), respectively, with crystallographic and in solution structural characterization of the DEPt region of DEPTOR and biochemical analysis. The core architecture of the cryo-EM reconstructions of the two mTOR complexes in association with DEPTOR largely resemble that of their DEPTOR-free states (Fig. 2.1a, b, c)[53,54]. In the mTORC1 and mTORC2 complexes associated with DEPTOR, the mTOR active site adopts a non-activated conformation[53,54](Fig. 2.1-S. 3g) and is not occupied by substrates. Inositol-hexakis-phosphate (IP6) was recently found to bind to mTORC1 and mTORC2, albeit without clear activating or inhibitory effect[54,63], and its binding is undisturbed in DEPTOR-bound mTORC1 and mTORC2 complexes. Binding sites for short linear TOS and RAIP motifs in mTORC1 substrates remain empty in the mTORC1-DEPTOR complex[73-75]. Consistent density for DEPTOR is observed in two regions of the FAT domain of mTOR for both mTORC1 and mTORC2, in agreement with a regulatory effect of DEPTOR on both complexes[182].

The DEPTOR-mTOR interaction occurs in two steps. In one step, the DEPTOR PDZ domain binds the mTOR FAT domain. The PDZ domain core (aa_{DEPTOR}326-409) adopts a canonical PDZ fold and binds the TRD2 subdomain[179] of the mTOR FAT domain (Fig. 2.2a, b; Fig. 2.2-S.1a). The interaction interface is formed by a conserved surface of the PDZ domain and three mTOR

helices (aa_{mTOR}1525-1578) (Fig. 2.1, 2a, b; Fig. 2.2-S.1a, b, c). The canonical PDZ domain peptide binding groove[218] is present, but remains unoccupied in the interaction of the DEPTOR PDZ domain with mTOR (Fig. 2.2-S1. d). This opens the possibility that binding of other, yet unknown protein partners via a canonical PDZ-peptide interaction to the DEPTOR PDZ domain could further strengthen or inhibit the mTOR-PDZ interaction. To the best of our knowledge, the mode of interaction of the DEPTOR PDZ domain with mTOR has not been observed for other PDZ domains. The binding interface between mTOR and the DEPTOR PDZ domain is considerably enlarged by contributions from regions which are known or predicted to be disordered in isolated mTOR complexes or DEPTOR. A loop in the Horn (also known as N-HEAT)[53,180] region of mTOR (aa_{mTOR}290-350, DEPTOR-binding loop) (Fig. 2.2c) was disordered in previous reconstructions of mTOR-complexes in the absence of DEPTOR, and its function remained elusive[53,54]. In complex with DEPTOR, residues aa_{mTOR}304-317 are ordered and the backbone of residues aa_{mTOR}290-303 connecting to the Horn is visible at lower resolution (Fig. 2.2-S. 1e). Residues aa_{mTOR}304-306 interact with the DEPTOR PDZ domain and residue F_{mTOR}306 is inserted between the DEPTOR PDZ and mTOR FAT domains as an integral part of the interface (Fig. 2.2-S. 1f). The DEPTOR PDZ domain together with the DEPTOR-binding loop forms a structural link between the Horn and FAT domain of mTOR, positioned to mediate conformational crosstalk between different subregions of the mTOR complexes. The DEPTOR linker connecting DEPt and the PDZ domain remains largely unresolved (aa_{DEPTOR}231-303), and only the C-terminal region of the linker (aa_{DEPTOR} 304-325) is ordered when DEPTOR is bound to mTOR complexes. Residues aa_{DEPTOR}309-325 provide an N-terminal extension to the PDZ core domain, while aa_{DEPTOR}304-308 bind a groove formed by α-helices 14-16 of the mTOR FAT domain (Fig. 2.2d). The linker-mTOR interaction enlarges the interface formed by the PDZ core domain suggesting functional relevance of linker residues aa_{DEPTOR}304-308 for DEPTOR-mediated regulation of mTOR.

The other step of the DEPTOR-mTOR interaction is mediated by the DEPTOR DEPt region and the mTOR FAT domain (Fig. 2.1a, c; Fig. 2.3a). The DEPt region bound to mTOR is less well resolved in overall high-resolution reconstructions as a consequence of local flexibility and partial occupancy. 3D-variability analysis, focused classification and local refinement (Fig 1-S.1a, 2a) led to clear visualization of the overall fold and individual secondary structure elements (Fig. 2.3-S. 1a) at a local resolution of approx. 4-6 Å (Fig. 2.1-S. 3e, f). To obtain a pseudo-atomic model of the second DEPTOR-mTOR binding interface, we determined an X-ray crystal structure of a recombinant DEPt region (aa_{DEPTOR} 1-230) at 1.93 Å resolution in a domain-swapped conformation as revealed by small-angle Xray scattering (SAXS) in solution (Fig. 2.3-S. 1b, c). Each of the two domains in DEPt adopt a characteristic DEP domain fold comprising an alpha-

helical core and a protruding beta-hairpin arm. In the DEPt domain tandem, the two DEP domains are interacting via their N-terminal α-helices and a C-terminal extension of the second DEP domain that folds back onto the first DEP domain (Fig. 2.3-S. 1b). Binding of DEPt to mTOR preserves the overall fold of DEPt, but is linked to a 3.6Å translation and 39° rotation between the two DEP domains (Fig. 2.3-S. 1d).

The DEPt region binds on top of the helical repeats of the mTOR FAT domain in the region aa_{mTOR}1680-1814 (Fig. 2.3a). The binding interface of DEPt with mTOR is smaller than that of the PDZ-and-linker interaction site (~950Å^2 compared to ~1100Å^2). The N-terminal DEP domain, including the linker to the second DEP domain, forms the major part of the interface (~700Å^2 compared to ~250Å^2) and is better ordered than the C-terminal DEP domain (Fig. 2.1-S. 3e, f; Fig. 2.3-S. 1a). Notably, the N-terminal DEP domain is absent in one of the two known isoforms of human DEPTOR[219], likely abolishing DEPt-mTOR association. The protruding beta-hairpin of the N-terminal DEP domain inserts into a crevice between the FAT and kinase domains of mTOR (Fig. 2.3b), where residue R_{mTOR}2505 is located. This residue is altered to proline in a cancer-associated mutation that weakens DEPTOR binding to mTOR[220,221] and cannot be compensated by DEPTOR overexpression, underlining the functional relevance of this interaction (Fig. 2.3b)[222]. mTOR interacting residues of DEPt are highly conserved (Fig. 2.3-S. 1e) and the surface electrostatic potentials around the interface are complementary (Fig. 2.3-S. 1f). Notably, two positively charged patches in DEPt, which are involved in mTOR interaction, were found to bind phosphatidic acid (PA)[213]. PA has been reported to displace DEPTOR from mTOR complexes[196].

Previously described mechanisms of mTOR inhibition include ATP-competitive binding to the kinase active site in mTORC1 and 2 (e.g. Torin1)[87], steric hindrance of access to the active site by the FKBP12-Rapamycin complex[8,53], and competition with substrate-guiding interactions specific to mTORC1 by the FRB domain binding protein inhibitor PRAS-40. Competitive binding at other substrate recognition elements, such as the TOS and RAIP motif binding sites in mTORC1[53,73-76,144] or C-terminal parts of mSIN1[223] in mTORC2, provide alternative target sites for mTOR inhibition. Recently developed small molecule mTOR inhibitors either utilize the above inhibitory mechanisms or their detailed mode of action is still unkown[224-227].

Notably, DEPTOR is not only a modulator of mTORC1 and mTORC2 activity, but also a substrate of mTOR in mTORC1 and mTORC2[182,188-190]. Indeed, we observe weak residual density in the DEPTOR-mTORC1 complex at a binding site for helical peptide segments of substrates and the inhibitor PRAS40 on the FRB domain, which might represent a dynamically interacting segment of DEPTOR or copurified interacting proteins (Fig. 2.4-S. 1a). Based on distance constraints, binding of the linker of DEPTOR with an extended helix as in PRAS40 to the FRB-site is incompatible with the DEPTOR association to mTOR via its PDZ and DEPt regions; a smaller

association patch cannot be ruled out, but would require fully extended surrounding linker regions. Still, it is sterically impossible that all sites for mTOR-mediated phosphorylation in the DEPTOR linker (aa_{DEPTOR} 244, 265, 286, 293, 295, 296, 299[182,188-190]) could reach the mTOR active site when DEPTOR is associated with mTORC1 via its PDZ and DEPt regions. Thus, a secondary linker-mediated, low affinity binding mode of DEPTOR (or in trans- phosphorylation without recruiting signal) is required and provides a plausible explanation for the residual signal at the FRB domain.

To test the relevance of DEPTOR interactions in the regulation of mTOR activity, we analyzed phosphorylation of 4E-BP1 by Rheb-activated mTORC1. An equivalent *in-vitro* activity assay with activated mTORC2 has not been described. Insect-cell and *E. coli* expressed DEPTOR, which are partially phosphorylated or unphosphorylated, respectively, show a 60-70% inhibition of 4E-BP1 phosphorylation at $T_{4E\text{-}BP1}37/46$ (Fig. 2.3c, Fig. 2.3 – source data 1). This inhibition is partially abolished by a single mutation and fully reverted by a triple mutation of the core PDZ interface (Fig. 2.3c, Fig. 2.3-S. 2). Notably, mutations in the interface between DEPt and mTOR lead to stimulation of 4E-BP1 phosphorylation (Fig. 2.3c, Fig. 2.3-S. 2), suggesting that DEPt mediates the inhibitory effect of DEPTOR on mTOR-complexes, while the binding of DEPt interface mutants only via the PDZ domain even mildly activates Rheb-bound mTORC1(Fig. 2.3c).

2.5 Discussion

Our structural and mutational analyses suggest a model for DEPTOR action on mTOR complexes, in which DEPTOR provides an additional layer of control with the ability to stimulate or inhibit the mTOR complexes (Fig. 2.4a). In this model DEPTOR associates with high-affinity via its PDZ domain anchor, possibly modulated by other PDZ-binding proteins, followed by lower-affinity association of DEPt based on avidity. DEPTOR partially inhibits mTOR activity by a dominant negative effect of DEPt association or moderately stimulates mTOR activity via the influence of the PDZ domain, if DEPt is prevented from mTOR association by PA binding (Fig. 2.4b). A suppression of non-stimulated basal mTORC1 or 2 would only be observed at high concentration of DEPTOR (Fig. 2.4b) that result in additional substrate-like binding of DEPTOR to mTORCs.

The isolated DEPt region of DEPTOR has been reported to lack significant binding to mTORC1 and to have no effect on mTORC1 activity, resulting in the hypothesis that DEPt is not involved in controlling mTOR activity in the context of full-length DEPTOR[182,228]. However, our data show that DEPt, when anchored via the PDZ domain, binds to a region of the mTOR FAT domain and suppresses allosteric activation of mTOR. Avidity of combined strong PDZ and weak DEPt interactions is supported by the earlier observation that full-length DEPTOR inhibits mTORC1 activation already at a lower concentration than required for binding of the isolated PDZ domain: The isolated PDZ domain binds with a K_d of 0.6 µM to the mTORC1variant A_{mTOR}1459P that mimics activation by Rheb, but the IC_{50} value for DEPTOR in the same system is 30-50nM[228]. The functional relevance of a similar interplay of strong and extremely weak association has recently been demonstrated for two mTORC1-binding motifs in 4E-BP1, the high affinity TOS motif and the very low affinity RAIP motif [144].

We observed an unexpected, weak activation of Rheb-stimulated mTORC1 activity in mutants of the DEPt interface which we attributed to an effect of PDZ domain binding. This effect is consistent with the observation of increased 4E-BP1 phosphorylation by mTORC1 in the presence of equimolar isolated PDZ domain (at overall nanomolar concentrations, cf. Fig.2S1/Fig.6S1 in Ref.[228]). It has also been reported that the PDZ domain has an approximately 10-fold higher affinity (K_d 0.6 µM vs 7 µM) for binding to activated vs. non-activated mTORC1[228], despite a lack of differences in the interface in static structures of activated and non-activated mTOR complexes[53]. Together, these data suggest that association of the PDZ domain is linked to changes in the dynamics of its binding site on mTOR, which are allosterically coupled to mTOR activation. Binding of other proteins to DEPTOR based on a canonical peptide-PDZ domain interaction via the empty PDZ-peptide binding groove may modulate the affinity of the PDZ to mTOR or even its effect on activity when bound to mTOR.

Why are low concentrations of DEPTOR inhibiting Rheb-stimulated mTORC1 but much higher concentrations of DEPTOR are required[228] for the reported inhibition of non-stimulated mTORCs[182,189,196,206]?

Facilitated by PDZ binding to mTOR, DEPt associates with non-activated mTOR-complexes without inducing structural changes in the FAT region, as visualized here for mTORC1 and mTORC2. We suggest that DEPt association with a region of the FAT domain, that transduces allosteric activation by Rheb, specifically suppresses the conformational coupling between the Rheb binding and the kinase site and consequently reduces only the stimulation of mTORC1 activity. This may occur by increasing the population of a state of the FAT region that is less competent for transmitting allosteric activation, either directly the state observed in non-activated mTOR or other intermediate states. Such a mode of action suggests the absence of inhibition of non-stimulated basal mTORC activity at low concentrations of DEPTOR. An alternative explanation for the lack of inhibition at low DEPTOR concentrations[228] could be the failure to associate with mTORCs as a result of the differential interaction of the PDZ domain with stimulated vs. non-stimulated mTORC1, K_d of 0.6 µM vs 7 µM[228], respectively. However, based on our demonstration of an additional interface for DEPt binding, the avidity of combined DEPt and PDZ association suggests that the association of full-length DEPTOR still occurs at a concentration lower than the approx. 15-50 µM required for effective inhibition of non-stimulated mTORC1[228]..

A plausible explanation for inhibition of mTORC1 and mTORC2 at higher concentrations could be a secondary, lower affinity binding mode at excess concentrations of DEPTOR over mTOR that does not involve interactions of PDZ and DEPt with mTOR. Indeed, DEPTOR is a substrate for mTORC1 and mTORC2[182,188-190]. Substrate recruitment by TOR complexes involves specific substrates recruitment via medium and low affinity interactions outside the kinase domain for many substrates[53,73-75,144,223], but the primary DEPTOR binding via PDZ and DEPt domains is not suitable for recruitment, suggesting lower-affinity secondary binding modes to mTORC1 and mTORC2. Indeed, such an alternative, substrate-like weak interaction is indicated by residual density observed here in a known substrate recruitment site for mTORC1. We have previously shown that the core substrate recognition regions in mTORC2 are flexibly disposed, explaining why substrate interactions are not visualized in the current type of cryoEM analysis[54].

Substrate-like association of DEPTOR, via the FRB domain or other regions in mTORC2, and simultaneous recruitment of other substrates with their respective binding motifs, e.g. 4E-BP1 with its TOS and RAIP motifs, would result in a mutual restriction of access to the mTOR active site that may partially be uncoupled from solution concentrations and dominated by local protein dynamics. At the same time, we consider that the core mechanism for the high-affinity mode of

inhibition of activated mTOR complexes by DEPTOR is unlikely to be based on a PRAS40-like FRB-interaction because (1) the binding site on the FRB domain is not accessible in mTORC2 (Fig. 2.4-S. 1b), (2) this would leave the conserved characteristic DEPt domain and its mTOR interaction involving $R_{mTOR}2505$ without assigned function, and (3) it provides no additional explanation for differential effects on stimulated and non-stimulated mTORC1, as the binding site on the FRB domain is not coupled to allosteric activation.

Notably, the interface of DEPt and mTOR suggested here to mediate inhibition of mTOR inhibition involves regions of DEPt that have been recently implicated in PA interaction[213]. We hypothesize that DEPt interaction with PA may control DEPt association with mTOR, resulting in either PDZ-based activation or DEPt-based down-regulation of activated mTOR complexes. This would create a mechanistic link between PA-signaling and mTOR activation on membranes (Fig. 2.4b)[229].

DEPTOR has been characterized as a modulator of mTOR activity with a profound impact on metabolism and cancer[211]. However, its divergent and orthogonal effects on cell physiology, including its apparently antagonistic roles as an oncoprotein and tumor suppressor, have remained enigmatic. Here, we provide a structure-guided model of the complex interplay of DEPTOR with mTORC1 and mTORC2 that identifies orthogonal contributions by different interacting regions of DEPTOR, and further potential for modulation by crosstalk from other signaling pathways. The molecular insights provided here will be a crucial component for targeted dissection of DEPTOR effects on mTOR signaling to further understand the divergent effects of DEPTOR in physiology and disease.

2.6 Figures

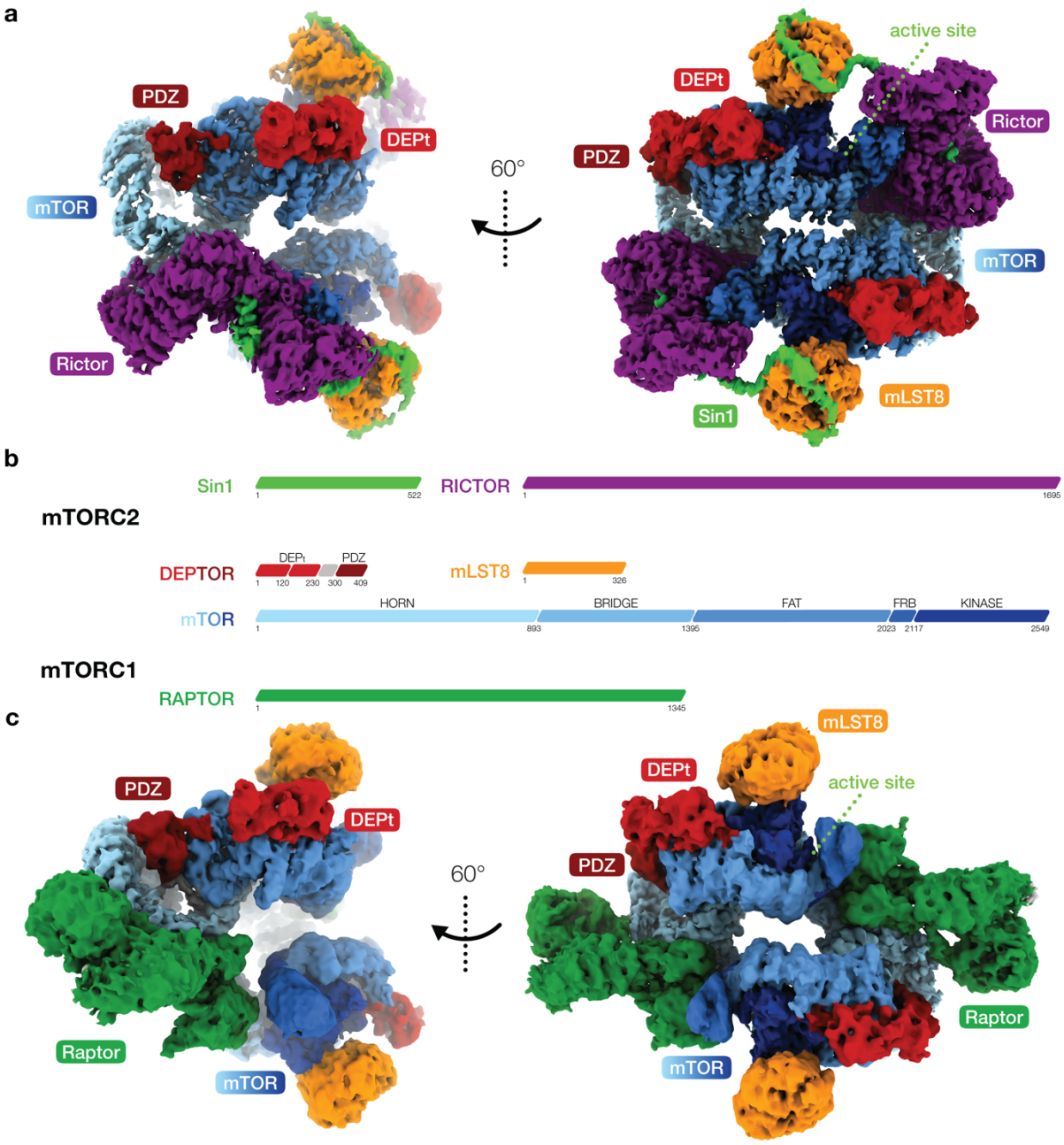

Figure 2.1 : cryo-EM reconstruction of DEPTOR-bound mTOR complexes 1 and 2
(a) Composite map of overall and local focussed cryo-EM reconstructions of DEPTOR-bound mTORC2 (b) Schematic representation of the domain architecture of mTORC1, mTORC2 and DEPTOR (c) Composite map of overall and local focussed cryo-EM reconstructions of DEPTOR-mTORC1. In (a) and (c) proteins are colored according to the schemes in (b). DEPTOR binds to mTORC1 and mTORC2 in virtually identical manner via its extended PDZ-linker and DEPt regions associating with the FAT domain of mTOR.

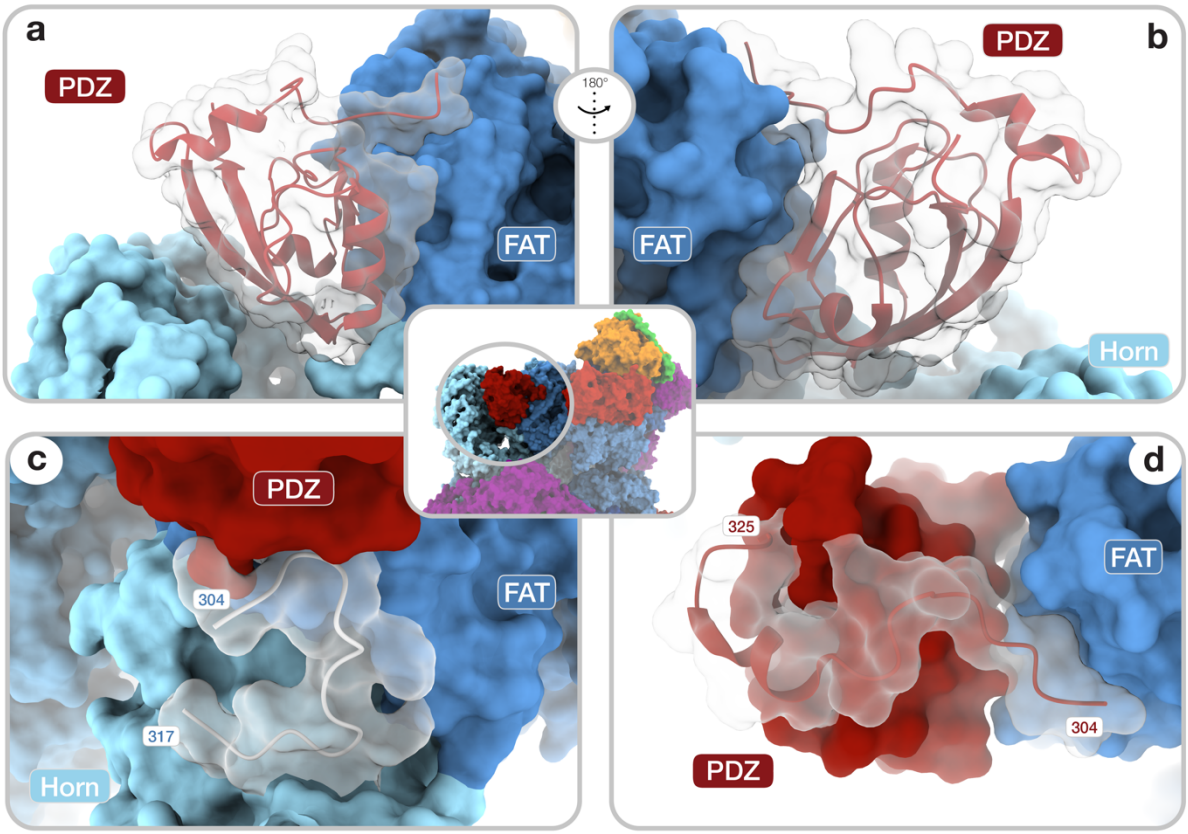

Figure 2.2: Architecture of the DEPTOR PDZ domain and its interaction with mTOR
(a),(b) Front (a) and back (b) view of DEPTOR PDZ bound to the mTOR FAT domain. The PDZ domain (shown as transparent surface with red cartoon) binds to a hinge in the FAT domain of mTOR.
(c) Loop region (aa_{mTOR}290-350) in the mTOR Horn-region (transparent with cartoon) is disordered in free mTOR complexes and contributes to the mTOR-PDZ interface and thereby creates a link between the Horn-region and the FAT domain of mTOR and the DEPTOR PDZ domain.
(d) The PDZ domain N-terminal extension stretches towards the FAT domain. The adjacent N-terminal linker inserts into a groove on the FAT domain and substantially contributes the PDZ-mTOR interface.

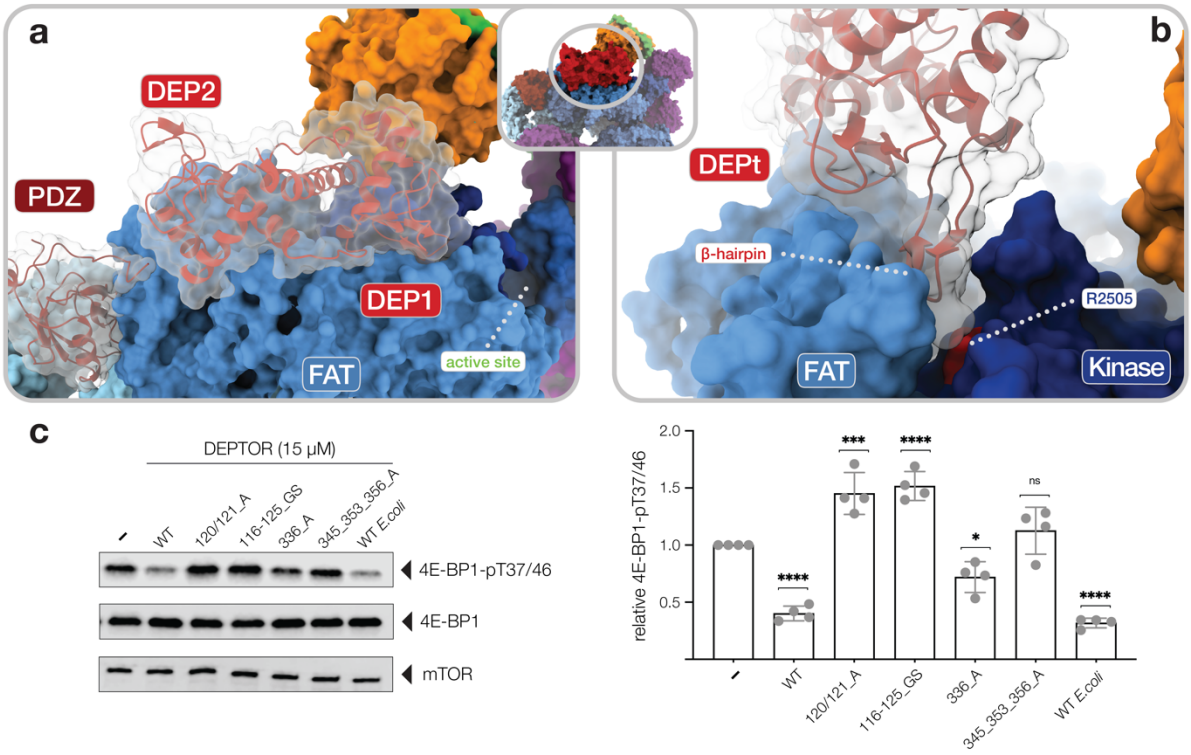

Figure 2.3: Interactions of the DEPTOR DEPt region with mTOR
(a) Surface representation of DEPTOR (transparent with cartoon in red) bound to mTORC2. The DEPt region binds centrally on top of the helical repeats of the FAT domain.
(b) The protruding hairpin of the first DEP domain of DEPt inserts into a crevice between the kinase and FAT domain of mTOR. The DEPTOR-displacing mutant R2505P[220] is located in close proximity.
(c) Analysis of the impact of wild-type and mutant forms of DEPTOR on Rheb-stimulated mTORC1 activity. Mutants are described in Fig. 2.3-S. 2. mTORC1 was incubated with 4E-BP1 and Rheb for stimulation, in the presence of DEPTOR wild-type and mutants. Reactions were separated by SDS-PAGE and analyzed by Western Blot. 4E-BP1 phosphorylation was detected with an antibody specific to phosphorylation of residues T37/46. Quantification (mean ± SD) of western blots in 4E-BP1-pT37/46 signals were normalized to total 4E-BP1 signals and the statistical significance of changes between control (0µM DEPTOR) and DEPTOR variants determined by One-way ANOVA. ****p<0.0001, ***p<0.001, *p<0.05, ns p>0.05, n=4.

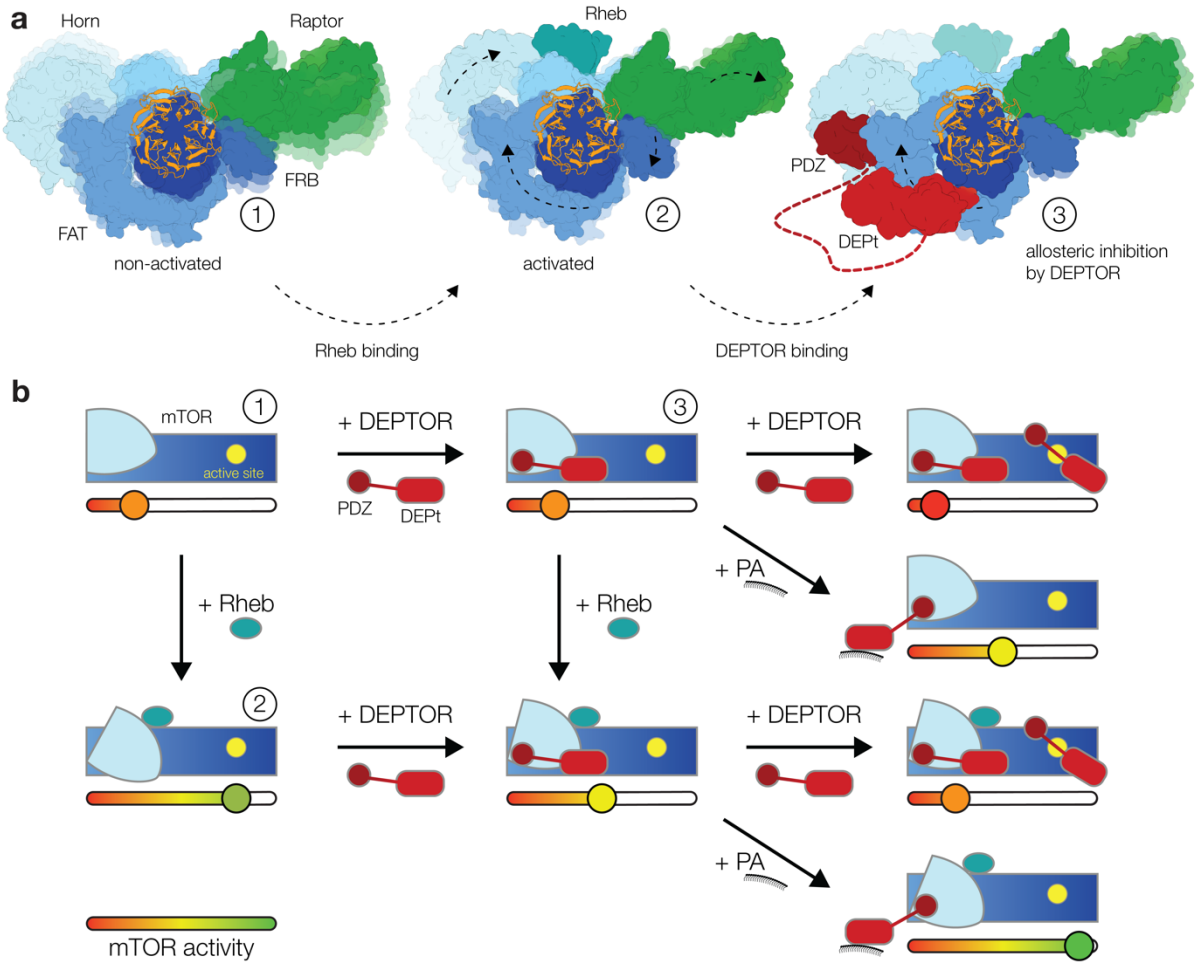

Figure 2.4: Model for the DEPTOR-mediated regulation of mTOR activity
(a) Structure-based representation of (1) the basal state of non-activated mTORC1 (based on PDB: 6BCX) (2) the allosteric activation of mTORC1 by Rheb binding (based on PDB: 6BCU) and (3) the impact of DEPTOR association via the PDZ domain and DEPt domain on the conformational state and activity of mTORC1. Possible transitions in subpopulations of conformational states are indicated by shadowing.
(b) Schematic diagram of the suggested regulatory interactions between DEPTOR and mTOR complexes. Structurally characterized states shown in (a) are indicate by numbers. DEPTOR binding via the PDZ and DEPt domains prevents allosteric activation. At high concentrations, DEPTOR binds to mTORC1 in a secondary binding mode as a substrate and sterically influences access of other substrates to the active site. PA may interfere with the DEPt-mTOR association, relieving the allosteric inhibition of mTORCs. The remaining bound PDZ domain mildly stimulates kinase activity in activated and non-activated mTOR complexes.

2.7 Supplementary Material

2.7.1 Supplementary Figures

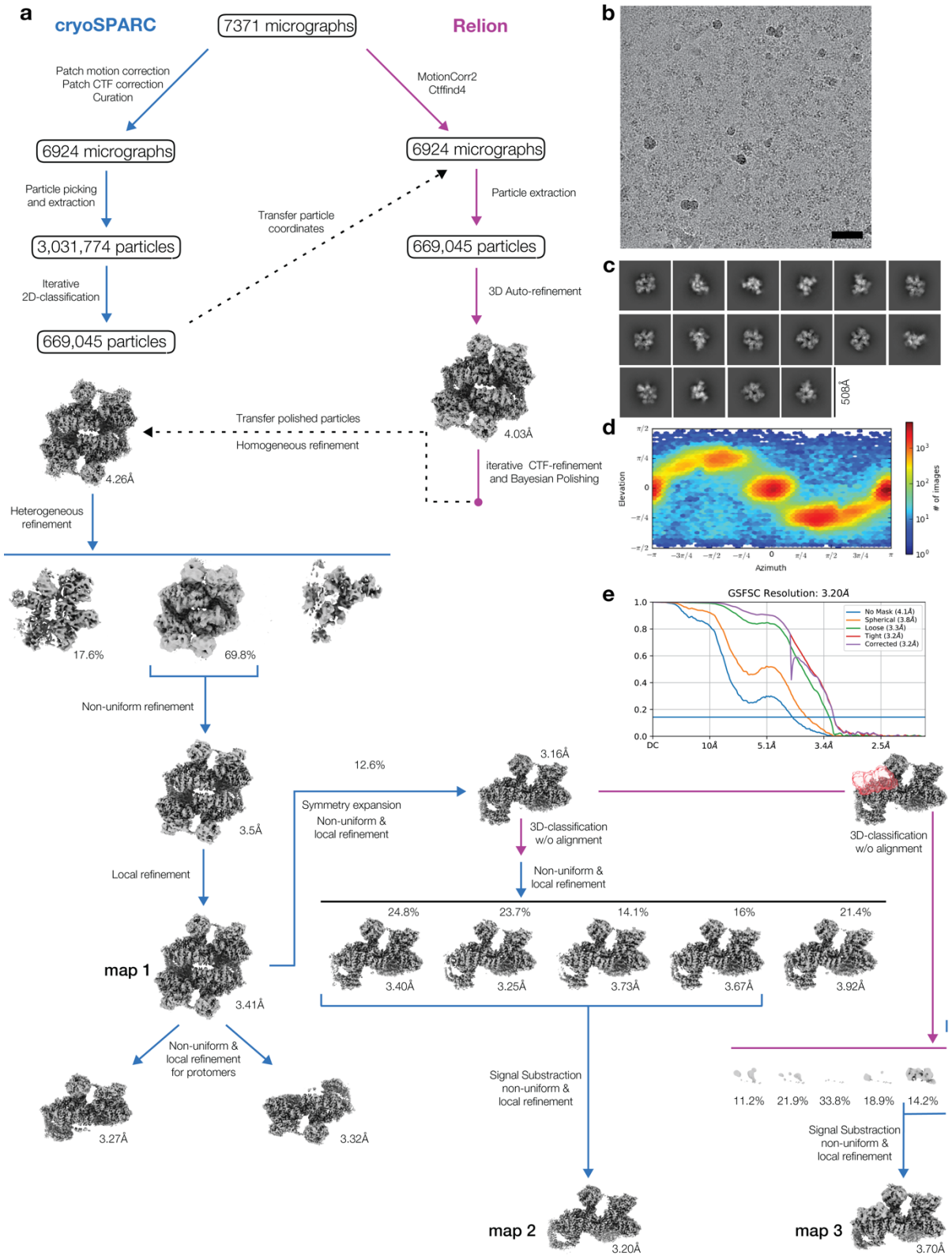

Figure 2.1 - figure supplement 1: Cryo-EM data processing DEPTOR-mTORC2
(a) Scheme of the cryo-EM data processing workflow. DEPTOR-mTORC2 overall refinement (map 1), focussed refinement on symmetry-expanded protomer (map 2) and focussed refinement on one protomer classified for the DEPt region (map 3) were used for modelling and illustration
(b) Representative micrograph of the DEPTOR-mTORC2 dataset is shown; scale bar equals 500Å
(c) 2D-class averages (d) Viewing direction distribution of the DEPTOR-mTORC2 overall refinement (map 1) (e) Fourier shell correlation (FSC) curves for unmasked, spherical, loose and tight masks, and corrected FSC curve for the map 2 reconstruction, yielding a gold standard FSC resolution of 3.20 Å.

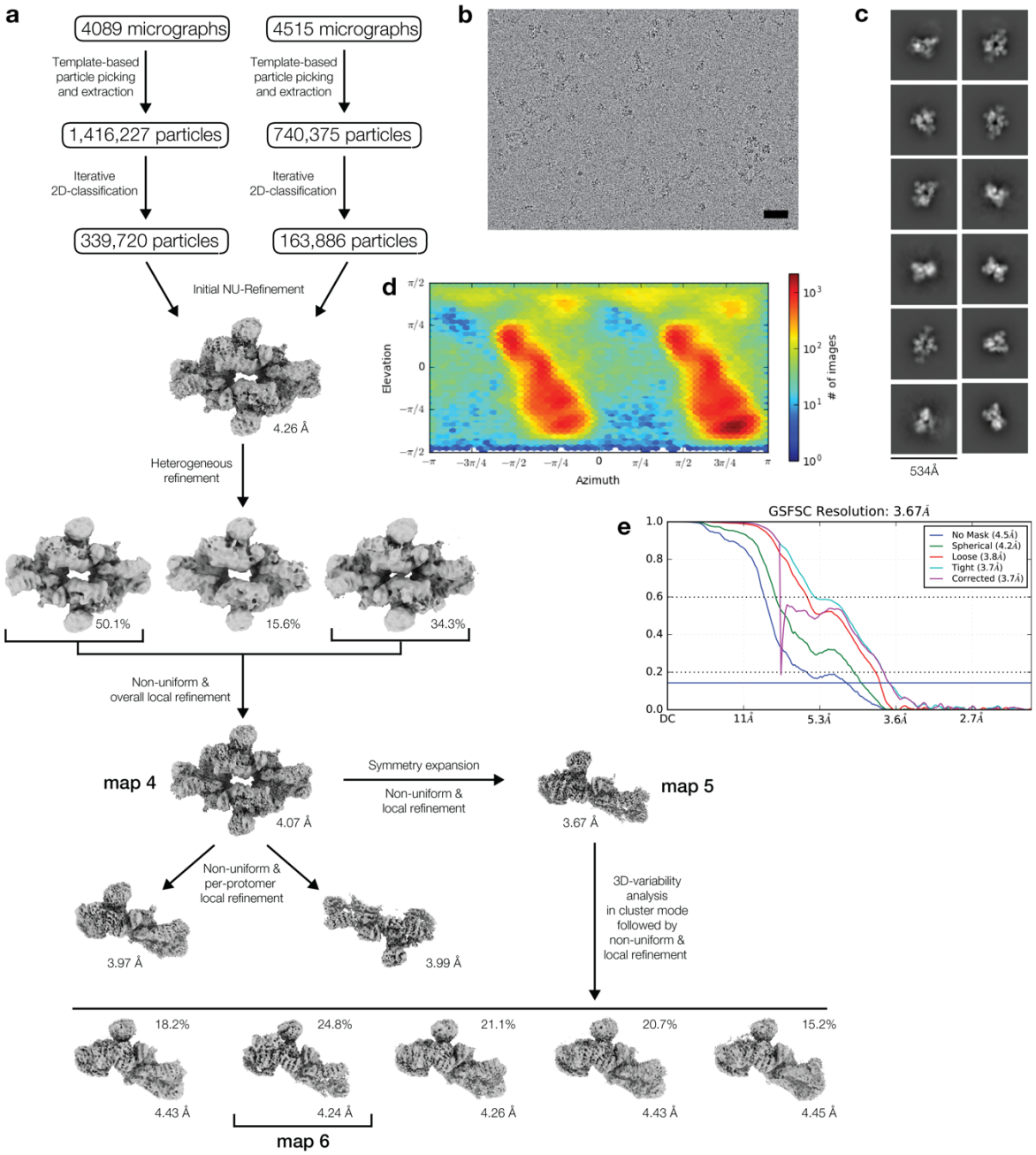

Figure 2.1 - figure supplement 2: Cryo-EM data processing of DEPTOR-mTORC1
(a) Scheme of the cryo-EM data processing workflow. DEPTOR-mTORC1 overall refinement (map 4), focussed refinement on symmetry-expanded protomer (map 5) and focussed refinement on one protomer classified for the DEPt region (map 6) were used for modelling and illustration (b) Representative micrograph of the DEPTOR-mTORC2 dataset is shown; scale bar equals 500Å (c) 2D-class averages (d) Viewing direction distribution of the DEPTOR-mTORC1 overall refinement (map 1) (e) Fourier shell correlation (FSC) curves for unmasked, spherical, loose and tight masks, and corrected FSC curve for the map 5 reconstruction, yielding a gold standard FSC resolution of 3.67 Å.

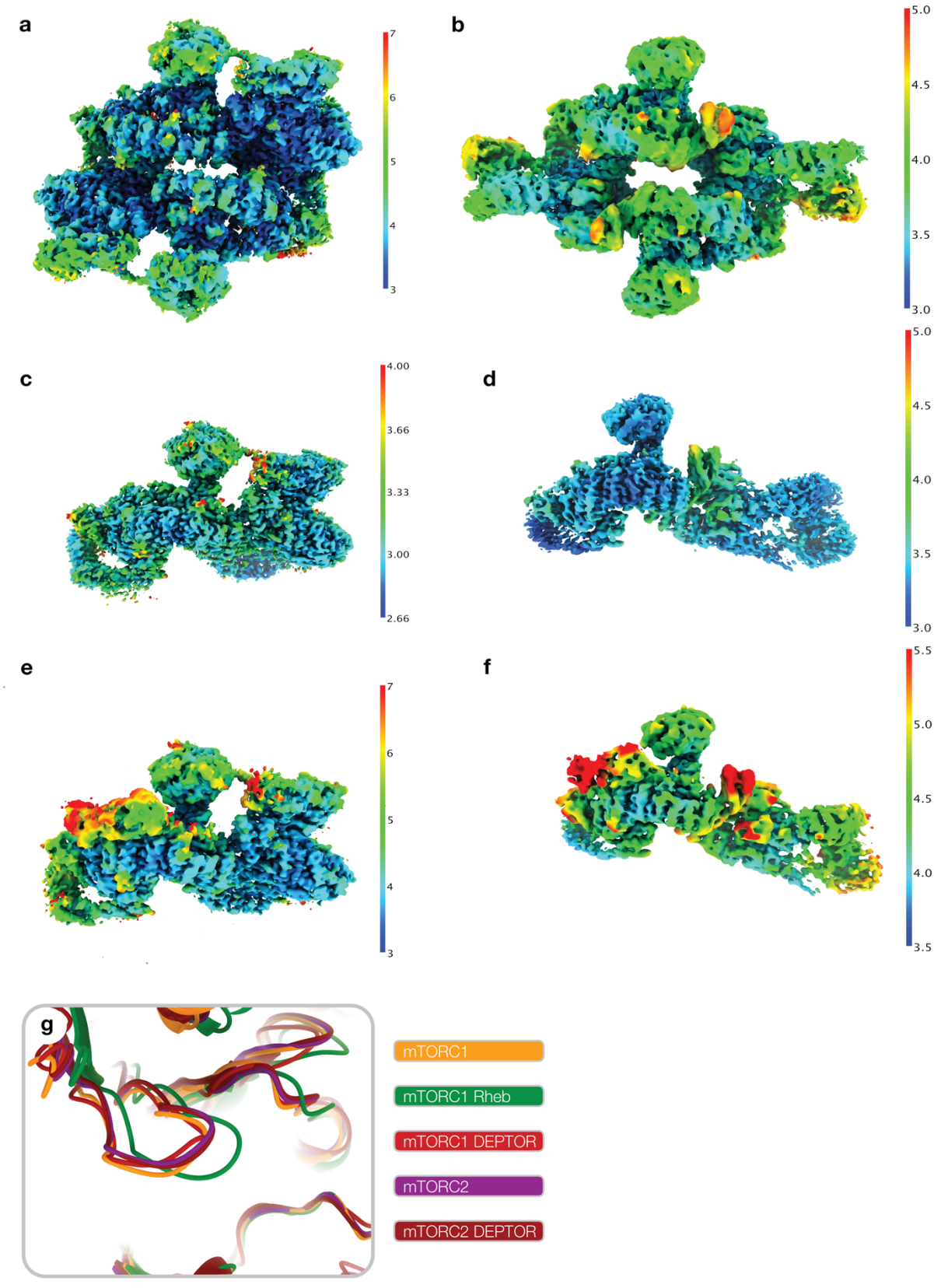
a
7
6
5
4
3
b
5.0
4.5
4.0
3.5
3.0
c
4.00
3.66
3.33
3.00
2.66
d
5.0
4.5
4.0
3.5
3.0
e
7
6
5
4
3
f
5.5
5.0
4.5
4.0
3.5
g
mTORC1
mTORC1 Rheb
mTORC1 DEPTOR
mTORC2
mTORC2 DEPTOR

Figure 2.1 - figure supplement 3: Local resolution and active site state of mTOR complexes in cryo-EM reconstructions

Cryo-EM reconstructions used for modelling colored by local resolution calculated using cryoSPARC at 0.143FSC cutoff **(a)** map 1, **(b)** map 4, **(c)** map 2, **(d)** map 5, **(e)** map 3, **(f)** map 6 (Fig. 2.1-S. 1a; Fig. 2.1-S. 2a). **(g)** Superimposition of free mTORC1 (6BCX[53]), Rheb-activated mTORC1(6BCU[53]), free mTORC2 (6ZWM[54]) and DEPTOR-bound mTORC1 and mTORC2 (this study). DEPTOR-bound mTOR-complexes resemble the non-Rheb activated state of the mTOR kinase active site.

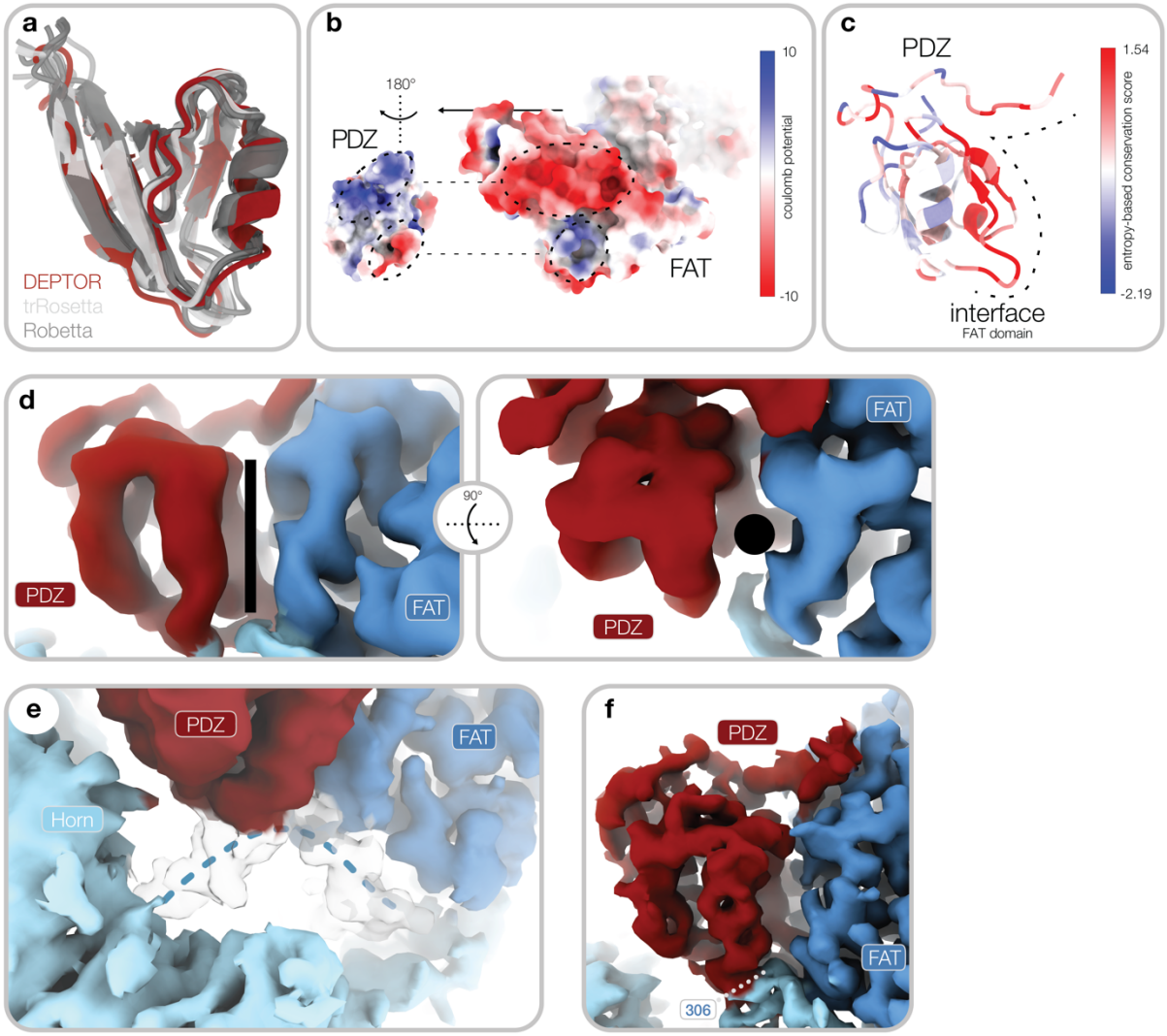

Figure 2.2 - figure supplement 1: PDZ domain interaction with mTOR complexes.
(a) Superimposition of models for the PDZ core obtained from trRosetta (light grey) and Robetta (dark grey) and the final model based on the cryo-EM reconstruction (red) (map 2, Fig. 2.1-S. 1a)
(b) Complementary surface electrostatic potential is observed for the two binding interfaces between DEPTOR and the mTOR FAT domain. **(c)** Sequence conservation of the PDZ domain mapped onto the structure. The interface to mTOR is schematically indicated by a dashed line. mTOR interacting residues are highly conserved. **(d)** map 2 (Fig. 2.1-S. 1a) lowpass-filtered to 5Å. The canonical binding groove of the PDZ domain (indicated by a black rod/dot) is empty and not peptide-bound. This mode of interaction allows regulation of the PDZ mTOR association by binding of additional interaction partners to the canonical binding groove. **(e)** map 2 (Fig. 2.1-S. 1a) lowpass-filtered to 3.5Å resolution. A linker of the Horn-region (indicated by blue dotted line) adopts a structured conformation upon PDZ-binding and provides a structural link between the Horn-region, the FAT domain and the PDZ domain **F** Quality of the cryo-EM reconstruction for the PDZ. The binding interface is well defined with a local resolution of around 3Å. Local resolution for the PDZ domain decreases due to flexibility with increasing distance from the interface to around 4 Å (Fig. 2.1-S. 3c). Continuous density is observed for the PDZ N-terminal extension and the transition into the FAT-bound linker. $F_{mTOR}306$ (labelled) is an integral part of the PDZ-mTOR interface.

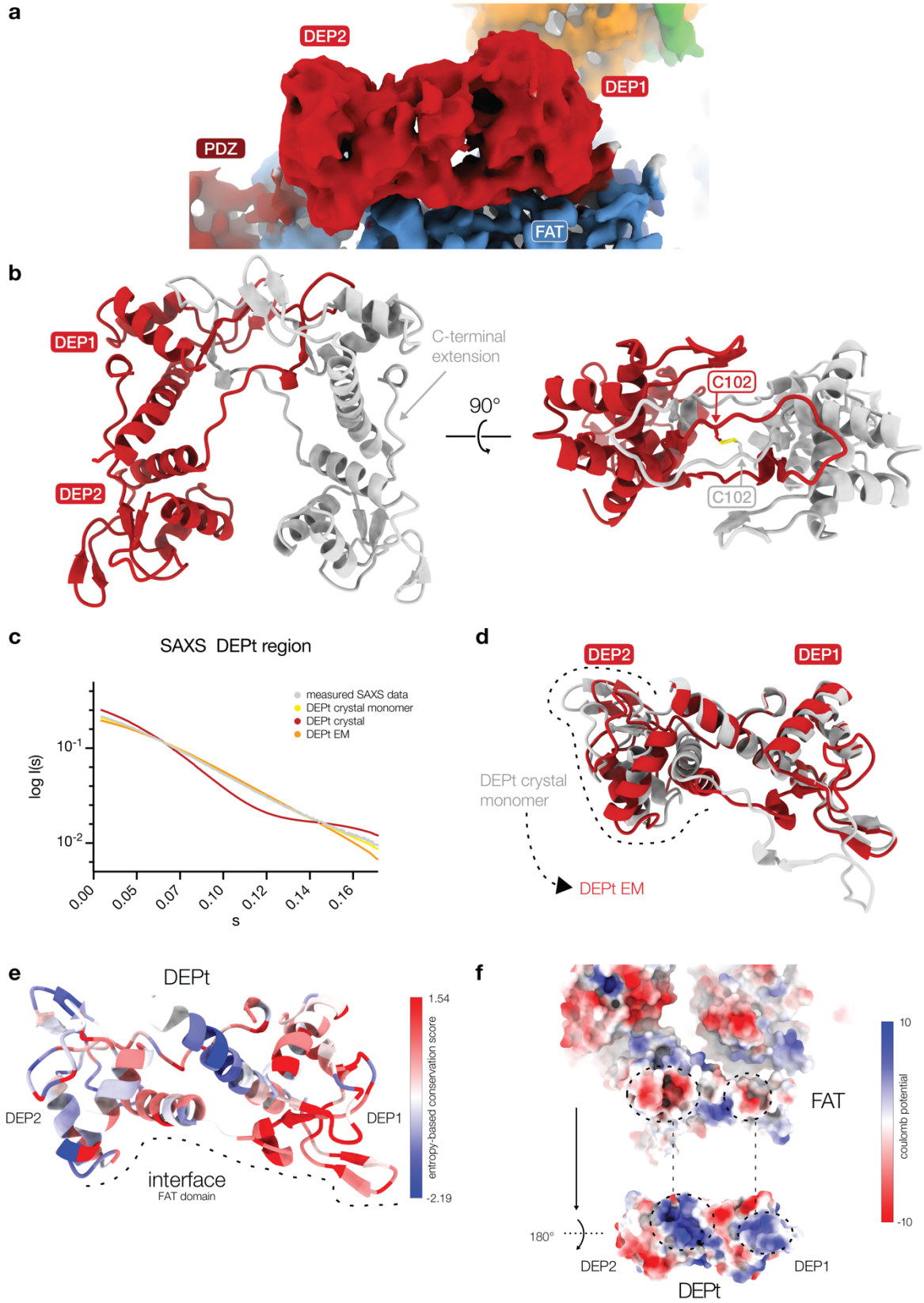
a
DEP2
DEP1
PDZ
FAT
b
DEP1
DEP2
C-terminal
extension
90°
C102
C102
c
SAXS DEPt region
measured SAXS data
DEPt crystal monomer
DEPt crystal
DEPt EM
log I(s)
10-1
10-2
0.00
0.05
0.07
0.10
0.12
0.14
0.16
s
d
DEP2
DEP1
DEPt crystal
monomer
DEPt EM
e
DEPt
DEP2
DEP1
interface
FAT domain
1.54
entropy-based conservation score
-2.19
f
FAT
10
coulomb potential
-10
180°
DEP2
DEP1
DEPt

Figure 2.3 - figure supplement 1: DEPt domains in crystals and associated with mTORC2.
(a) Cryo-EM reconstruction of the DEPt (map 3 (Fig. 2.1-S. 1a)) based on local refinement. The local resolution of 4-6 Å allows to identify secondary structure elements and fold, but not individual amino acid sidechains. **(b)** The DEPt of DEPTOR crystallized as a domain-swapped dimer. The domain-swapped dimer is stabilized by a non-native disulfide bridge between C102 of the protomers. **(c)** SAXS data and fitted curves for three different DEPt models. DEPt crystal monomer c^2:0.59; DEPt crystal dimer c^2:49.27; DEPt EM c^2: 5.88. The DEPt is monomeric in solution in a conformation corresponding to the conformation found in the crystal structure, which is related to the mTOR bound state by a simple domain rotation with minor translation component. **(d)** Superimposition based on the DEP1 of DEPt from the crystal structure and bound to mTOR. The FAT-bound confirmation of DEPt differs from the free form by a 3.6 Å translation and 39° rotation of DEP2 relative to DEP1. **(e)** Sequence conservation of DEPt mapped onto the structure of DEPt. The interface to mTOR is schematically indicated by a dashed line. mTOR interacting residues are highly conserved in DEPt. DEP1 of DEPt, which mainly mediates interaction of DEPt and mTOR, is more conserved than DEP2. **(f)** Complementary surface electrostatic potential is observed for the binding interface between DEPt and the mTOR FAT domain. The two positively charged patches in DEPt were recently described to bind to PA[213].

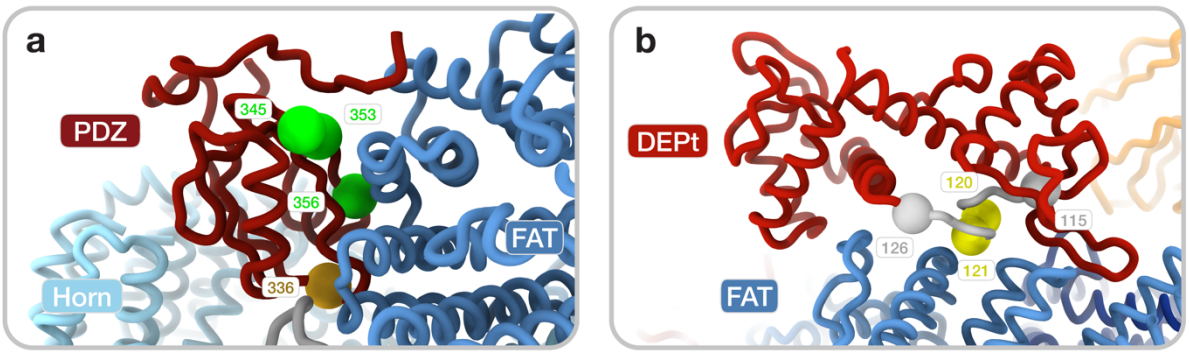

Figure 2.3 - figure supplement 2: Mutations in PDZ and DEPt interface.
(a) Mutants targeting the PDZ-mTOR interface: single mutant D336A (golden) and triple mutant R345A/Q353A/D356A (green). (b) Mutants targeting the DEPt-mTOR interface: double mutant D120A/D121A (yellow) and a linker substitution mutant where 116-125$_{DEPTOR}$ are substituted with a glycine serine linker (GS)5 (grey).

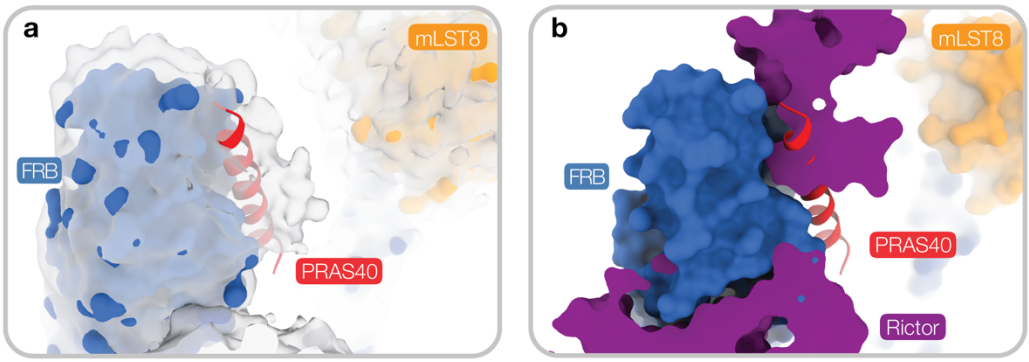

Figure 2.4 - figure supplement 1: Residual density in a substrate recruitment site at the FRB domain for DEPTOR-bound mTOR complex 1.
(a) In cryo-EM reconstructions of DEPTOR-mTORC1, additional density is observed at a site of the FRB, where substrates and PRAS40 (red, 5WBU[53]) bind. Unsharpened map at low contour level is shown to illustrate additional density. (b) This substrate recruitment site on the FRB is occupied in mTORC2 by Rictor. Same view shown as in panel (a).

2.7.2 Supplementary Tables

Supplementary Table 1. Cryo-EM data collection and refinement statistics of DEPTOR-mTORC2 complex

DEPTOR-mTORC2			
	Dimer (map1, Fig. 1-S1a)	Protomer (map2, Fig. 1-S1a)	DEPt-Protomer (map3, Fig. 1-S1a)
Data acquisition and processing			
EMDB accession #	13347	13348	13349
Magnification	65,000x		
Voltage (kV)	300		
Exposure (e^-/ Å^2)	50		
Frames	40		
Defocus range (μM)	-1.0 to -3.0		
Pixel size (Å)	1.058		
Symmetry imposed	C1		
Initial particles	3,031,774		
Final particles	467,078	750,254	132,837
FSC resolution (masked, Å)*	3.41	3.20	3.70
Model refinement			
PDB ID	7PE7	7PE8	7PE9
Model resolution (Å)	3.7/3.3	3.4/3.1	3.9/3.5
FSC threshold	0.50/0.143	0.50/0.143	0.50/0.143
Bond length (Å)	0.002	0.001	0.003
Bond angle (°)	0.440	0.388	0.535
Favored (%)	96.62	96.79	96.33
Allowed (%)	3.33	3.21	3.67
Disallowed (%)	0.05	0	0
Rotamer Outliers (%)	0.98	1.62	1.33
MolProbity score	1.43	1.59	1.68
Clashscore	4.31	4.43	6.16

*gold-standard FSC criterion: 0.143

Supplementary Table 2. Cryo-EM data collection and refinement statistics of DEPTOR-mTORC1 complex

DEPTOR-mTORC1			
	Dimer (map4, Fig. 1-S2a)	Protomer (map5, Fig. 1-S2a)	DEPt-Protomer (map6, Fig. 1-S2a)
Data acquisition and processing			
EMDB accession #	13350	13351	13352
Magnification			
Voltage (kV)	200		
Exposure (e^-/ Å^2)	50		
Frames	40		
Defocus range (μM)	-1.0 to -2.5		
Pixel size (Å)	0.556		
Symmetry imposed	C1		
Initial particles	2,156,602		
Final particles	425,076	850152	211021
FSC resolution (masked, Å)*	4.07	3.67	4.24
Model refinement			
PDB ID	7PEA	7PEB	7PEC
Model resolution (Å)	6.3/4.0	4.3/3.6	4.7/4.1
FSC threshold	0.50/0.143	0.50/0.143	0.50/0.143
Bond length (Å)	0.002	0.002	0.002
Bond angle (°)	0.455	0.505	0.470
Favored (%)	95.26	94.86	95.43
Allowed (%)	4.71	5.09	4.54
Disallowed (%)	0.03	0.06	0.03
Rotamer Outliers (%)	4.24	2.69	4.99
MolProbity score	1.99	1.91	2.13
Clashscore	3.95	4.50	5.32

*gold-standard FSC criterion: 0.143

Supplementary Table 3. X-ray data collection and refinement for DEPTOR DEPt

*Values in parentheses are for highest-resolution shell

	DEPt (PDB 7PED)
X-ray data collection	
Space group	P 1 2_1 1
Cell dimensions	
a, b, c (Å)	50.9, 99.0, 68.2
α, β, γ (°)	90.0, 109.7, 90.0
Resolution (Å)	99.01-1.93 (1.98-1.93) *
R_{merge}	0.036 (1.41)
$CC_{1/2}$	0.999 (0.405)
I/σI	14.2 (0.6)
Completeness (%)	97.4 (87.6)
Redundancy	4.3 (3.1)
Refinement	
Resolution (Å)	49.51-1.93
No. reflections	46,321(4,170)
R_{work}/R_{free}	0.211/0.226
No. atoms	
Protein	3572
Water	204
B-factors	
Protein	63.35
Water	56.97
R.m.s. deviations	
Bond lengths (Å)	0.006
Bond angles (°)	1.04
Ramachandran plot	
favored (%)	98.6
allowed (%)	1.4
outliers (%)	0.0

2.8 Material and methods

2.8.1 Protein expression and purification

Sf21 insect cells (Expression Systems) were grown in HyClone insect cell media (GE Life Sciences) and baculovirus was generated according to Fitzgerald *et al.*[230]. mTORC2 was expressed and purified as previously described with an internal FLAG-tag inserted after D258.[54] Purified mTORC2 was concentrated in gel filtration buffer, supplemented with 5% w/v glycerol and stored at -80°C until further use.

For expression of human mTORC1, Sf21insect cells were infected with baculovirus of as described previously[180]. Cells were harvested 72 hours after infection by centrifugation at 800x*g* for 15 min and stored at –80°C until further use. Cell pellet was lysed in 50 mM bicine (pH 8), 250 mM NaCl, and 5 mM $MgCl_2$ using a dounce homogenizer and the lysate was cleared by ultracentrifugation. Soluble protein was incubated with 7 ml of anti-DYKDDDDK agarose beads (Genscript, Piscataway, USA) for 1 hour at 4°C. The beads were transferred to a 50-ml gravity flow column (Bio-Rad) and washed four times with 200 ml of wash buffer containing 50 mM bicine (pH 8), 150 mM NaCl, and 5 mM $MgCl_2$. Protein was eluted by incubating beads for 60 min with 10 ml of wash buffer supplemented with synthetic DYKDDDDK peptide (0.6 mg/ml) (Genscript, Piscataway, USA). The eluate was combined with three additional elution steps using synthetic DYKDDDDK peptide (0.1 mg/ml) and 5-min incubation time. The eluted protein was concentrated using a 100,000-Da molecular mass cut-off centrifugal concentrator with regenerated cellulose membrane (Amicon) and purified by size exclusion chromatography on a custom Superose 6 Increase 10/600 GL gel filtration column equilibrated with 25 mM bicine (pH 8.0), 200 mM NaCl, 5% Glycerol and 2 mM tris(2-carboxyethyl)phosphine (TCEP). Purified mTORC1 was concentrated in gel filtration buffer and stored at -80°C until further use.

Full-length human WT DEPTOR coding sequence was amplified from pRK5 FLAG human DEPTOR, which was a gift from David Sabatini (Addgene plasmid no 21334)[182], and was cloned into a pAceBAC2 expression vector (Geneva Biotech, Geneva, Switzerland) with an N-terminal His10-Myc-FLAG tag by Gateway cloning. For expression of human WT DEPTOR, Sf21 cells were infected with baculovirus, harvested 72 hours after infection by centrifugation at 800x*g* for 15 min and stored at –80°C until further use. The cell pellet was lysed in lysis buffer (50 mM PIPES (pH 6.8), 500 mM NaCl, 50 mM imidazole, 2 mM $MgCl_2$ and 2mM TCEP) using sonication, and the lysate was cleared by ultracentrifugation. The cleared lysate was loaded onto a 25-ml Ni-column (Genscript High Affinity Ni-charged resin), washed with 10 column volumes (CV) of lysis buffer containing 1mM ATP and eluted with a linear gradient (5CV) to lysis buffer containing

500 mM imidazole. The tag was cleaved overnight using TEV-protease, followed by an orthogonal Ni-column (25 ml, Genscript High Affinity Ni-charged resin) to remove Tag and the tagged TEV-protease from the sample. The protein was subjected to a final gel filtration chromatography step in 20 mM PIPES (pH 6.8), 150mM NaCl, 5% glycerol and 1 mM TCEP. DEPTOR containing fractions were concentrated to 10 mg/ml and stored at -80°C until further use.

DEPt (aa_{DEPTOR}1-230) was cloned into the vector pETG-10A and expressed in *E.coli* BL21DE3 cells. Cells were grown in 2xYT medium at 37°C. At an OD_{600} of 0.8, isopropyl-β-D-thiogalactoside (IPTG) was added to a final concentration of 0.75 mM. The cells were further grown for 4-6h and harvested by centrifugation. Cells were lysed by sonication in 50mM HEPES (pH8), 250mM NaCl, 40mM imidazole,1mM TCEP and the lysate was cleared by ultracentrifugation. The cleared lysate was loaded onto a 5-mL Ni-column (Genscript High Affinity Ni-charged resin), washed with 13CV of lysis buffer and eluted with a linear gradient over 5CV to 50 mM HEPES (pH 8), 150 mM NaCl, 500 mM imidazole and 1mM TCEP. The tag was cleaved overnight using TEV-protease, followed by an orthogonal Ni-column Ni-column (5 ml, Genscript High Affinity Ni-charged resin) to remove Tag and tagged TEV-protease from the sample. The protein was subjected to a final gel filtration chromatography step in 20 mM HEPES (pH 8), 150mM NaCl, 5% glycerol and 1 mM TCEP. DEPt containing fractions were concentrated to 14.9 mg/ml and stored at -80°C until further use.

DNA coding for human WT Rheb (aa_{Rheb} 1-171) (GenBank: D78132) was synthesized by Genscript and cloned into the vector pETG30A coding for a His_6-GST-Tag for expression. *E.coli* SoluBL21 cells were grown in ZY medium at 37°C. At an OD_{600} of 0.65, isopropyl-β-D-thiogalactoside (IPTG) was added to a final concentration of 0.5 mM. The cells were further grown for 8 h and harvested by centrifugation. Cells were lysed using a French Press in 50 mM bicine (pH8), 500 mM NaCl, 5 mM $MgCl_2$ and 5 mM beta-mercaptoethanol (bME) and the lysate was cleared by ultracentrifugation. The cleared lysate was loaded onto a 5 mL His-Trap HP (GE Healthcare), washed 20 CV with lysis buffer supplemented with 20 mM imidazole and eluted with a linear gradient (5 CV) to 50 mM Bicine (pH8), 250 mM NaCl, 500 mM imidazole, 5 mM $MgCl_2$ and 5 mM bME. The tag was cleaved overnight using TEV-protease, followed by an orthogonal Ni-column Ni-column (5 mL His-Trap HP (GE Healthcare)) to remove Tag and tagged TEV-protease from the sample. The protein was subjected to a final gel filtration chromatography step (HiLoad 16/600 Superdex 75 pg, Cytiva) in 10 mM bicine (pH 8), 150mM NaCl, and 1 mM TCEP. Rheb containing fractions were collected, concentrated with a 3,000-Da molecular mass cut-off centrifugal concentrator (Amicon) and supplemented with 5 % w/v glycerol and stored at -80°C until further use.

2.8.2 In vitro mTORC1 activity assays

mTORC1 kinase activity assays were performed in final concentrations of 50 mM Hepes (pH 7.5), 75 mM NaCl, 2.4% Glycerol, 6 mM $MgCl_2$ and 1 mM TCEP. 4E-BP1 was expressed and purified as previously described[144]. For Rheb-activated mTORC1, Rheb was loaded with 2 mM GTPγS (Jena Biosciences) and 5 mM EDTA for 1 hour at room temperature and locked by the addition of $MgCl_2$ to 10 mM final concentration. For the activity assays, 2 nM purified mTORC1 were mixed with 15 µM Deptor (wild-type or mutants), 5 µM Rheb and 320 nM 4E-BP1 as the substrate. Reactions were started by the addition of 1 mM ATP, incubated for 10 min at room temperature and quenched with 5x SDS-sample buffer. Samples were resolved by SDS-PAGE and transferred onto 0.2 µM pore size nitrocellulose membranes via the Trans-Blot Turbo Transfer System (Bio-Rad). Signals were detected by the LI-COR Fc system (LI-COR Biosciences) using the following antibodies: mTOR (1:1000, RRID:AB_2105622), 4E-BP1-p(T37/46) (1:1000, RRID: AB_560835, 4E-BP1 (1:1000, RRID: AB_331692) and IRDye 800CW goat anti-rabbit IgG (1:17.500, RRID: AB_621843). All antibodies were diluted into an equal mix of TBST and LI-COR intercept (TBS) blocking buffer. Statistical analysis was performed by GraphPad Prism (RRID:SCR_002798), using One-way ANOVA.

2.8.3 Crystallization, X-ray data collection and structure determination

The DEPt region (aa_{DEPTOR} 1-230) was crystallized at 4°C using the sitting-drop vapor diffusion method at a protein concentration of 14.9 mg/ml and using a reservoir (12% w/v PEG 3350, 0.2M NaCl) to protein ratio of 1:1 in a total drop volume of 0.4 µl. Crystals were transferred into cryoprotectant (reservoir solution with added ethylene glycol to 20% v/v) and vitrified in liquid nitrogen. Crystallographic data were collected at the Swiss Light Source (Paul Scherrer Institute) beamline X06SA at 100 K using an Eiger16M detector (Dectris). Data were collected at a wavelength of 1.0 Å with an exposure time of 0.1s, a rotation angle of 0.25° for 240° and a detector distance of 299.7977 mm.

Data were processed with DIALS and scaled using aimless(RRID:SCR_015747)[231]. The structure was solved by molecular replacement using the crystal structure of 4F7Z.pdb[232] as search model with the program PHASER(RRID:SCR_014219)[233]. Model building was done with COOT(RRID:SCR_014222)[234] and the structures were refined with PHENIX(RRID:SCR_014224)[235]. MolProbity(RRID:SCR_014226)[236] was used to validate the model. Data and refinement statistics are summarized in Supplementary File 3. The final model

contains two chains with residues 20-230 of DEPTOR, 19 residues at the N-terminus were not resolved, presumably due to flexibility.

2.8.4 SAXS data collection and analysis

SAXS data of purified DEPt in gel filtration buffer at 2-14mg/ml was collected in batch-mode experiments on the B21 beamline at Diamond Light Source (DLS), UK. Solution scattering of the dimeric crystal structure, one monomer of the crystal structure and the DEPt model based on the cryo-EM reconstruction, was evaluated and fitted to the experimental scattering curves using PRIMUS and CRYSOL[237,238]. Fits generated from CrYSOL were plotted using GraphPad Prism version 9.1.0.

2.8.5 Cryo-EM sample preparation and data collection

Freshly thawed mTORC2 aliquots were mixed with freshly thawed DEPTOR aliquots in 1:8 molar ratio and dialysed in 20 mM bicine (pH 7.5), 100 mM NaCl, 5 mM $MgCl_2$, 2 mM TCEP and 0.25% glycerol before preparing grids. For each grid 4 µl of the sample at 1.2 mg/ml were applied to a Quantifoil R2/2 holey carbon copper grid (Quantifoil Micro Tools), which was mounted in a Vitrobot (Thermo Fisher Scientific) whose chamber was set to 4°C and 100% humidity. The grid was immediately blotted with a setting of 2.5 to 4 seconds blotting time and rapidly plunge-frozen in liquid ethane. Data were collected using a Titan Krios (Thermo Fisher Scientific FEI) transmission electron microscope equipped with a K2 Summit direct electron detector (Gatan) using SerialEM(RRID:SCR_017293)[47](Supplementary File 1) in counting mode. During data collection, the defocus was varied between -1 and -3 µm and five exposures were collected per holes. Stacks of frames were collected with a pixel size of 1.058 Å/pixel and a total dose of about 50 electrons/$Å^2$.

Freshly thawed mTORC1 aliquots were mixed with freshly thawed DEPTOR aliquots in 1:12 molar ratio and dialysed in 20 mM bicine (pH 7.5), 100 mM NaCl, 5 mM $MgCl_2$, 2 mM TCEP and 0.25% glycerol before preparing grids. For each grid 4 µl of the sample at 1.4 mg/ml were applied to a Quantifoil R2/2 holey carbon copper grid (Quantifoil Micro Tools), which was mounted in a Vitrobot (Thermo Fisher Scientific) whose chamber was set to 4°C and 100% humidity. The grid was blotted after 10 seconds incubation with a setting of 2.5 to 4 seconds blotting time and rapidly plunge-frozen in liquid ethane.

Two datasets were collected using a Glacios (Thermo Fisher Scientific FEI) transmission electron microscope equipped with a K3 direct electron detector (Gatan) using SerialEM[239]

(Supplementary File 2) in correlated double sampling (CDS) mode. During data collection, the defocus was varied between -1 and -2.5µm. Stacks of frames were collected with a super-resolution pixel size of 0.556 Å/pixel and a total dose of about 50 electrons/Å^2.

2.8.6 Cryo-EM data processing

The DEPTOR-mTORC2 dataset, consisting of 7371 micrographs, was corrected for beam-induced drift using Patch Motion, and the contrast transfer function (CTF) parameters for each micrograph were determined using Patch CTF in cryoSPARC(RRID:SCR_016501)[240]. After curation of micrographs, we selected 6924 micrographs for further processing. Particles were picked with the blob picker function in cryoSPARC and subjected to reference-free 2D classification. 2D-classes showing structural features were used as templates for particle picking using the template picker in cryoSPARC. Iterative 2D-classification was used to sort particles. Particle coordinates were transferred to Relion(RRID:SCR_016274) and particles were extracted from micrographs, which have been previously motion-corrected using Relion[241] own implementation of MotionCor2(RRID:SCR_016499)[242] and the CTF estimated using CTFFIND4.1(RRID:SCR_016732)[243]. An initial 3D-autorefinement yielded a reconstruction at 4.03 Å. Particles were subjected to iterative CTF-refinement and Bayesian particle polishing[244]. Polished particles were imported into cryoSPARC followed by a homogeneous refinement. To prune the dataset, particles were classified by Heterogeneous Refinement in three classes. The most populated class was selected and particles used in a non-uniform homogeneous refinement followed by an local refinement using a global mask yielding a reconstruction at 3.41 Å (map 1; Fig. 2.1-S1a)[245]. By subsequent local refinements focussing on one protomer respectively, we obtained reconstructions at 3.27Å and 3.32 Å. Particles of the global refinement were symmetry-expanded based on the C2 symmetry of mTORC2. A local non-uniform refinement focussed on one protomer yielded a map at 3.16 Å. To reduce heterogeneity, particles were classified without alignment in five classes in Relion. After separate local refinement of these classes in cryoSPARC, four classes were selected. On these particles, signal subtraction of one protomer was performed followed by a local non-uniform refinement focussed on the remaining protomer. A final protomer map at a resolution of 3.2 Å was obtained (map 2; Fig. 2.1-S1a). Due to partial occupancy and high flexibility the DEPt region remained poorly resolved in these reconstructions. Sorting for this region was done by 3D-classification without alignment into 5 classes in Relion using the symmetry-expanded particle stack and a mask for the DEPt region. Only one class showed structural features. Partial signal subtraction of one protomer followed by

focussed local non-uniform refinement yielded a reconstruction at 3.7 Å (map 3; Fig. 2.1-S1a). A processing scheme can be found in Fig. 2.1-S1a.

For the DEPTOR-mTORC1 dataset, micrographs from two data collections were corrected separately for beam-induced drift using patch motion, and the contrast transfer function (CTF) parameters for each micrograph were determined using Patch CTF in cryoSPARC[240]. We selected a total of 8604 movies after manual curation for further processing. Particles were picked with the blob picker function in cryoSPARC and subjected to reference-free 2D classification. 2D-classes showing structural features were used as templates for particle picking using the template picker in cryoSPARC. The particle stack was cleaned by iterative 2D-classification. Extracted particles from both datasets were subjected to an initial non-uniform refinement with an ab-initio reconstruction as starting model. To sort for heterogeneity the particles were sorted into 3 classes using heterogeneous refinement. Particles of the two most populated classes representing a “wide” and “tight” mTORC1 conformation were used in a non-uniform homogeneous refinement followed by an local refinement using a global mask[245]. This yielded a reconstruction of DEPTOR-mTORC1 at 4.07 Å (map 4; Fig. 2.1-S2a). Subsequent non-uniform local refinements focussing on individual protomers resulted in reconstructions at 3.97 Å and 3.99 Å. Symmetry expansion was performed on the particles of the overall refinement utilizing the C2 symmetry of the complex. Using non-uniform local refinement of symmetry-expanded particles focussed on one protomer a final map at 3.67 Å was obtained (map 5; Fig. 2.1-S2a). Sorting for occupancy of the DEPt region was achieved by 3D-variability analysis using 5 principle modes[246]. Particles were classified in 5 clusters based on the principle modes. Non-uniform local refinement of the cluster with highest DEPt occupancy resulted in a reconstruction at 4.24 Å (map 6; Fig. 2.1-S2a). A processing scheme can be found in Fig. 2.1-S2a.

2.8.7 Cryo-EM model building and refinement

One protomer of the cryo-EM structure of mTORC2 (PDB: 6ZWM[54]) was used as initial model and was rigid-body fitted in map 2 (Fig. 2.1-S1a). Minor adjustment of the manual to fit the density were done using COOT[234]. The linker of mTOR, which becomes structured upon DEPTOR binding was identified based on continuous density in maps filtered to lower resolution connecting it to modelled parts of mTOR, but only the better-ordered residues aa_{mTOR} 304-317 were built into full-resolution maps *de novo* using COOT. Initial models and secondary structure definitions for the PDZ domain were generated using trRosetta and Robetta[247] (RRID:SCR_021181, RRID:SCR_018805)(Fig. 2.2-S1a). These initial model were rigid-body fitted into the map and adjusted in COOT to fit the density. The N-terminal PDZ extension and following

linker binding mTOR (aa_{DEPTOR} 325-304) were built *de novo* using COOT, guided by continuous density for this region visualized in softened or low-pass filtered maps with higher disorder reducing side-chain visibility. The structure was finally real-space-refined using phenix.real_space_refine[248]. The resulting structure was rigid-body fitted into map 3 (Fig. 2.1-S1a). One monomer of the DEPt crystal structure was fitted into the extra density. Using the cryo-EM reconstruction and the second monomer of the crystal structure as template the domain-swapped crystal structure was un-swapped *in silico* to obtain a physiologically-relevant DEPt monomer model. Individual domains were fitted to the map and minor adjustment were carried out manually in COOT. The final model was real-space-refined using phenix.real_space_refine.
For model building of DEPTOR-mTORC1, one protomer of pdb:6BCX[53] was used as initial model. Individual proteins were rigid-body fitted into map 5 (Fig. 2.1-S2a), keeping residues with unassigned identity as in the higher resolution 6BCX. The model of the PDZ domain, obtained from the DEPTOR-mTORC2 reconstruction, was rigid-body fitted into the density. The final model was real-space-refined using phenix.real_space_refine. The obtained model was rigid-body fitted into map 6 (Fig. 2.1-S2a). Additionally, the DEPt model, obtained from the respective DEPTOR-mTORC2 reconstruction, was rigid-body fitted into map 6 (Fig. 2.1-S2a) to yield an mTORC1-protomer with PDZ domain and DEPt bound. The final model was real-space-refined using phenix.real_space_refine. To obtain a model for the mTORC1 dimer with PDZ domain bound, two copies of the PDZ-bound protomer were rigid body fitted into map 4 (Fig. 2.1-S2a) followed by real-space-refinement using phenix.real_space_refine. All models were validated using phenix and MolProbity[236].

2.8.8 Structural analysis and figure generation

Properties of individual protein interfaces between DEPTOR and mTOR were analyzed using PISA(RRID:SCR_015749)[249].To analyze sequence conservation of DEPTOR, we aligned 136 full-length DEPTOR sequences with Clustal Omega(RRID:SCR_001591)[250]. The final alignment was used as input for AL2CO[251] to map conservation onto the DEPTOR structure using ChimeraX(RRID:SCR_015872)[252]. To analyze motion of the DEP2 of DEPt induced by binding to mTOR, the DEPt crystal and cryo-EM structure were superimposed onto DEP1. Rotation and translation of DEP2 was analyzed using the PSICO extension of Pymol(RRID:SCR_000305)[253]. All density and structure representations, and the movies were generated using UCSF ChimeraX[252]. Local resolution was estimated using cryoSPARCv3 (Structura Biotechnology Inc.).

2.9 Acknowledgments

We thank T Sharpe at the Biophysics facility and A Schmidt at the Proteomics Core Facility of Biozentrum, the Biozentrum Bio-EM lab, and the sciCORE scientific computing facility, all of University of Basel. We acknowledge the staff of beamlines X06DA and X06SA at the Paul Scherrer Institute, Villigen, Switzerland, for support with crystallographic data collection. We would like to thank DLS for beamtime and the staff of beamline B21 for SAXS data collection. MW and FM were supported by a Fellowship for Excellence from the Biozentrum Basel International PhD program. KB is supported by a Boehringer Ingelheim Fonds PhD Fellowship and has received support by a Biozentrum PhD Fellowship. LMC and MNH were supported by H2020 (ITN Healthage, grant agreement number 812830). This work was supported by the Swiss National Science Foundation (SNSF) via the National Center of Excellence in RNA and Disease (141735, 182880) to MNH and SNSF project and R'Equip funding to TM (179323, 177084).

2.10 Author contributions

MW, TM, KB and LMC designed experiments. MW expressed and purified proteins, prepared samples for cryo-EM, carried out data processing, structure modelling and analyzed data. KB expressed and purified proteins, performed activity assays and analyzed data. FM expressed and purified proteins. ES established the mTORC2 purification procedure. SI cloned mTORC2, contributed to data analysis and manuscript preparation. MW and TM wrote the original draft of the manuscript. MW, KB, FM, SI, LMC, ES, MNH and TM participated in the writing of the manuscript.

2.11 Data availability

Structure factors and model coordinates for the DEPt X-ray crystal structure is deposited to the RCSB protein data bank with PDB ID 7PED. Cryo-EM reconstructions and model coordinates are deposited to the EMDB and PDB for the mTORC2:DEPTOR dimer (EMDB ID: EMD-13347, PDB ID: 7PE7), mTORC2:DEPTOR protomer (EMDB ID: EMD-13348, PDB ID: 7PE8), mTORC2:DEPTOR protomer:DEPt (EMDB ID: EMD-13349, PDB ID: 7PE9), mTORC1:DEPTOR dimer (EMDB ID: EMD-13350, PDB ID: 7PEA), mTORC1:DEPTOR protomer(EMDB ID: EMD-13351, PDB ID: 7PEB), mTORC1:DEPTOR protomer:DEPt (EMDB ID: EMD-13352, PDB ID: 7PEC).

3 mTOR substrate phosphorylation: mechanisms, motifs, functions, and structures

Reproduced from:

mTOR substrate phosphorylation: mechanisms, motifs, functions, and structures
Stefania Battaglioni[1], Don Benjamin[1], Matthias Wälchli, Timm Maier and Michael N. Hall

[1]Authors contributed equally

Review submitted to Cell

3.1 Abstract

TOR (Target of Rapamycin), discovered 30 years ago, is a highly conserved serine/threonine protein kinase that plays a central role in regulating cell growth and metabolism. It is activated by nutrients, growth factors, and cellular energy. TOR forms two structurally and functionally distinct complexes, TORC1 and TORC2. TOR signaling activates cell growth, defined as an increase in biomass, by stimulating anabolic metabolism while inhibiting catabolic processes. Despite the large number of reviews on TOR, none focuses specifically on TOR substrates. With an emphasis on mammalian TOR (mTOR), we comprehensively reviewed the literature and identified all reported direct substrates. We discuss how mTORC1 and mTORC2, despite having a common catalytic subunit, phosphorylate distinct substrates. We conclude that the two complexes recruit different substrates to phosphorylate a common, minimal motif.

3.2 Introduction

Rapamycin is a secondary metabolite produced by a bacterium originally isolated from a soil sample collected on Easter Island (Rapa Nui) in 1965. Initially identified as an antifungal agent, it was later found to possess immunosuppressive and anti-cancer activity [6,7]. The resulting interest in rapamycin led to the hunt for its cellular target. The Target of Rapamycin (TOR) was first described in yeast [16-19] and then in mammalian cells [20-23]. A second milestone in the field was the realization in the late 1990s that TOR is a central controller of cell growth [254]. A third milestone was the discovery in the early 2000s that TOR is found in two functionally distinct complexes which, like TOR itself, are conserved from yeast to human [66,71,72]. Over the years, dysregulation of mTOR has been linked to major diseases such as diabetes and cancer. Given its importance in fundamental biology and medicine, the study of mTOR has become a large and complex research field.

3.3 Main text

mTORC1 and mTORC2

mTOR is a member of the PIKK (phosphatidylinositol (PI) kinase-related kinase) family of atypical protein kinases [255]. Despite common ancestry with PI kinases, mTOR and other PIKKs have no known lipid kinase activity but rather serine/threonine protein kinase activity. The N-terminus of mTOR contains multiple HEAT repeats and the middle section of mTOR is characterized by a FAT (FRAP/ATM/TRRAP) domain followed by the FRB (FKBP-rapamycin binding) domain. The C-terminus contains the kinase domain (Figure 3.1).

mTOR nucleates two functionally distinct complexes, mTOR complex 1 (mTORC1) and mTORC2 [66,256,257]. mTORC1 is composed of mTOR, mLST8 (mammalian lethal with SEC13 protein 8) and RAPTOR (regulatory-associated protein of mTOR) [66,71,72]. mTORC1 is a dimer of mTOR-mLST8-RAPTOR heterotrimers [53,180,181,258]. RAPTOR is the defining subunit of mTORC1. It is responsible for recognizing at least some mTORC1 substrates and for targeting mTORC1 to the surface of the lysosome [258].

mTORC2 is a dimer of heterotetramers composed of mTOR, mLST8, RICTOR (rapamycin-insensitive companion of mTOR) and mSIN1 (mammalian stress-activated map kinase-interacting protein 1) [54,66,79,81,259]. RICTOR and mSIN1 are unique to and thus the defining subunits of mTORC2. mSIN1, via its N-terminus, is embedded in RICTOR and then folds around mLST8.

Flexible middle and C-terminal regions of mSIN1 have not been resolved within the overall mTORC2 structure. A CRIM (conserved region in the middle) domain of mSIN1 is important for mTORC2 substrate recruitment [54,223]. An mSIN1 C-terminal PH domain is required for mTORC2 localization to membranes [260,261]. The function of RICTOR, other than anchoring mSIN1 within mTORC2, is unknown.

mLST8 is common to both complexes, binding close to the kinase site in mTOR. mLST8, like RICTOR, knockout embryos die at day 10.5 whereas mTOR or RAPTOR knockout embryos die at day 3.5, suggesting that mLST8 may not be critical for mTORC1 function [69,70]. Indeed, mLST8 knockout MEFs retain the ability to phosphorylate mTORC1 substrates S6K1 (ribosomal protein S6 kinase 1) and 4E-BP1 (eukaryotic translation initiation factor 4E-binding protein 1) but not mTORC2 substrates AKT (also known as PKB) and PKCα (protein kinase C α) [69]. mLST8 stabilizes mTORC2 via direct interactions with mSIN1 and mTOR [68-70]. Furthermore, a recent cryo-EM structure of mTORC2 revealed that mLST8 interacts with mSIN1 to position the mSIN1 substrate interacting CRIM domain [54]. mLST8 does not appear to have an equivalent function in mTORC1.

Upstream regulation

mTORC1. mTORC1 integrates nutrients, growth factors, and cellular energy inputs to promote anabolism and cell growth while repressing catabolism. Nutrient availability is sensed by mTORC1 through the small GTPases RAG-A, -B, -C and -D. RAGs form heterodimers, either RAG-A or -B with RAG-C or -D. The active configuration of the RAGs is GTP-bound RAG-A or -B (RAG-A/BGTP) and GDP-bound RAG-C or- D (RAG-C/DGDP) [229,262]. This configuration recruits mTORC1 to the lysosome where mTORC1 encounters and is activated by the small GTPase RHEB (Ras homolog enriched in brain). The RAGs bind Ragulator, a pentameric complex composed of the five LAMTOR proteins (LAMTOR 1-5), on the surface of the lysosome [89]. RAG-C/D is activated by the folliculin complex, composed of FLCN and FNIP1 or FNIP2, that has GTPase-activating protein (GAP) activity [263,264]. RAG-A/B is activated upon inhibition of its direct upstream inhibitor GATOR1 (GTPase activating proteins toward RAGs), a complex of three proteins [92]. GATOR1 is inhibited by GATOR2, a complex of five proteins, which is negatively controlled by the amino acid sensors SESTRIN2 and CASTOR1 [92]. In starved conditions, SESTRIN2 and CASTOR1 bind and thereby prevent GATOR2 from inhibiting GATOR1. Upon arginine stimulation, arginine binds CASTOR1. CASTOR1 then releases GATOR2 to inhibit GATOR1, thus permitting RAG-A/B activation (by an unknown mechanism) and subsequent mTORC1 recruitment to the lysosome [101-104]. SESTRIN2 performs a function similar to CASTOR1 but in response to leucine [99,265]. Recently, a new regulatory component, SAR1B, was reported to

work in concert with SESTRIN2 in leucine sensing and GATOR2 regulation [266]. SESTRIN binds leucine with low affinity whereas SAR1B binds with high affinity and thus requires a lower leucine concentration for release of GATOR2. As SAR1B and SESTRIN2 bind distinct sites on GATOR2, there is a possible interplay between SAR1B and SESTRIN2 in modulating leucine-dependent mTORC1 activity [100]. Another interacting partner of GATOR1 is KICSTOR, a complex of four proteins. KICSTOR anchors GATOR1 to the lysosome to ultimately inhibit RAG-A/B and mTORC1 [93,94]. Furthermore, SAMTOR, an S-adenosylmethionine (SAM) sensor upstream of mTORC1, indirectly senses methionine availability via SAM. High levels of methionine lead to increased SAM levels which in turn lead to dissociation of SAMTOR-GATOR1, and thereby GATOR1 inactivation and mTORC1 activation [106]. Finally, alpha-ketoglutarate produced by glutaminolysis also regulates RAG activity, by promoting RAG-B GTP loading and consequently promoting mTORC1 localization to the lysosome [116].

Growth factors activate mTORC1 via the PI3K-AKT-TSC axis. Receptor tyrosine kinases are stimulated by insulin or other growth factors on the cell surface, leading to PI3K (phosphatidylinositol-3-OH kinase) activation. PI3K converts PIP2 (phosphatidylinositol-4,5-bisphosphate) to PIP3 (phosphatidylinositol-3,4,5-triphosphate). PDK1 (phosphoinositide-dependent kinase 1) binds PIP3 in the plasma membrane where it activates AKT, which itself binds PIP3, by phosphorylating AKT-Thr308. Active AKT phosphorylates and inhibits the TSC complex, formed by Tuberous Sclerosis Complex 1 (TSC1), TSC2 and TBC1D7 proteins [125,126,267]. The TSC complex is a GAP for the small GTPase RHEB. RHEB is located on the lysosome and in its active GTP-bound state binds and activates mTORC1 by inducing a conformational change [53,258]. Therefore, PI3K-AKT dependent TSC complex inhibition activates mTORC1 by locking RHEB in its active GTP bound state [262,268,269].

Energy stress inhibits mTORC1 via AMPK (AMP activated protein kinase). Low ATP production causes a rise in the intracellular AMP:ATP and ADP:ATP ratios which lead to allosteric activation of AMPK. AMPK in turn restores ATP production by promoting glucose uptake and increasing β-oxidation [270]. AMPK also activates autophagy by phosphorylating ULK1 (unc-51-like kinase), a component of the autophagic complex that is negatively regulated by mTORC1. Thus, AMPK and mTORC1 are mutually antagonistic. AMPK inhibits mTORC1 upon energy stress in two separate ways. First, it phosphorylates TSC2 at Thr1271 and Ser1387 to activate TSC complex GAP activity toward RHEB, thereby preventing mTORC1 activation [132]. Second, it directly phosphorylates RAPTOR on Ser722 and Ser792 to inhibit mTORC1 [133,271,272]. Conversely, mTORC1 directly phosphorylates AMPK catalytic subunit α1 (Ser347) or αα2 (Ser345 and Ser377) which diminishes Thr172 phosphorylation in the AMPK activation loop, thereby limiting AMPK activity [273,274]. Interestingly, AMPK phosphorylates mTOR (Ser1261) specifically in

mTORC2 and RICTOR on multiple sites to increase mTORC2 activity independent of the mTORC1 negative feedback loop (see section below). It has been suggested that the purpose of AMPK-dependent mTORC2 activation is to activate anti-apoptotic AKT signaling to promote cell survival during acute energetic stress [275].

mTORC2. mTORC2 is activated by growth factors via PI3K. The mTORC2 core component mSIN1 contains a phosphoinositide-binding PH domain that also binds mTOR to autoinhibit mTORC2. Upon activation of PI3K, the mSIN1 PH domain binds newly generated PIP3, thereby releasing mTOR and allowing activation of mTORC2 [261]. The PIP3-bound PH domain also serves to recruit mTORC2 to the plasma membrane where it can phosphorylate membrane-bound substrates such as AKT. PI3K also promotes association of mTORC2 with the ribosome, which is required for mTORC2 activation [276]. Once activated, mTORC2 phosphorylates AKT on Ser473 to fully activate AKT [277] (see below for other mTORC2 substrates).

mTORC2 activity is also regulated via a negative feedback loop from mTORC1. The mTORC1 substrates S6K and GRB10 (growth factor bound-receptor protein 10) downregulate PI3K signaling by inhibiting the insulin receptor and IRS1 [278-280], thereby dampening mTORC2 activity. S6K also phosphorylates RICTOR and mSIN1 on Thr1135 and Thr86/Ser389, respectively, to destabilize mTORC2 [281-283].

The cellular localization of mTORC2 is more diverse than that of mTORC1. mTORC2 has been reported to be associated with the plasma membrane, ribosomes, mitochondria, Golgi, endosomes, ER and MAM (mitochondria-associated ER membrane) [170]. How mTORC2 is activated at these different sites is poorly understood. It is also unclear if there are functionally insulated pools of mTORC2.

mTOR inhibition

Rapamycin. mTOR is inhibited by rapamycin and so-called rapalogs. Rapamycin forms a complex with the small endogenous protein FKBP (FK506-binding protein) and this complex then binds and inhibits mTOR. FKBP-rapamycin binds the FRB domain in mTOR adjacent to the catalytic cleft and thereby sterically hinders access of substrates to the catalytic site [179,180]. Rapamycin alone binds mTOR but does not have sufficient bulk to block access to the catalytic site. Furthermore, while mTORC1 is acutely sensitive to rapamycin, mTORC2 is insensitive. RICTOR partially overlays the FRB domain of mTOR (Figure 3.1 and Figure 3.2) [54,180]. Thus, RICTOR masks the mTOR FRB domain in mTORC2, preventing FKBP-rapamycin binding [54]. However, long-term rapamycin treatment inhibits mTORC2 indirectly. FKBP-rapamycin

presumably binds free, nascent mTOR protein to prevent mTORC2 assembly, thereby inhibiting mTORC2 in addition to mTORC1 [84].

Rapalogs are rapamycin derivatives with minor modifications. Their mode of action is identical to rapamycin but with improved drug-like properties. They are clinically prescribed for immunosuppression and to counter restenosis and cancer. ATP-competitive mTOR active site inhibitors have been developed that effectively inhibit both mTORC1 and mTORC2. However, no active site inhibitor has been approved for clinical use to date [225].

DEPTOR. mTORC1 and mTORC2 have a common endogenous inhibitor, DEPTOR (DEP domain-containing mTOR-interacting protein). DEPTOR directly binds and weakly inhibits mTOR in both complexes [182,183]. Exactly how DEPTOR partially inhibits mTOR activity has long been a topic of discussion. Two recent studies revealed that DEPTOR regulates mTOR allosterically [228,284]. The C-terminal PDZ domain of DEPTOR binds mTOR with high affinity and mildly stimulates mTOR activity. The PDZ domain serves as a high-affinity anchor for the lower affinity association of the N-terminal DEPt (DEP domain tandem) domain of DEPTOR which then hinders mTOR in adapting an active conformation. Furthermore, mTOR directly phosphorylates DEPTOR on Ser293, Thr295 and Ser299, leading to its degradation by the proteasome [182,188,189]. At high concentrations, DEPTOR binds in a separate, substrate-like mode to the mTOR FRB domain via the linker region between the PDZ and DEPt domains [228,284]. Interestingly, DEPTOR deletion increases only mTORC1 activity while DEPTOR overexpression promotes mTORC2 activity. This paradoxical effect of DEPTOR, an mTOR inhibitor, on mTORC2 is probably due to inhibition of the mTORC1 negative feedback loop (see above) [183]. DEPTOR's ability to both promote and decrease mTOR activity provides a good example of how complex and contextual mTOR regulation can be.

PRAS40. mTORC1 has a specific endogenous inhibitor, PRAS40 (proline-rich Akt substrate of 40 kDa). PRAS40 contains a TOS motif, a five amino acid sequence present in several mTORC1 substrates (see below and Table 1) [75]. RAPTOR binds the TOS motif to recruit substrates to mTORC1. PRAS40 competes with other substrates for mTORC1 binding and thereby inhibits downstream signalling. AKT phosphorylates PRAS40 on Thr246, which induces its release from mTORC1 and cytoplasmic sequestration by 14-3-3 proteins [285]. mTORC1 also phosphorylates PRAS40, on Ser183, Ser212 and Ser221, to induce PRAS40 release from mTORC1 [286,287].

Well characterized mTORC1 substrates: S6K, 4E-BP, ULK1 and TFEB

The best described mTOR substrates are S6K and 4E-BP. They are widely used as readouts of mTORC1 activity, due to the availability of antibodies that specifically recognize the phosphorylated forms of these two proteins.

S6K. There are two S6Ks in mammals, encoded by separate genes, of which S6K1 is the best characterized. S6K belongs to the AGC kinase family. AGC kinase family members are frequently mTOR, in particular mTORC2, substrates. S6K is the only AGC kinase that is an mTORC1 substrate. S6K1 was originally identified as the kinase for ribosomal protein S6, but is now known to have many more substrates, involved in cell growth, transcription, translation and cell survival [288,289]. It is phosphorylated and activated by mTORC1 and PDK1 (Figure 3.1). mTORC1 phosphorylates Thr389 in the hydrophobic motif (HM) of the linker region in S6K. PDK1 phosphorylates Ser229 in the T-loop of the S6K kinase domain [141,145]. Phosphorylation of both sites is necessary for full S6K1 activation, as mutation at either site abolishes S6K1 activity [146,290-292]. Furthermore, S6K1 has an autoinhibitory C-terminus which is released, upon mitogen stimulation, by phosphorylation of Ser411, Ser418, Ser421 and Ser424 [145,293,294]. Release of the autoinhibitory domain relaxes S6K structure, allowing phosphorylation by mTORC1 and PDK1. mTORC1 also phosphorylates Ser371 in the S6K turn motif (TM). This phosphorylation is also essential for S6K1 activity, however, few experiments have been conducted to elucidate its specific function [295]. S6K, like 4E-BP, possesses a TOS motif that is necessary for recognition and phosphorylation by mTORC1. Phosphorylation of other AGC kinase family members by mTORC2 is discussed below.

4E-BP. There are three isoforms of 4E-BP in mammals, all similarly regulated by mTORC1 [141,296-298]. In its unphosphorylated state, 4E-BP binds and inhibits eIF4E to prevent translation initiation [299-301]. 4E-BP is phosphorylated by mTORC1 sequentially, first on Thr37/Thr46 and then on Ser65/Thr70 (Figure 3.1) [142,302-304]. Phosphorylation of Thr37/Thr46 reduces the 4E-BP-eIF4E binding affinity 100-fold. The subsequent phosphorylation of Ser65/Thr70 reduces the affinity an additional 40-fold. This releases 4E-BP, allowing eIF4E to bind eIF4G and initiate translation [304-306]. A recent publication elucidated how mTORC1 recognizes 4E-BP and phosphorylates it in an hierarchical manner [144]. mTORC1, via RAPTOR, binds TOS and RAIP motifs in 4E-BP. The RAIP (Arg-Ala-Ile-Pro) motif is found only in 4E-BP [74]. The binding of these motifs by RAPTOR orients the phosphorylation sites in 4E-BP toward the mTORC1 active site. This occurs even when 4E-BP is bound to eIF4E. eIF4E covers the Ser65/Thr70 sites, preventing their phosphorylation in the absence of prior phosphorylation of Thr37/Thr46 [144]. Interestingly, phosphorylation of

Thr37/Thr46 is rapamycin-insensitive while phosphorylation of Ser65/Thr70 is rapamycin-sensitive [304]. Thr37/Thr46 have access to the mTORC1 active site despite FKBP-rapamycin being bound to the FRB domain in mTORC1. However, phosphorylation of Thr37/Thr46 induces a conformational change in otherwise intrinsically disordered 4E-BP that impedes the interaction of Ser65/Thr70 with the catalytic site in rapamycin-inhibited mTORC1 [144].

ULK1. ULK1 forms a complex with ATG13 and FIP200 to initiate autophagy. This step is tightly controlled by the opposing kinases mTORC1 and AMPK. In nutrient rich conditions, mTORC1 interacts with the ULK complex and phosphorylates ULK1 on Ser757 and Ser638, and ATG13 on Ser259, to inhibit the complex and consequently block autophagy (Figure 3.1) [163,307,308]. Under starvation conditions, however, AMPK activates autophagy by concomitantly inhibiting mTORC1 and activating ULK1 and ATG13 [309]. Activated ULK1 also promotes autophagy by inhibiting mTORC1, via phosphorylation of RAPTOR on multiple sites (including the Ser792 site that is phosphorylated by AMPK) which hinders substrate interaction with RAPTOR [310].

TFEB. TFEB (transcription factor EB) and the less well characterized TFE3 are homologous helix-loop-helix leucine zipper transcriptional factors that regulate genes involved in lysosome biogenesis, autophagy and lipid metabolism[311-313]. TFEB and TFE3 translocate into the nucleus upon starvation to activate target genes. Upon nutrient replete conditions, they are phosphorylated by mTORC1 and consequently retained in the cytoplasm by 14-3-3 proteins[164,314-316]. Neither TFEB nor TFE3 contains a TOS motif. They appear to be recruited to mTORC1 via interaction with GDP-bound RAG-C/D (Figure 3.1)[317,318]. mTORC1 phosphorylates TFEB at Ser122, Ser142 and Ser211. Ser211 phosphorylation mediates 14-3-3 binding and cytoplasmic sequestration. The corresponding site in TFE3 (Ser321) is also phosphorylated by mTORC1 with similar results[316]. Mutation of TFEB Ser142 or Ser211 to alanine causes constitutive nuclear localization of the transcription factor[319]. Moreover, in addition to controlling TFEB localization, Ser142 and Ser211 phosphorylation induces STUB1-mediated TFEB ubiquitination and degradation[320].

Well characterized mTORC2 substrates: AKT, PKC and SGK

All well characterized mTORC2 substrates, AKT, PKC (in its various isoforms), and SGK (serum and glucocorticoid induced kinases), belong to the AGC kinase family. They have similar domain structures characterized by an N-terminal regulatory domain and a C-terminal catalytic region consisting of the kinase domain and the C-tail. The key phosphorylation sites in AKT, PKC and SGK are in the so-called T-loop (or activation loop) in the kinase domain, and the turn motif (TM)

and hydrophobic motif (HM) in the C-tail (Figure 3.1)[321]. Phosphorylation of at least the T-loop and HM sites is important for full activation of the kinases. The order of phosphorylation is likely similar in all three cases, initial phosphorylation of the T-loop by PDK1 in response to upstream stimulation by PI3K followed by mTORC2 (which is also activated by PI3K generated PIP3) phosphorylation of HM (see below for discussion of TM). However, it should be noted that in the absence of PDK1 and thus T-loop phosphorylation, mTORC2 can still phosphorylate the HM in AKT [322]. Furthermore, unlike the other AGC kinases, AKT also contains an N-terminal PH domain that is inhibitory in the absence of PIP3. Thus, PIP3 dependent membrane localization is also a prerequisite for T-loop (Thr308) and HM (Ser473) phosphorylation in AKT[323-326].

TM phosphorylation is notably different from T-loop and HM phosphorylation. In AKT and PKCα, the TM site (Ser450 and Thr638, respectively) is co-translationally phosphorylated by mTORC2. This phosphorylation is constitutive, independent of upstream inputs and is required for stability of the kinase[172,327-330]. Whether this mode of TM phosphorylation also applies to other AGC kinases remains to be demonstrated. The consequence of phosphorylation of the three sites also varies among the different kinases. In AKT and PKC, phosphorylation of the T-loop and HM determines kinase activity while TM phosphorylation determines stability of the protein[327]. In AKT, T-loop phosphorylation is required for catalytical activity, while HM phosphorylation is required to obtain maximal AKT activity[324,331]. There is less information on the role of SGK phosphorylation, although, similar to the other AGC kinases, SGK is phosphorylated at its T-loop (Thr256) by PDK1 and at its HM (Ser422) by mTORC2[332,333]. The SGK TM kinase is yet to be identified, but TM phosphorylation is growth factor sensitive and is required for full kinase activity[334]. Finally, Ser477 and Thr479 at the extreme C-terminus of AKT are phosphorylated by mTORC2 or Cdk2, depending on the context, to increase AKT activity[335].

Recently, a new model has been proposed challenging the conventional view of HM phosphorylation in AGC kinases[336]. Baffi et al. identified an evolutionarily conserved motif, F-X-X-X-F-T (F = phenylalanine, X = any amino acid, T = phospho-acceptor threonine), termed the TOR interaction motif (TIM). TIM is N-terminal to TM and, at least in AKT1 and PKC β II, is phosphorylated by mTORC2. Threonine to alanine mutation of the phosphorylation site in both TIM and TM abolishes PKC β II kinase activity, whereas mutation of the phosphorylation site only in TIM is sufficient to abolish AKT activity. Contrary to conventional views, Baffi et al. propose that HM phosphorylation in AKT1 and PKC β II (and by implication in other AGC kinases) is not by mTORC2 but rather is due to AKT and PKC β II autophosphorylation. In this model, mTORC2 phosphorylates TIM which in turn promotes T-loop phosphorylation by PDK1 and then autophosphorylation of the HM by AKT1 and PKC β II. This new model has important implications

for mechanistic studies of mTORC2 as most of the known mTORC2 substrates are AGC kinases. However, this model also raises several questions. First, TIM is also required for binding the mSIN1 CRIM domain during substrate presentation to mTORC2. In light of current structural information, it is difficult to understand how TIM can be phosphorylated by mTORC2 while remaining bound to mSIN1. Second, TIM is part of an alpha-helix which should not fit into the mTOR catalytic site. Third, the T-loop can still be phosphorylated by PDK1 in mTORC2 deficient cells and AKT HM can still be phosphorylated in PDK1-/- cells, suggesting that T-loop and HM phosphorylation are independent rather than sequential events[82,322,329]. Nonetheless, this is an interesting new development in the field that should spur further studies on mTORC2 phosphorylation of AGC kinases.

A comprehensive survey of all mTORC1 and mTORC2 substrates

A comprehensive survey of the mTOR literature, for this review, has revealed that there are numerous reports of putative mTOR substrates. Most studies were performed in cells treated with mTOR inhibitors and thus do not distinguish direct versus indirect phosphorylation. Additionally, many of the studies have not been followed up and thus lack independent confirmation. Furthermore, the actual phosphorylation site in many cases remains unknown. We considered only those reports where there is experimental evidence for direct phosphorylation by mTOR and the phosphorylation site was identified, at least tentatively. One exception was to include AGC kinases with known phosphorylation motifs as mTORC2 substrates, although not all have indeed been experimentally verified as substrates. We omitted datasets from global phosphoproteomic studies in which phosphorylation status correlated with mTOR inhibition or activation, as sites identified in such studies require further validation as bona fide mTOR targets. Adhering to these criteria, we found 56 and 25 mTORC1 and mTORC2 substrates, respectively, including the well characterized substrates discussed above (Tables 3.1 and 3.2). These substrates contain, in total, 104 and 48 phosphorylation sites for mTORC1 and mTORC2, respectively. Interestingly, p53 was shown to be phosphorylated by both mTOR complexes, on the same residue (Ser15). No other substrate is common to both complexes.

mTORC1. Proteins phosphorylated by mTORC1 are listed in Table 1. There is a marked preference for serine (90 sites) over threonine (14 sites) as the phospho-acceptor in mTORC1 substrates. This is well above the relative abundance of serine and threonine residues in the human proteome (~8% and ~6%, respectively). The vast majority of substrates lack a TOS, RAIP or any other discernible recognition motif (see below). Substrates lacking a known recognition

motif may bind mTORC1 in an idiosyncratic fashion. Resolving such motif-less interactions may require structure determination and docking simulations.

Grouped according to function, there appears to be a clustering of substrates in translation, autophagy and transcription (Figure 3.2). Translational regulation via 4E-BP is one of the earliest described roles of mTOR signaling. Direct mTORC1 phosphorylation of other translation factors or regulators (e.g., eIF2β, eIF4E, eEF2K, and S6K) may be built-in functional redundancy to ensure failure-proof regulation of a central function of mTOR signaling. Alternatively, not incompatible with the previous possibility, the apparent redundancy could be multiple layers of mTOR regulation to fine-tune translation. A similar line of reasoning can be applied to the various autophagy factors (e.g., AMBRA1, ATG13, ATG14, DAP1, NRBF2, PACER, TRPML1, ULK1 and WIPI2) that are direct mTORC1 targets. For these autophagy factors, the consequence of phosphorylation by mTORC1 is consistently in the direction of suppressing autophagy. The sum total of their individual contributions may be to strengthen the final signaling output. The reader is referred to other reviews[309,337,338] for a more in-depth discussion of the relationship between mTORC1 and autophagy.

mTORC1 also phosphorylates and regulates components of signaling (e.g., AMPK, IRS1, GRB10) and metabolic pathways (e.g., LIPIN1, CRTC2). The direct, mutual inhibitory phosphorylation of AMPK and mTORC1 is discussed above. A striking observation is the number of substrates involved in mTOR signaling itself, including core complex component RAPTOR. In general, mTOR signaling is characterized by feedback loops and stringent upstream regulation to prevent inappropriate activation. Phosphorylation of signaling pathway components may be a built-in control system to ensure appropriate signaling. That these substrates are direct phosphorylation targets may satisfy a need for rapid regulation to make immediate changes in signaling output.

mTORC2. Proteins phosphorylated by mTORC2 are listed in Table 2. mTORC2 has fewer identified substrates than mTORC1. Most validated mTORC2 targets belong to the AGC kinase family (e.g., AKT, PKC and SGK). The non-AGC kinase substrates listed in Table 2 do not easily fall into functional categories. Of interest is mTOR autophosphorylation at Ser2481 in mTORC2[339,340]. This autophosphorylation is conserved in vertebrates but its significance is unknown. We note that there is also evidence that this site is autophosphorylated in mTORC1[341]. AMOTL2, MST1 and YAP belong to the Hippo pathway controlling organ size. The presence of three Hippo components among the handful of described mTORC2 substrates is highly suggestive of cross-talk between the pathways. The ratio of serine (25 sites) to threonine (19 sites) phospho-acceptor residues is lower for mTORC2 compared to mTORC1. However, this

lower ratio for mTORC2 sites is distorted due to the number of AGC kinases that contain a conserved threonine at TIM and TM. Considering only the non-AGC kinase substrates of mTORC2, there are 14 serines and no threonines as phospho-acceptors, resulting in a similar serine:threonine ratio for the two complexes. Finally, IGF1R and INS-R are each reported to be phosphorylated on two tyrosine residues [342]. The sequence immediately surrounding the phospho-tyrosines are highly conserved and identical in both proteins. While interesting, the claim that mTOR has an additional tyrosine kinase activity requires confirmation.

mTOR target phosphorylation motif: S/T-P

As described above, we found evidence of 104 and 48 target phosphorylation sites in 56 mTORC1 and 25 mTORC2 substrates, respectively (Table 3.1 and 3.2). Based on these in vivo substrates, we generated a common consensus phosphorylation motif for mTORC1 and mTORC2 (Figure 3.3A). We note that we did not detect an mTORC1- or mTORC2-specific phosphorylation motif (when excluding the bias created by over-represented, related AGC kinases as mTORC2 substrates). mTOR substrates are more likely to contain a serine than a threonine (77% and 23%, respectively) as a phospho-acceptor residue. Importantly, mTOR substrates contain mainly a proline at position +1. Leucine, glutamic acid, phenylalanine, tyrosine and glutamine are also favored, albeit weakly, in this position. The preference for proline and the large hydrophobic amino acids leucine and phenylalanine in this position is not easily explained based on the available static structure of the mTOR catalytic site. The phosphorylation reaction may involve a specific conformational adaptation or other effects beyond the direct kinase-substrate interaction, such as post-translational modification. Notably, there is no preference for any amino acid at position -1 when considering all substrates. However, when focusing solely on AGC kinases as substrates, including S6K, phenylalanine and leucine are dominant at this position (Figure 3.3B).

Structural insights on the interaction of a catalytic site and its target phosphorylation motif were recently provided by SMG1 and ATM, both PIKK family members structurally related to mTOR. Overlays of the structures of the catalytic site of these two PIKKs with active and inactive conformations of mTOR in mTORC1 reveal similarities, but also important differences, in phosphorylation site interaction. An important difference is that residues in mTOR do not make specific interactions with the +1 and -1 position residues of the phosphorylation motif. mTOR has the possibility to accommodate larger residues in these positions, possibly at the cost of lower overall affinity (Figure 3.3C)[52,179,343,344]. There is strong specificity for glutamine in the +1 position of substrates of SMG1, ATM and possibly other PIKKs, but not in mTOR substrates. This specificity is due to a hydrogen bond between the sidechain of the substrate glutamine and

the backbone amide and carbonyl groups in a short loop segment of SMG1 and ATM. Such a hydrogen bond is precluded for mTOR because, in this case, the corresponding loop region is flipped away from the substrate peptide. Another important difference is the replacement of a small valine residue (position 2367) in the SMG1 loop with a larger and rotatable phenylalanine residue (position 2371) in mTOR. Conformational plasticity of Phe2371 and Tyr2542 in mTOR may explain its ability to accommodate proline, leucine and phenylalanine residues in the +1 position of substrates. The +1 glutamic acid found in some substrates could also be accommodated as mTOR residues Lys2370 or Arg2368 may move into the pocket to stabilize binding of negatively charged glutamic acid.

The pocket regions in SMG1 and mTOR near the -1 position of the target phosphorylation motif exhibit similar backbone conformations. However, the three residues of the SMG1 pocket arrayed around the -1 leucine of the SMG1 substrate peptide are replaced with smaller residues in mTOR (Phe2215 - His2274, Asp2339 - Ser2342, Leu2338 - Pro2341). These smaller residues in mTOR create space that could accommodate the bulky phenylalanine residue typically observed in the -1 position of the phosphorylation motif in AGC kinases.

A study in 2011, based on in vitro phosphorylation of a peptide library, proposed an mTOR consensus phosphorylation motif. The proposed motif consists of the phosphorylated serine or threonine followed at the +1 position by proline, phenylalanine, leucine, tryptophan, tyrosine or valine in decreasing order of preference [345]. Other than the +1 position, no strong preference for any particular residue was discerned for positions -5 to +4. The new structural evidence discussed above and the now longer list of mTOR substrates confirm that mTOR has relaxed sequence requirements for its target phosphorylation sites. Thus, any sequence other than S/T-P is of limited use in identifying putative mTOR sites.

mTOR substrate recognition: TOS and RAIP motifs

mTORC1 and mTORC2 phosphorylate different substrates despite having the same catalytic subunit. This is paradoxical as the kinase sites in mTORC1 and mTORC2 are structurally similar, if not identical, and fully contained within mTOR with no significant interaction with neighboring subunits. Furthermore, we did not detect an mTORC1- or mTORC2-specific phosphorylation motif. The mechanism(s) that account for mTORC1 and mTORC2 phosphorylating different substrates likely involves subunits specific to each mTOR complex. Indeed, evidence suggests that subunits unique to each complex bind substrates for presentation to a common kinase site. In mTORC1, RAPTOR binds the TOS motif, a five amino acid sequence defined as F-X-Φ-(E/D)-Φ, where Φ represents a hydrophobic residue and X is any residue [53,75]. The TOS motif was first identified in S6K and 4E-BP and subsequently in other mTORC1 substrates (Table 1). 4E-BP

has, in addition, a RAIP motif that acts synergistically with the TOS motif to strengthen 4E-BP interaction with RAPTOR[74,75,144]. However, most mTORC1 substrates do not possess a sequence resembling a TOS or RAIP motif. Other RAPTOR binding motifs have been reported, such as the so-called SAIN (SHC and IRS1 NPXY) domain in IRS1 [346] and the S/P-X-P-X-P-P motif in eIF4E, ULK1, LARP1 and DAP1. These proteins are direct mTORC1 substrates that lack a TOS motif [347]. Furthermore, some substrates can interact with mTORC1 independently of RAPTOR. For example, TFEB and TFE3 bind RAG-C/D which results in sufficient proximity to mTORC1 for their phosphorylation[317,318].

In mTORC2, evidence is emerging that the CRIM domain of mSIN1 is responsible for substrate recruitment. The CRIM domain is highly flexible and adjacent to mLST8 and the mTOR kinase site[54]. Whether there is a sequence motif in mTORC2 substrates equivalent to a TOS or RAIP motif that is recognized by the CRIM domain remains to be determined.

As discussed above, current evidence suggests that substrate specificity is determined at the level of recruitment. The mTOR subunit itself appears to exercise little discrimination, readily phosphorylating substrates recruited by other subunits. This model explains why truncated mTOR alone (without any other subunits) is able to indiscriminately phosphorylate 4E-BP, S6K and AKT in vitro[348]. This model can also account for why S6K, an AGC kinase with a target phosphorylation sequence very similar to that of other AGC kinases but the sole AGC kinase family member with a TOS motif, is phosphorylated by mTORC1 rather than mTORC2.

3.4 Conclusion

Our knowledge of TOR has increased enormously since its discovery 30 years ago[16-19]. Given the central role of mTOR in cellular physiology, it appears to have relatively few substrates. However, mTOR is able to exert wide-ranging effects via targets like 4E-BP and S6K that regulate translation and through it the levels of numerous proteins. In addition, mTOR controls the levels and activity of many transcription factors and hence the expression of many genes. Thus, direct phosphorylation of only a handful of mTOR targets is sufficient to have wide impact.

Despite three decades of active research, much remains to be determined. How the majority of substrates are recognized and recruited to either mTORC1 or mTORC2 is still unknown. The weak specificity of the phosphorylation motif leads mTOR to rely on ancillary motifs, such as TOS, to select its targets. As only a few mTOR substrates bear known motifs, this raises the possibility of more such motifs to be discovered.

Finally, one of the greatest challenges presently facing the field is resolving the intracellular localization of TOR complexes. It has long been suspected that there are functionally distinct sub-pools of mTOR complexes and that intracellular localization may compartmentalize their activity. Advances in live-cell imaging and visualization of tagged proteins will provide the necessary tools to address this challenge.

3.5 Acknowledgements

We acknowledge support from the ERC (MERiC), the Swiss National Science Foundation, the Sjöberg Foundation, and the Louis Jeantet Foundation.

3.6 Figures and Tables

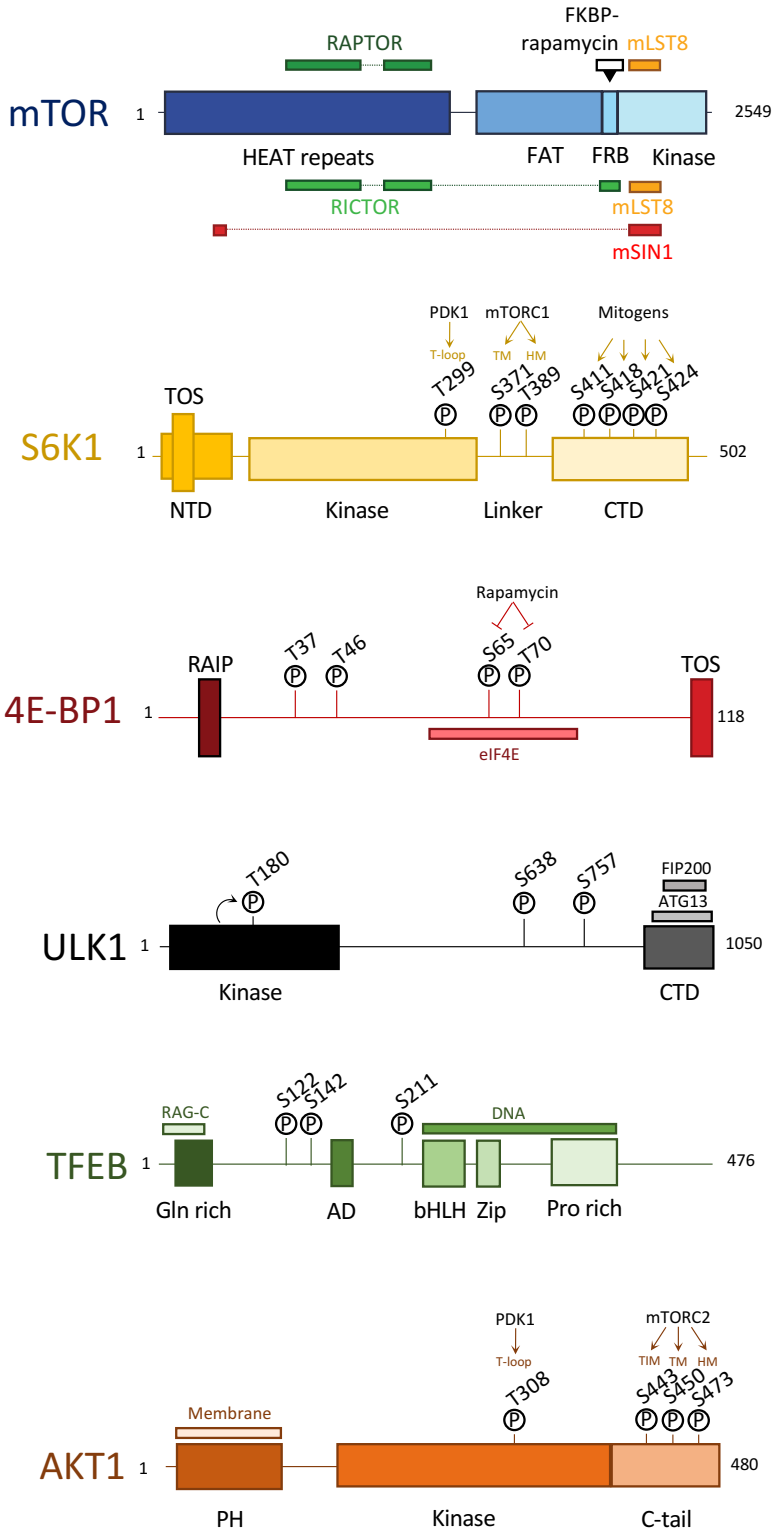

Figure 3.1 : Schematic representation of mTOR and selected substrates.
Domains are drawn to scale. Horizontal bars indicate the interaction with specific proteins, DNA or membrane. Where not specifically indicated, sites are phosphorylated by mTORC1.
AD, activation domain; bHLH, basic helix-loop-helix; CTD, C-terminus domain; Gln rich, glutamine rich; FAT, FRAP ATM TRRAP; FRB, FKBP-Rapamycin binding, HM, hydrophobic motif; NTD, N-terminus domain; PH, Pleckstrin homology; Pro rich, proline rich; TM, turn motif; TOS, TOR signaling.

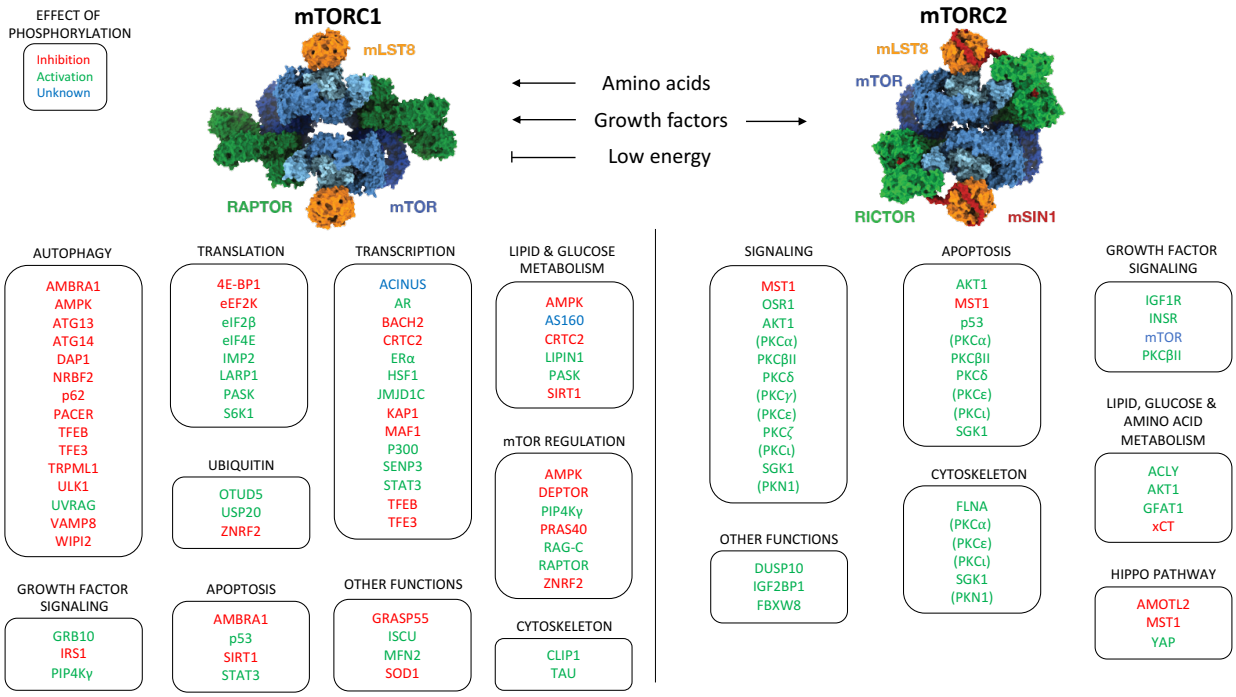

Figure 3.2 : Structure of mTORC1 and mTORC2 with their respective substrates.
Only the main function of the substrates is indicated. AGC kinases not experimentally verified as mTORC2 substrates are shown in parentheses.(mTORC1 PDB: 6BCX[53]; mTORC2 PDB: 6ZWM[54])

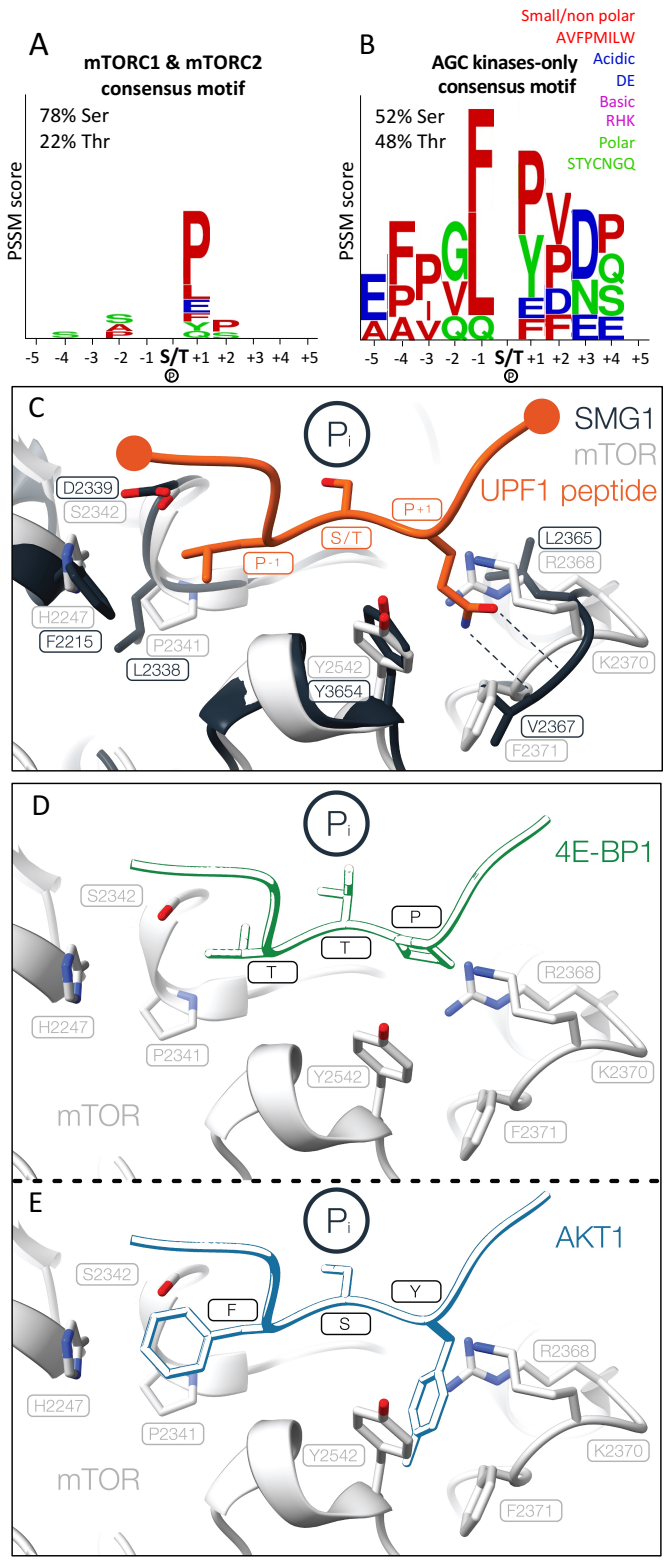

Figure 3.3 : mTORC1 and mTORC2 consensus motif.
Manually curated from [349], version 2.8.2. **A** Consensus motif generated from all mTORC1 and mTORC2 substrates listed in Table 1 and 2. **B** Consensus motif generated from AGC kinases (HM and TM only). **C** Superposition of the substrate binding grooves of SMG1 (grey) and mTOR (white) (PDB ID:7PE8) with an UPF1 substrate peptide (orange) (PDB ID:6Z3R) [64] [284]. An inversion in backbone conformation around Lys2370 in mTOR abolishes the specific recognition of glutamine in the UPF1 +1 position by hydrogen bonding that is present in the SMG1 backbone. **D and E** Illustration of mTOR-substrate peptide interactions, 4E-BP1 (green) (D) and AKT1 (blue) (E). The representation is based on modeling standard rotamers of +1 and -1 side chains of mTOR substrate peptides onto the UPF1 peptide backbone [64]. The positioning of the peptide in the mTOR active site is based on a domain-wise mTOR-SMG1 superposition. Small side chains of a 4E-BP1 substrate peptide (D) are not filling the existing pockets while steric overlap of an AKT1 substrate peptide (E) with mTOR suggests a requirement for structural rearrangements upon binding.

Substrate	Uniprot ID	Phosphorylated site(s)	Phosphorylated site(s) and adjacent residues	TOS motif	Purpose of phosphorylation	Function	Remarks	Reference
4E-BP1[a]	Q13541	T37,T46	GDYSTTPGGTLFSTTPGGTR	FEMDI	Inhibitory	Translation regulation	Rapamycin insensitive	[145]
		S65,T70	MECRNSPVTKTPPRDL		Inhibitory		Rapamycin sensitive	[303]
ACINUS	Q9UKV3	S240,S243	RAAKLSEGSQPAEE		Unknown significance	EJC, splicing		[350]
AMBRA1	Q9C0C7	S52	VELPDSPRSTF		Inhibitory	Autophagy		[351]
AMPKα1	Q13131	S356[b]	FYLATSPPDSF		Inhibitory	Signaling		[273]
AMPKα2	P54646	S345	FYLASSPPSGS		Inhibitory	Signaling		[273]
		S377	PLIADSPKARC		Specific activation	Glucose uptake		[274]
AR	P10275	S96	QGEDGSPQAHR		Activating	Signaling		[352]
AS160	O60343	S666	AQGVRSPLLRQ	FEMDI	Unknown	Signaling	Sensitive to TOS mutation and rapamycin	[353]
ATG13	O75143	S259[c]	TSFSTSPPSQL		Inhibitory	Autophagy		[308]
ATG14	Q6ZNE5	S3	MASPSGKG		Inhibitory	Autophagy		[354]
		S223,T233	PADVSSESDSAMTSSTVSKLA					
		S383	LMYLVSPSSEH					
		S440	WENLPSPRFCD					
BACH2	Q9BYV9	S510[d]	KVCPRSPPLET		Inhibitory	Transcriptional regulator		[355]
		S536[d]	DGSGGSPCSLP					
CLIP1	P30622	Multiple sites			Activating	Microtubule organization		[356]
CRTC2	Q53ET0	S136	SPAYLSPPPES		Inhibitory	SREBP1 processing		[357]
DAP1	P51397	S3	MSSPPEGK		Inhibitory	Autophagy		[358]
		S51	EWESPSPPKPT					
DEPTOR	Q8TB45	S293, T295, S299	GYFSSSPTLSSSPPVLC		Degradation	Signaling	mTORC1 regulation	[359,360]
eEF2K	O00418	S78	GSPANSFHFKE		Inhibitory	Translation regulation		[361]
		S396	DSLPSSPSSAT					
eIF2b	P20042	S2	MSGDEMI	FDIDE	Activating	Translation regulation		[362]

		S67	RKKDASDDLDD					
eIF4E	P06730	S209	ATKSGSTTKNR		Activating	Translation regulation	TPTPNPP Raptor binding motif	363
ERa	P03372	S104,S106	PLNSVSPSPLMLL	FPATV	Activating	Signaling		364
GRASP55	Q9H8Y8	Undetermined			Localization	Protein transport		365
GRB10	Q13322-1	S474,476[e]	MNILGSQSPLHPS		Protein stabilization	Signaling		345,366
HSF1	Q00613	S326	VDTLLSPTALI		Activating	Transcription		367
IMP2	Q9Y6M1	S162,S164	DEEVSSPSPPQRA		Activating	Translation regulation		368
IRS1	P35568-1	S422,S423	DGGFISSDEYGS		Protein degradation	Signaling		369
		S636,S639	DYMPMSPKSVSAPQ		Protein degradation	Signaling	SAIN domain binding to Raptor	346,370
ISCU	Q9H1K1	S14	LRRAASALLLR		Protein stabilization	Protein folding		371
JMJD1C	Q15652	T505	VSRPPTPKCVI		Activating	Histone demethylase		372
KAP1	Q13263	S824	GAGLSSQELSG		Inhibitory	Transcriptional repressor		373
LARP1	Q6PKG0	26 S/T residues			Activating	TOP mRNA translation		374,375
LIPIN1	Q14693-3	S106	MHLATSPILSE		Localization	Lipid metabolism	Rapamycin sensitive	155
		S470[f]	RSANQSPQSVG				Rapamycin insensitive	
MAF1	Q9H063	S60,S68,S75	VLEALSPPQTSGLSPSRLSKSQGGEE		Inhibitory	RNA polIII repressor		150
MFN2	O95140	S200	LVLMDSPGIDV		Activating	Mitochondrial fusion		376
OTUD5	Q96G74-5	S323,S332	EPIRVSYHRNIHYNSVVNPN		Protein stabilization	Deubiquitination	mTORC1 and	377
		S503	ADRATSPLVSL		Activation		mTORC2 regulation	
NRBF2	Q96F24	S113,S120	DAEGQSPLSQKYSPSTEK		Inhibitory	Autophagy		378
p300	Q09472	S2271,S2279	QQQMGSPVQPNPMSPQQHM		Activating	Protein acetylation		379
		S2291	PNQAQSPHLQG					
		S2315	PQPVPSPRPQS					
p53	P04637	S15	VEPPLSQETFS		Protein stabilization	Tumor suppressor	mTORC1 & mTORC2 dependent	380
p62	Q13501-1	S349[g]	KEVDPSTGELQ		Inhibitory	Autophagy		381

PACER	Q9H714	S157	GILATSPYPET		Inhibitory	Autophagy		[382]
PASK	Q96RG2	T640,T642	GLSFGTPTLDEPW		Activating	Signaling		[383]
		S949,S953,S956	RLFLASLPGSTHSTAAEL					
PIP4kγ	Q8TBX8	S324,S328	PALVGSYGTSPEGIG		Inhibitory	Signaling	mTORC1 regulation	[384]
PRAS40	Q96B36	S183	QQYAKSLPVSV	FVMDE	Substrate competition	Signaling	mTORC1 regulator	[286]
		S212,S221	NGPPSSPDLDRIAASMRALV		Inhibitory	Signaling	S212 rapamycin insensitive	[287]
RAG-C	Q9HB90	S21	YGAADSFPKDF		mTORC1 destabilization	Signaling	Rapamycin insensitive	[385]
RAPTOR	Q8N122	S859,S863	SSLTQSAPASPTNKG		Activating	Signaling	mTORC1 core component	[386,387]
S6K1	P23443-2[h]	S371	QTPVDSPDDST	FDIDL	Priming	Signaling, translation		[295]
		T389	VFLGFTYVAPS		Activating			[145]
SENP3	Q9H4L4	S25,S26	IPPAYSSPRRER		Nucleolar localization	Ribosome biogenesis		[388]
		S141,T142,T145	LLYSKSTSLTFHWKL					
SIRT1	Q96EB6	S47	PGLERSPGEPG	FDVEL	Inhibitory	Protein deacetylation		[389]
SOD1	P00441	T40	SIKGLTEGLHG		Inhibitory	ROS detoxification		[390]
STAT3	P40763	S727	IDLPMSPRTLD		Activating	Signaling		[391,392]
TAU	P10636-8[i]	S214	RSRTPSLPTPP		Aggregation	Microtubule organization		[393]
		T231	VAVVRTPPKSP					
		S356	QSKIGSLDNIT					
TFEB	P19484	S122	PPPAASPGVRA		Localization	Transcription factor		[319]
		S142	NSAPNSPMAML					[315]
		S211	GVTSSSCPADL					[164,314]
TFE3	P19532	S321[j]	ITVSNSCPAEL		Inhibitory	Transcription factor		[316]
TRPML1	Q9GZU1	S572,S576	CGRDPSEEHSLLVN		Inhibitory	Autophagy		[394]
ULK1	O75385	S757	VFTVGSPPSGS		Inhibitory	Autophagy		[163]
USP20	Q9Y2K6	S132,S134	ADEGESESEDDDL		Activating	Deubiquitination		[395]
UVRAG	Q9P2Y5	S498	SGGIPSPDKGH		Repressor activation	Autophagy		[396]
		S550	TSLSSSLDTSL		Activating	Autophagy		[397]
		S571	EDLVGSLNGGH					

VAMP8	Q9BV40	T48	HLRNKTEDLEA		Inhibitory	Autophagy		[398]
WIPI2	Q9Y4P8-4	S395	TYVPSSPTRLA		Degradation	Autophagy		[399]
ZNRF2	Q8NHG8	S145	RLVIGSLPAHL		Translocation	Signaling	mTORC1 regulation	[400]

Table 3.1 : Direct substrates of mTORC1.
Numbering is based on the human protein. Adjacent residues from -5 to +5 to the phosphorylated site are shown. [a] There are 3 4EBP isoforms, all of which are phosphorylated by mTORC1 at the cognate sites. [b] Ser347 in reference. [c] Ser258 in reference. [d] Ser509 and Ser535 in reference. [e] Positions in canonical isoform 3. [f] position Ser472 in reference. [g] Ser351 in reference. [h] alpha II isoform. [i]TAU-F isoform. [j] homologous to TFEB Ser211, no in vitro evidence for direct phosphorylation by mTORC1.

Substrate	Uniprot ID	Phosphorylated site(s)	Phosphorylated site(s) and adjacent residues	Purpose of phosphorylation	Function	Remarks	Reference
ACLY	P53396	S455	PSRTASFSESR	Activating	Metabolism		[401]
AMOTL2[a]	Q9Y2J4-2	S760	SQRAASLDSVA	Inhibitory	YAP signaling repressor		[402]
DUSP10	Q9Y6W6	S224, S230	REGKDSFKRIFSKEIIV	Protein stabilization	p38 phosphatase		[403]
FBXW8	Q8N3Y1-1	S86	ASRSRSPLARE	Protein stabilization	Ubiquitination		[404]
FLNA	P21333	S2152	RRRAPSVANVG	Localization	Cytoskeleton		[405]
GFAT1[b]	Q06210-2	S243	LSRVDSTTCLF	Activating	Metabolism		[406]
IGF1R[c]	P08069	Y1161, Y1166	MTRDIYETDYYRKGGK	Activating	Growth factor signaling	Tyr phosphorylation	[342]
IGF2BP1	Q9NZI8	S181	QPRQGSPVAAG	Activating	mRNA binding		[407]
INSR[d]	P06213-1	Y1185, Y1190	MTRDIYETDYYRKGGK	Activating	Growth factor signaling	Tyr phosphorylation	[342]
MST1	Q13043	S438	YEFLKSWTVED	Inhibitory	Hippo signaling		[408]
mTOR	P42345	S2481	PESIHSFIGDG	Unknown significance	Signaling	mTORC2 autophosphorylation	[339,340]
OSR1	O95747	S339	GGWEWSDDEFD	Activating	Signaling		[409]
p53	P04637	S15	VEPPLSQETFS	Protein stabilization	Tumor suppression	Substrate of mTORC1 & mTORC2	[380]
xCT	Q9UPY5	S26	NGRLPSLGNKE	Inhibitory	Solute carrier		[410]
YAP	P46937	S436	QSTLPSQQNRF	Activating	Transcriptional regulator	Hippo pathway	[411]

AGC Kinases	Uniprot ID	Phosphorylated site(s)	Phosphorylated site(s) and adjacent residues	Purpose of phosphorylation	Motif	Experimentally verified	Reference
AKT1[e]	P31749	T443	FDEEFTAQMIT	Priming	TIM	NO	[336]
		T450	QMITITPPDQD	Stability	TM	YES	[329,330]
		S473	HFPQFSYSASG	Activating	HM	YES	[412]
		S477, T479	FSYSASGTA	Activating		YES	[335]
PKCα	P17252	T631	FDKFFTRGQPV	Priming	TIM	NO	[336]

		T638	GQPVLTPPDQL	Stability	TM	NO	329,330
		S657	DFEGFSYVNPQ	Activating	HM	NO	79,330
PKCβII	P05771-2	T634	FDRFFTRHPPV	Priming	TIM	YES	336
		T641	HPPVLTPPDQE	Stability	TM	NO	330
		S660	EFEGFSFVNSE	Activating	HM	NO	330
PKCδ	Q05655	S664	AFAGFSFVNPK	Activating	HM	YES	413
PKCγ	P05129	T648	FDKFFTRAAPA	Priming	TIM	NO	336
		T655	AAPALTPPDRL	Stability	TM	NO	330
		T674	DFQGFTYVNPD	Activating	HM	NO	330
PKCε	Q02156	T703	FDQDFTREEPV	Priming	TIM	NO	336
		T710	EEPVLTLVDEA	Stability	TM	NO	330
		S729	EFKGFSYFGED	Activating	HM	NO	330
PKCζ	Q05513	T553	FDTQFTSEPVQ	Priming	TIM	NO	336
		T560	EPVQLTPDDED	Stability	TM	YES	414
		S573	KRIDQSEFEGF	Activating	HM	NO	-
PKCι	P41743	T557	FDSQFTNEPVQ	Priming	TIM	NO	336
		T564	EPVQLTPDDDD	Stability	TM	NO	-
		S577	RKIDQSEFEGF	Activating	HM	NO	-
SGK1[f]	O00141	T390	FDPEFTEEPVP	Priming	TIM	NO	336
		S397	EPVPNSIGKSP	Stability	TM	NO	-
		S422	AFLGFSYAPPT	Activating	HM	YES	333
PKN1[g]	Q16512	T909	FDEEFTGEAPT	Priming	TIM	NO	336
		S916	EAPTLSPPRDA	Stability	TM	NO	415
		T925	DARPLTAAEQA	Activating	HM	NO	-

Table 3.2 : Direct substrates of mTORC2.
Numbering is based on the human protein. [a] Isoform 2. [b] Isoform 2. [c,d] Tyrosine phosphorylation, identical sequences in both proteins. In reference [342], sites are Y1131, Y1136 in IGF1R and Y1146, Y1151 in INSR. [e] There are 3 Akt isoforms with highly conserved sequences surrounding the cognate phosphorylated sites. [f] There are 3 SGK isoforms with highly conserved sequences surrounding the cognate phosphorylated sites. There is no direct evidence for mTORC2 phosphorylation of the respective sites for many of the AGC kinases. mTORC2 phosphorylation is assumed from cell based experimental data or inferred from homology. [g] There are 3 PKN isoforms with highly conserved sequences surrounding the cognate phosphorylated sites. TIM, TOR interacting motif; TM, turn motif; HM, hydrophobic motif.

4 Discussion and Outlook

DEPTOR is an inhibitor of mTOR-complexes with an enigmatic role of being tumor suppressor and oncogene. In this thesis, I present important insights into the complex regulatory interplay of DEPTOR and mTORCs enabled by structural and biochemical studies of DEPTOR and its effect on mTORC1 and mTORC2 activity.

The DEPTOR PDZ domain was proposed to be crucial for binding and inhibiting mTOR-complexes. I could show that the PDZ domain indeed binds to the FAT domain of mTOR. cryo-EM reconstructions at high resolution enabled *de novo* building of a model for the DEPTOR PDZ domain and analysis of the binding interface with mTOR. The PDZ domain of DEPTOR adopts a canonical PDZ domain fold. In addition to the core fold, the domain extends at the N-terminus towards the FAT domain and enlarges the binding interface. The DEPTOR PDZ domain interacts with mTOR in a non-canonical manner which does not resemble other interactions with a PDZ binding protein. The peptide binding groove of the PDZ domain is located at the interface, but remains unoccupied. This represent a novel binding mode of PDZ domains, which to our best knowledge has not been observed so far. The binding interface is further enlarged by a linker of the mTOR Horn region spanning residues 290-350. This linker, like some other linkers or regions of mTOR complexes, could not be visualized in previous reconstructions of mTOR-complexes due to high degree of flexibility or intrinsic disorder[53,54,180,181]. The linker undergoes a partial disorder-to-order transition upon DEPTOR-PDZ binding and provides a structural link between FAT domain, DEPTOR and Horn region. Surprisingly and in contrast to existing literature, I could show that DEPTOR and mTOR form a second interaction interface via the DEPTOR DEPt domain. Solving the crystal structure of isolated DEPt and docking it into the cryo-EM density allowed pseudo-atomic analysis of the interaction.

Using *in vitro* activity assays in combination with mutational studies, we investigated the role of the two DEPTOR domains and revealed the complex mode of inhibition. The PDZ domain anchors the DEPt domain and counteracts allosteric activation of mTOR. Binding of the PDZ alone on the other hand stimulates allosteric mTOR activation. This peculiar feature makes DEPTOR a bidirectional regulator, not only an inhibitor of mTOR as has been published[182,183].

In summary, DEPTOR interacts with mTOR by binding of the PDZ and DEPt domains to the FAT domain at two distinct sites. Moreover, there is no apparent difference in DEPTORs interaction with mTORC1 or mTORC2. We were able to determine the functional role of the individual domains of DEPTOR. Our work unraveled a novel, allostery-based inhibition mechanism of mTOR.

Concurrently with our paper, Heimhalt *et al.* published a related study on the function of DEPTOR on mTOR [228]. Their findings confirm the importance of the PDZ domain as anchoring domain. However, Heimhalt and colleagues did not reveal the interaction of DEPt with mTOR and the role of DEPt in mTOR inhibition. The mechanism proposed by this group is based on the DEPTOR linker binding to the FRB domain of mTOR and thereby competing with substrates. Functional inhibition of mTOR by DEPTOR is observed at significantly lower concentration than necessary for detecting substrate competition effects. Therefore, we consider their proposed mechanism as substrate binding mode of DEPTOR (as discussed in chapter 2), being not relevant in understand the mTOR inhibition mechanism by DEPTOR.

The inhibition of mTOR by DEPTOR revealed by our work differs fundamentally from all previously known possible modes of inhibition. The rapamycin-FKBP12 complex restricts access to the active site and hinders substrates from binding to the FRB domain [180]. PRAS40 blocks substrate recruitment to mTORC1 by binding to the FRB domain and the TOS site in Raptor [53,76]. ATP-analogs like Torin1 compete with ATP in the active site and thereby prevent substrate phosphorylation [87]. The described inhibition mechanisms have a strong effect on mTORC1 activity and diminish substrate phosphorylation almost completely. In contrast, DEPTOR allosterically counteracts the activation of mTOR-complexes leading to non-complete inhibition. Thereby, knowledge on DEPTOR function adds an important aspect to mTOR regulation which is independent of the AND-gate logic for mTORC1 activation.

There are important aspects of the interplay between DEPTOR and mTOR which remain to be answered. Is DEPTOR differentially regulated in mTORC1 and mTORC2 signaling? How can DEPTOR inhibition be substrate-specific in certain cellular context[206]? The mechanistic understanding of DEPTOR presented in this work paves the way for future studies to understand the role of DEPTOR in mTOR signaling.

4.1 The signal integrator DEPTOR links mTORC1 and lipid signaling

As outlined in the previous chapters, the integration of input signals and modulation of kinase activity accordingly is the key characteristic of mTOR signaling. Information on the cellular state converges on the signaling mediators Rheb and Rag Our findings suggest that DEPTOR represents as well one of these mediators in the mTOR signaling network, with an important role in health and disease.

DEPTOR PDZ interacts with mTOR in a non-canonical fashion. The unoccupied peptide binding groove opens the possibility for other proteins to modulate the mTOR-DEPTOR interaction. Binding of C-terminal peptides to this groove could either stabilize the interaction of DEPTOR with mTOR or compete with mTOR binding. A potential binding partner could be the Glycine N-

Methyltransferase (GNMT). GNMT has been shown to interact with the PDZ domain, disrupt its interaction with mTOR and promote mTORC1 activity[416]. GNMT is a tumor suppressor in different cancers[417,418]. Using DEPTORs PDZ domain as a bait to identify novel binding partners could lead to new insights into regulation of PDZ binding to mTOR and thereby mTOR signaling. Binding competition assays and characterization of their function by deletion, overexpression or mutation of the binding partner while monitoring mTOR activity would be necessary to validate and understand their role on mTOR signaling through via DEPTOR.

Our work established the DEPt as the inhibitory domain of DEPTOR. A recent study revealed that DEPTORs DEPt binds phospholipids like PA[419]. DEPTOR displacement from mTOR by PA has been attributed to PA binding to the FRB domain[196]. In light of our results, one can assume that PA disrupts the binding of DEPt to mTOR and thus mitigates mTOR inhibition by DEPTOR. Beyond direct activation of mTOR, the lipid binding capability of DEPTOR could also influence subcellular localization of mTOR-complexes by targeting them to different membrane compartments.

4.2 Allosteric activation and inhibition in the PIKK family

The PIKK kinase family is characterized by their conserved domain arrangement and sequence similarity to phosphatidyl inositol kinases. Besides the highly conserved FATKIN region, structural architecture of PIKKs diverges in terms of oligomerization and organization of the N-terminal HEAT repeats. Due to their fundamental role in cellular homeostasis and stress-induced signaling is mechanistic understanding of PIKK regulation crucial to develop therapeutic strategies targeting dysregulated PIKKs in context of diseases.

Regulation of mTOR-complexes

The mTOR catalytic site in non-activated mTORC1 and mTORC2 adopts the same conformation[53,54]. mTORC1 is activated by the GTPase Rheb using an allosteric mechanism: Rheb binds mTOR at a tripartite interface consisting of N-HEAT, M-HEAT and FAT domain, which induces a conformational change via a pull and twist movement of the FAT domain towards the active site(Figure 4.1 b). This conformational change realigns the kinase C- and N-lobes to gain maximum activity[53]. The identical active site conformation for apo-complexes in combination with he published activation mechanism for mTOR led Scaiola *et al.* to the conclusion that mTORC2 must be activated as well by a unknown mechanism[54]. Based on our novel findings from chapter 2 (i) there is no difference in the interaction between DEPTOR and mTOR in context of the different complexes and (ii) DEPTOR counteracts the allosteric activation mechanism described

for mTORC1. It is thus temping to speculate that mTORC2 is activated via a similar, potentially GTPase-driven, mechanism as mTORC1. Since the Rheb-binding site of mTOR is accessible in the context of mTORC2, it is intriguing to speculate that Rheb could potentially activate mTORC2 *in vitro* as well, although opposite has been reported [173]. It is compelling to check the capability of Rheb to activate mTORC2 in an *in-vitro* kinase assay using purified components. Importantly, this experiment does not reflect the cellular context. Probably activation of the two mTOR complexes is at least in part driven by colocalization with the respective activator at different subcellular sites to prevent crossactivation[171,173].

Several small GTPases have been reported to be important for mTORC2 activation. Structural and functional investigation of these GTPases in complex with mTORC2 and characterization using *in-vitro* kinase assays will be necessary to assess and compare mTORC1 and mTORC2 activation mechanisms.

Regulation of PIKKs

The FAT and kinase domains are highly conserved in sequence and structure among members of the PIKK family (Figure 1.4)[420]. The FAT domain partially encapsulates the kinase domain and was initially described as structural scaffold or protein binding domain prior to structural characterization[27]. Studies on the mTOR-complexes revealed the role of the FAT domain being a key regulatory element for mTOR function.

In a non-activated state, the FAT domain has an autoinhibitory function keeping the active site in a non-ideal conformation harboring basal kinase activity. During activation of mTORC1 the FAT domain transduces large conformational changes in the HEAT-repeats towards the active site thereby increasing kinase activity[53]. Our work on DEPTOR emphasizes the role of the FAT domain as region for allosteric regulation: the PDZ domain stimulates activation while the DEPt domain diminishes activation (chapter 2). This is in line with activating mutations observed in cancers that cluster in the mTOR FAT domain[220,222,228]. These mutations lead to destabilization of the FAT domain by disruption of helical stacking and thereby abolish its autoinhibitory function[228].

The findings above raise questions on the role of the FAT domain in other members of the PIKK family. Is the FAT domain just a structural scaffold? Does the FAT domain autoinhibit other PIKKs as well? Do the PIKKs share a common activation mechanism?

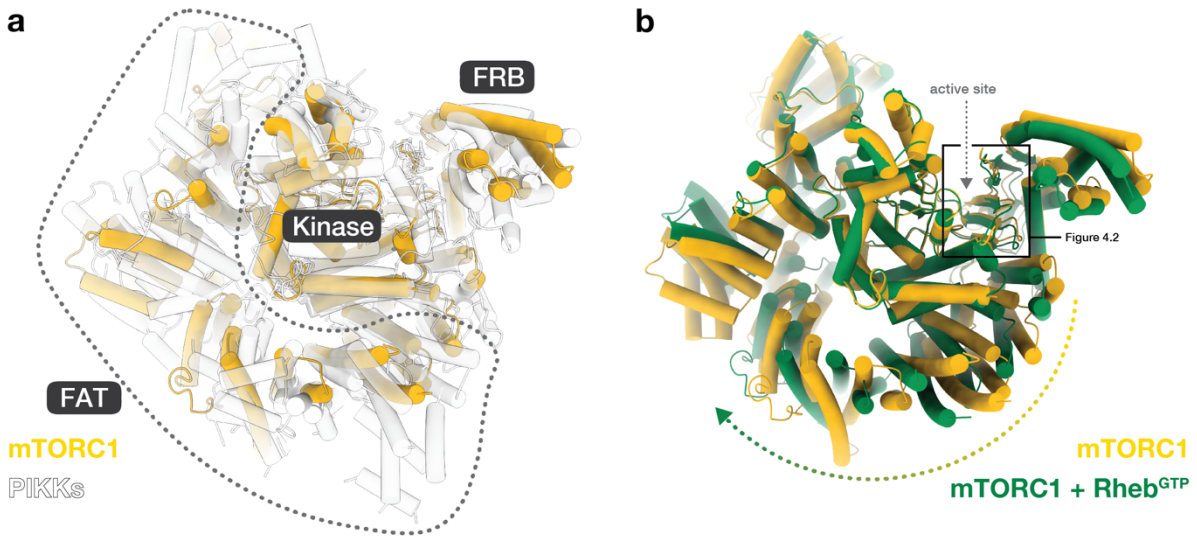

Figure 4.1 : The FAT domain as key regulatory element
(a) Superposition of PIKKs with functional active site; mTOR is colored yellow, other PIKKs colored in shades of blue (ATM (PDB: 7NI5[42]); ATR (PDB: 5YZ0[49]); DNA-PKcs (PDB: 7OTP[50]); SMG1 (PDB: 7PW4[52]); mTORC1 (PDB: 6BCX[53]) (b) Conformational changes in FAT domain and active site upon activation by Rheb (mTORC1 (PDB: 6BCX[53]); mTORC1-Rheb (PDB: 6BCU[53]))

The role of the FAT domain as structural unit is divergent in the PIKK family (Figure 1.4). In monomeric PIKKs, the FATKIN region forms a “head” unit onto which the HEAT region is anchored. As in mTOR-complexes, besides anchoring the HEAT repeats, the FAT domain has a minor role in the structural organization. In ATM and ATR, the two dimeric members of the family besides mTOR, the FAT domain mediates dimerization of the protomers and therefor is crucial for complex assembly and organization.

What is the role of the FAT domain for kinase activity in the different PIKKs? Comparison of the active site states of all PIKKs, for which high-resolution structural data is available (ATR excluded, cryo-EM resolution at 4.7Å), reveals that in their non-activate, apo-state harbor the identical conformation. A recent structural study on DNA-PKcs described its activation by Ku70/80 and DNA that mechanistically resembles activation of mTORC1[34]. DNA and Ku70/80 bind to DNA-PKcs in the HEAT-repeat region. The binding induced movement of the HEAT repeats is communicated via FAT domain towards the active site. As for mTORC1, this leads to a realignment of C- and N-lobe of the kinase (Figure 4.2). The conformational changes in the active site DNA-PKcs and mTORC1 upon activation are identical. It is justifiable to assume that other members of the PIKK family are activated using an analogous mechanism. Of special interest is how ATM and ATR, where the FATKIN is involved in dimer formation, transmit conformational changes via the FAT domain. This may require the dimer to adopt a new conformation. Structural characterization of activated ATM (in complex with DNA and the MRN-complex) and ATR (in

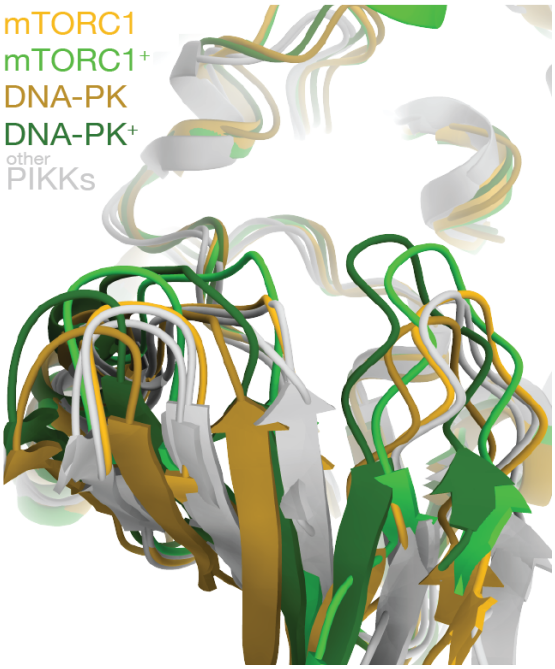

complex with DNA, RPA, TOPB1 and ETAA1) using cryo-EM could visualize the conformational change upon activation and eventually confirm a shared activation mechanism with the FAT domain as central element. If, as proposed above, PIKK share a common activation mechanism, also a shared inhibition mechanism like the one described for DEPTOR (chapter 2) could have emerged.

Figure 4.2 : Activation off PIKKs induces conformational changes in active site
Superposition of PIKK active site. Activation induces conformational changes and realignment of active site residues. Coloring according to legend.(mTORC1 PDB:6BCX, 6BCU[53]; DNA-PKcs PDB: 7K10, 7K11[34]; ATM PDB:7NI5[42]; SMG-1 PDB: 7PW4[52])

In several recent published structures of PIKKS, including this work, inositolhexakiphosphate (InsP6) has been observed at a distinct, positively charged cleft in the FAT domain[51,54,63]. This site has been suggested to be a common InsP6 binding site found in PIKKs[63]. Mutant of this binding site in mTORC2 showed decreased protein stability, but kinase activity and overall structure were not affected [54]. These findings led to a proposed structural role for InsP6 in mTOR folding or complex assembly, as observed for other protein complexes to stabilize helical regions [421,422]. However, considering the FAT domain as an allosteric regulatory element, changes in flexibility and stability have a significant effect on function as observed for DEPTOR. The *in vitro* kinase assays for mTORC2-mutants in this site have been conducted under non-activating conditions[54]. It would be important to revisit the role of InsP6 on kinase activity by executing kinase assays also under activating conditions. It is important to mention, that InsP6 might not be the native small molecule/metabolite recognized at this site, but copurified because of expression or purification conditions. A comparison of InsP6 binding for different published mTOR structures revealed that this site is not always occupied[54]. Isolation and characterization of endogenous mTOR under varying cellular conditions should allow to investigate which metabolite is bound by mTOR or other PIKKs at this site.

4.3 DEPTOR and mTOR as drug targets

mTOR is as master regulator off cell growth and metabolism, and misregulation of mTOR signaling is implicated in numerous diseases such as cancer or neurodegenerative disorders. This makes mTOR and proteins regulating mTOR activity prime targets for therapeutic intervention.

DEPTOR as drug target

DEPTOR plays an important role in modulating mTOR signaling, but the molecular mechanisms of DEPTOR functions in diseases is poorly understood. However, DEPTOR represents a promising drug target, especially in diseases associated to DEPTOR upregulation such as multiple myeloma or obesity[182,206]. A recent yeast-two-hybrid screen identified a compound that inhibits the interaction between DEPTOR and mTOR[423,424] and shows cytotoxic properties towards multiple myeloma cells correlating with the expression levels of DEPTOR. This finding suggests that targeting DEPTOR could be indeed a suitable therapeutic strategy. The structural work presented in this thesis will greatly facilitate structure-guided drug design on new target sites in DEPTOR or at the interface of the DEPTOR – mTOR interaction.

Attempts of targeting mTOR

mTOR was discovered as the “target of rapamycin” in 1991. Soon after this groundbreaking discovery rapamycin entered clinical development. Rapamycin was approved for immunosuppression after transplantations in 1999 [225]. Due to poor solubility and bad pharmacokinetic properties, rapamycin derivatives with improved characteristics have been developed and were termed rapalogs (class 1 mTOR inhibitors). Rapamycin and rapalogs entered development against different cancer indications, but showed disappointing efficacy. This is probably caused by the limited inhibitory potential to some substrates like 4E-BPs[225], and potential activation of negative feedback activation.

To efficiently block mTOR activity towards all substrates, ATP-competitive inhibitors have been developed (class 2 mTOR inhibitors). ATP-competitive mTOR inhibitors can be classified in two categories according to their selectivity: i) dual PI3K/mTOR inhibitors where the effective inhibitory concentration for both kinases is similar and ii) pan-mTOR inhibitors with higher selectivity for mTOR. In clinical studies these compounds have been not successful due to high toxicity and severe side effects.

The Class 3 inhibitors arose as a combination of class 1 and 2 inhibitors[425]. The so called Rapalinks fuse a rapalog moiety to an ATP-competitive inhibitor via a linker and thereby targeting

both the mTOR ATP binding site and FRB domain simultaneously. Importantly, the mTOR kinase forms the two structurally and functionally distinct signaling complexes mTORC1 and mTORC2, and each complex should be considered as individual drug targets. As described above, current targeting strategies focused on two functional sites respectively inhibition mechanisms of mTOR, namely blocking ATP binding and steric hindrance of access to the active site by targeting the FRB domain. Using these two approaches complex specificity is not achievable, because (i) the active site is identical and (ii) targeting the FRB domain affects in addition to mTORC1 also mTORC2 complex assembly. Therefore, new routes in targeting the mTOR pathway for therapeutic intervention must be considered and pursued by developing truly selective inhibitors that target either mTORC1 or mTORC2, or by targeting proteins that modulate the activity of either complex. A promising strategy might be exploiting inhibition mechanisms that are utilized by cellular protein inhibitors of mTOR such as PRAS40. PRAS40 prevents substrate recruitment by occupying the TOS site in Raptor. Identifying a small molecule that occupies the TOS site and mimics the effect of PRAS40 would allow specific inhibition of mTORC1 towards substrates which are dependent on recruitment via the TOS site (Figure 4.3).

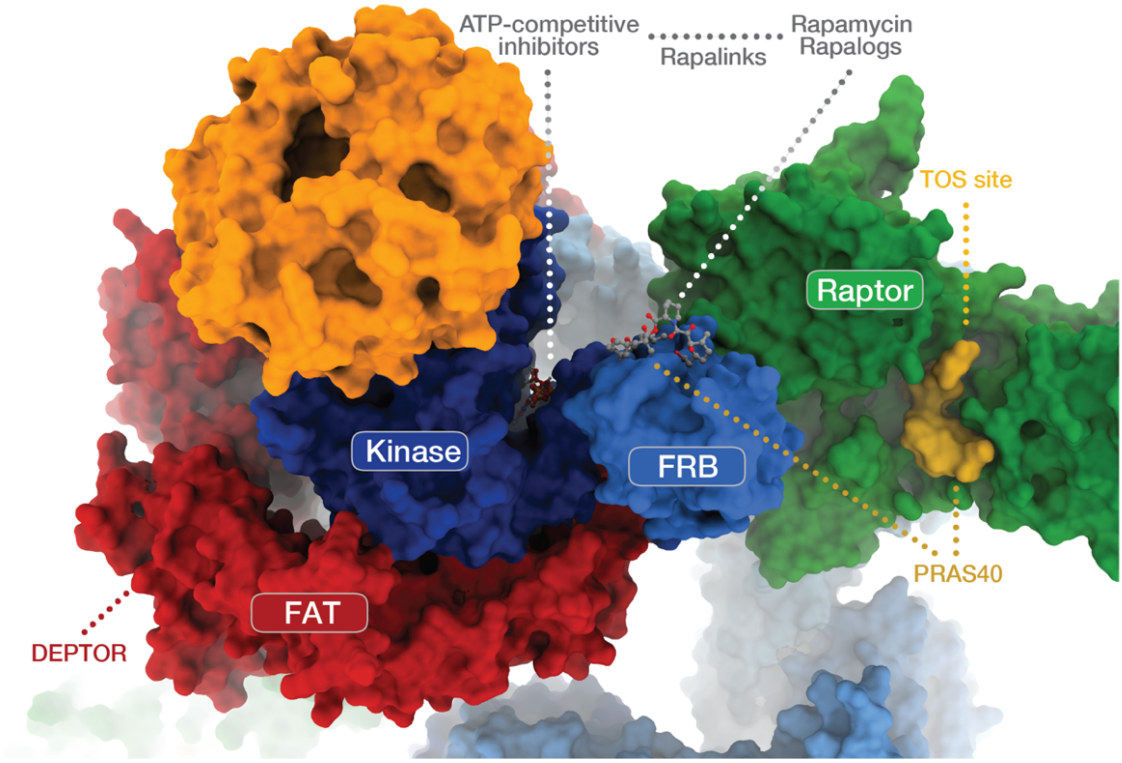

Figure 4.3 : Inhibition of mTORC1 by protein and small molecule inhibitors
Important functional sites in mTORC1 inhibition targeted by either small molecules or cellular protein inhibitors are visualized.

Our results reveal the importance of the FAT domain as allosteric regulation element for mTOR kinase activity. Small molecules with the potential to lock the FAT domain in an inhibited or activated conformation would allow fine tuning of kinase activity. This attempt may be superior to strategies that completely block kinase activity such as ATP-competitive inhibitors (Figure 4.3).

mTORC2

The availability of rapamycin as an mTORC1 inhibitor has largely accelerated and dominated research on mTORC1. Molecular mechanisms of mTORC2 signaling are to a large extend poorly understood. The identification of compounds that specifically target mTORC2 would provide a novel tool for studying its signaling network and answer elusive questions. Moreover, such compounds could find therapeutic utility. Recently, a small molecule inhibitor specific for mTORC2 has been identified [224]. The inhibitor disrupts the interaction of Rictor and mTOR, but the mode of action remains unknown.

Structural characterization of mTORC2 revealed novel target sites for interventions. The N-terminus of mSIN1 is inserted into a hydrophobic pocket formed by Rictor[54]. Mutational studies on N-terminal residues of mSIN1 have shown that abrogation of this interaction leads to defective mTORC2 assembly[54]. Small molecules binding to the hydrophobic pocket of Rictor may lead to a similar effect and mTORC2 specific inhibition. In addition, abrogating substrate recruitment by the CRIM domain of mSIN1 could be another promising option for specific mTORC2 inhibition. Structural information on how substrates are recognized and recruited to mTORC2 is not yet available.

Subcellular localization of mTORC2 appears to be not as narrow defined as for mTORC1 and might represent an important characteristic of its signaling. mTORC2 is recruited via the PH-domain to several membrane compartments to exerts is function[426]. Interfering with the localization of mTORC2 at membranes by targeting the PH-domain may represent another viable option for specific inhibition of mTORC2.

4.4 Outlook

Here we analyzed the function of the three-domain protein DEPTOR. The two DEP domains form one structural and functional unit. However, they can exert their function if the third domain, the PDZ domain, anchors them to mTOR. mTOR itself uses 4 domains to allosterically control activity of one domain. In eukaryotes 65% of the proteins consist of two or more domains, while in prokaryotes only 40% of the proteome are multi-domain proteins[427]. Multi-domain proteins evolved mostly through duplication of domains. A duplicated domain can obtain a novel function by diverging in sequence or recombination with other domains to form a multi-domain protein[428]. Importantly, the sequential order of domains in multi-domain proteins is conserved, probably due to evolution from a common ancestor[428]. Proteins consisting of multiple domains are sometimes considered as «balls on a string». While this model may apply for some examples, it is generally too simplistic. Protein functions are often still studied using domain fragments. This can result in incomplete conclusions and obstruct adequate interpretations. Our work highlights the necessity of analyzing intact proteins and the interplay thereof to study complex functional mechanisms.

However, cellular systems contain many more layers of complexity than what we are able to reconstruct with isolated proteins. Proteins evolved to exert their function at distinct subcellular locations interacting with membranes, binding partners and small molecules. The cellular context greatly influences and determines the structure and function of a protein. For mTORC1, the role of individual components and molecular mechanisms of signaling became more and more clear in recent years. However, many fundamental aspects, that are linked to the cellular environment, remain poorly understood. What is the role of the lysosomal membrane? How does interaction with lipids regulate mTORC1 signaling? How is this signaling hub consisting of membrane-tethered and cytosolic protein (-complexes) spatially organized?

Advances in cryo electron tomography enable us to visualize protein complexes in their cellular context. This permits investigation of assembly, spatial organization or dynamics of protein assemblies like mTORC1 at the lysosome under varying cellular stimuli. These methods can further be applied to study differences between healthy and patient samples and derive novel treatment approaches.

Ultimately, understanding the interplay of entire proteins in their native environment paves the way to truly decipher complex molecular mechanisms, taking all relevant aspects into account. This knowledge will facilitate the development of personalized and targeted therapeutic intervention.

5 Acknowledgements

First of all, I would like to thank my PhD committee for guiding me through the years of my PhD. Thanks to Timm, for having me in your lab, believing into my project, and a lot of insightful discussions. Thanks to Mike and Sandra for your input. It was a pleasure to share and discuss my work you.
I want to deeply thank my two dads in science! You taught me everything I can and, also needed to successfully do this PhD. You shared your passion for mTOR with me and always had the best ideas on what to try next. Thanks Imsi, for showing me the importance of nice figures and how to get them. Eddi, it was a pleasure being supervised by you! Special thanks to both of you for everything!
Franci, thanks for sharing all the highs and lows of a PhD with me. Your energy and Italian vibes made my days interesting. By the way, shouting would have not been necessary; I was always listening to you! Thanks for being there!
Leo, thanks for so many breaks, awesome discussions, being part of the big office crew, making time at the EM fun and of course legendary PhD retreats!
Anna, you convinced me to join this lab. Thanks for babysitting me doing my first steps in cryo-EM, your continuous support also from overseas and of course for sharing your table with us for storage of glassware!
Muri, thanks for the best drawing I have ever seen of myself!
Yves and Kai, studying with you was already a lot of fun, and fun continued. Thanks for sharing so many memories! Flu, thanks for sharing the gin passion and of course playing darts in the small office!
Roman, thanks for being the pillar of the lab! You taught me the most important rule of the wet lab: One eppi will always work!
Karo, thanks for all your support in fighting DEPTOR to reveal its secrets! It was a hard, but also fun time and means a lot me!
Elsa, thanks for so many discussions, fun and serious ones. I deeply enjoyed it having you and all the plants next to me!
Domi, thanks for being the greatest apero organizer and setting standards for happy hours and PhD defenses!
Flo, thanks for being so much fun and hitting the nail with what you say. Some of us are spheres, some are force of nature!
A special thanks to all former and current members of the Maier Lab. You made this lab a special place!
Lastly, I want to thank my family. Thanks for supporting me throughout my entire life in everything I needed and wanted to achieve. Thanks for always being there for me, in all the good and not so good days of life! DANKE für Alles!

6 References

1. Manning, G., Whyte, D.B., Martinez, R., Hunter, T. & Sudarsanam, S. The protein kinase complement of the human genome. *Science* **298**, 1912-34 (2002).
2. Chen, M.J., Dixon, J.E. & Manning, G. Genomics and evolution of protein phosphatases. *Science Signaling* **10**(2017).
3. Li, Z.Y. et al. dbPTM in 2022: an updated database for exploring regulatory networks and functional associations of protein post-translational modifications. *Nucleic Acids Research* **50**, D471-D479 (2022).
4. Olsen, J.V. et al. Global, in vivo, and site-specific phosphorylation dynamics in signaling networks. *Cell* **127**, 635-648 (2006).
5. Ardito, F., Giuliani, M., Perrone, D., Troiano, G. & Lo Muzio, L. The crucial role of protein phosphorylation in cell signaling and its use as targeted therapy. *International Journal of Molecular Medicine* **40**, 271-280 (2017).
6. Vezina, C., Kudelski, A. & Sehgal, S.N. Rapamycin (AY-22,989), a new antifungal antibiotic. I. Taxonomy of the producing streptomycete and isolation of the active principle. *J Antibiot (Tokyo)* **28**, 721-6 (1975).
7. Sehgal, S.N., Baker, H. & Vezina, C. Rapamycin (AY-22,989), a new antifungal antibiotic. II. Fermentation, isolation and characterization. *J Antibiot (Tokyo)* **28**, 727-32 (1975).
8. Choi, J., Chen, J., Schreiber, S.L. & Clardy, J. Structure of the FKBP12-rapamycin complex interacting with the binding domain of human FRAP. *Science* **273**, 239-42 (1996).
9. Lenz, K.D., Klosterman, K.E., Mukundan, H. & Kubicek-Sutherland, J.Z. Macrolides: From Toxins to Therapeutics. *Toxins* **13**(2021).
10. Park, S.R., Yoo, Y.J., Ban, Y.H. & Yoon, Y.J. Biosynthesis of rapamycin and its regulation: past achievements and recent progress. *J Antibiot (Tokyo)* **63**, 434-41 (2010).
11. Singh, K., Sun, S. & Vezina, C. Rapamycin (AY-22,989), a new antifungal antibiotic. IV. Mechanism of action. *J Antibiot (Tokyo)* **32**, 630-45 (1979).
12. Eng, C.P., Sehgal, S.N. & Vezina, C. Activity of rapamycin (AY-22,989) against transplanted tumors. *J Antibiot (Tokyo)* **37**, 1231-7 (1984).
13. Calne, R.Y. et al. Rapamycin for immunosuppression in organ allografting. *Lancet* **2**, 227 (1989).
14. Harding, M.W., Galat, A., Uehling, D.E. & Schreiber, S.L. A receptor for the immunosuppressant FK506 is a cis-trans peptidyl-prolyl isomerase. *Nature* **341**, 758-60 (1989).

15. Bierer, B.E. et al. Two distinct signal transmission pathways in T lymphocytes are inhibited by complexes formed between an immunophilin and either FK506 or rapamycin. *Proc Natl Acad Sci U S A* **87**, 9231-5 (1990).
16. Heitman, J., Movva, N.R. & Hall, M.N. Targets for cell cycle arrest by the immunosuppressant rapamycin in yeast. *Science* **253**, 905-9 (1991).
17. Cafferkey, R. et al. Dominant missense mutations in a novel yeast protein related to mammalian phosphatidylinositol 3-kinase and VPS34 abrogate rapamycin cytotoxicity. *Mol Cell Biol* **13**, 6012-23 (1993).
18. Kunz, J. et al. Target of rapamycin in yeast, TOR2, is an essential phosphatidylinositol kinase homolog required for G1 progression. *Cell* **73**, 585-96 (1993).
19. Helliwell, S.B. et al. TOR1 and TOR2 are structurally and functionally similar but not identical phosphatidylinositol kinase homologues in yeast. *Mol Biol Cell* **5**, 105-18 (1994).
20. Chiu, M.I., Katz, H. & Berlin, V. RAPT1, a mammalian homolog of yeast Tor, interacts with the FKBP12/rapamycin complex. *Proc Natl Acad Sci U S A* **91**, 12574-8 (1994).
21. Sabatini, D.M., Erdjument-Bromage, H., Lui, M., Tempst, P. & Snyder, S.H. RAFT1: a mammalian protein that binds to FKBP12 in a rapamycin-dependent fashion and is homologous to yeast TORs. *Cell* **78**, 35-43 (1994).
22. Sabers, C.J. et al. Isolation of a protein target of the FKBP12-rapamycin complex in mammalian cells. *J Biol Chem* **270**, 815-22 (1995).
23. Brown, E.J. et al. A mammalian protein targeted by G1-arresting rapamycin-receptor complex. *Nature* **369**, 756-8 (1994).
24. Barbet, N.C. et al. TOR controls translation initiation and early G1 progression in yeast. *Mol Biol Cell* **7**, 25-42 (1996).
25. Keith, C.T. & Schreiber, S.L. Pik-Related Kinases - DNA-Repair, Recombination, and Cell-Cycle Checkpoints. *Science* **270**, 50-51 (1995).
26. Andrade, M.A. & Bork, P. HEAT repeats in the Huntington's disease protein. *Nat Genet* **11**, 115-6 (1995).
27. Bosotti, R., Isacchi, A. & Sonnhammer, E.L. FAT: a novel domain in PIK-related kinases. *Trends Biochem Sci* **25**, 225-7 (2000).
28. Yousefzadeh, M. et al. DNA damage-how and why we age? *Elife* **10**(2021).
29. Gottlieb, T.M. & Jackson, S.P. The DNA-dependent protein kinase: requirement for DNA ends and association with Ku antigen. *Cell* **72**, 131-42 (1993).
30. Meek, K., Gupta, S., Ramsden, D.A. & Lees-Miller, S.P. The DNA-dependent protein kinase: the director at the end. *Immunological Reviews* **200**, 132-141 (2004).

31. Jette, N. & Lees-Miller, S.P. The DNA-dependent protein kinase: A multifunctional protein kinase with roles in DNA double strand break repair and mitosis. *Progress in Biophysics & Molecular Biology* **117**, 194-205 (2015).
32. Hammarsten, O. & Chu, G. DNA-dependent protein kinase: DNA binding and activation in the absence of Ku. *Proceedings of the National Academy of Sciences of the United States of America* **95**, 525-530 (1998).
33. West, R.B., Yaneva, M. & Lieber, M.R. Productive and nonproductive complexes of Ku and DNA-dependent protein kinase at DNA termini. *Molecular and Cellular Biology* **18**, 5908-5920 (1998).
34. Chen, X. et al. Structure of an activated DNA-PK and its implications for NHEJ. *Mol Cell* **81**, 801-810 e3 (2021).
35. Lavin, M.F. Ataxia-telangiectasia: from a rare disorder to a paradigm for cell signalling and cancer. *Nat Rev Mol Cell Biol* **9**, 759-69 (2008).
36. Savitsky, K. et al. A single ataxia telangiectasia gene with a product similar to PI-3 kinase. *Science* **268**, 1749-53 (1995).
37. Matsuoka, S. et al. Ataxia telangiectasia-mutated phosphorylates Chk2 in vivo and in vitro. *Proc Natl Acad Sci U S A* **97**, 10389-94 (2000).
38. Banin, S. et al. Enhanced phosphorylation of p53 by ATM in response to DNA damage. *Science* **281**, 1674-7 (1998).
39. Khanna, K.K. et al. ATM associates with and phosphorylates p53: mapping the region of interaction. *Nat Genet* **20**, 398-400 (1998).
40. Burma, S., Chen, B.P., Murphy, M., Kurimasa, A. & Chen, D.J. ATM phosphorylates histone H2AX in response to DNA double-strand breaks. *J Biol Chem* **276**, 42462-7 (2001).
41. Baretic, D. et al. Structures of closed and open conformations of dimeric human ATM. *Sci Adv* **3**, e1700933 (2017).
42. Stakyte, K. et al. Molecular basis of human ATM kinase inhibition. *Nat Struct Mol Biol* **28**, 789-798 (2021).
43. Warren, C. & Pavletich, N.P. Structure of the human ATM kinase and mechanism of Nbs1 binding. *Elife* **11**(2022).
44. Zou, L. & Elledge, S.J. Sensing DNA damage through ATRIP recognition of RPA-ssDNA complexes. *Science* **300**, 1542-8 (2003).
45. Kumagai, A., Lee, J., Yoo, H.Y. & Dunphy, W.G. TopBP1 activates the ATR-ATRIP complex. *Cell* **124**, 943-55 (2006).

46. Thada, V. & Cortez, D. ATR activation is regulated by dimerization of ATR activating proteins. *Journal of Biological Chemistry* **296**(2021).
47. Matsuoka, S. et al. ATM and ATR substrate analysis reveals extensive protein networks responsive to DNA damage. *Science* **316**, 1160-6 (2007).
48. Bartek, J. & Lukas, J. Chk1 and Chk2 kinases in checkpoint control and cancer. *Cancer Cell* **3**, 421-9 (2003).
49. Rao, Q. et al. Cryo-EM structure of human ATR-ATRIP complex. *Cell Res* **28**, 143-156 (2018).
50. Liang, S.K. et al. Structural insights into inhibitor regulation of the DNA repair protein DNA-PKcs. *Nature* (2022).
51. Herbst, D.A. et al. Structure of the human SAGA coactivator complex. *Nature Structural & Molecular Biology* (2021).
52. Langer, L.M., Bonneau, F., Gat, Y. & Conti, E. Cryo-EM reconstructions of inhibitor-bound SMG1 kinase reveal an autoinhibitory state dependent on SMG8. *Elife* **10**(2021).
53. Yang, H. et al. Mechanisms of mTORC1 activation by RHEB and inhibition by PRAS40. *Nature* **552**, 368-373 (2017).
54. Scaiola, A. et al. The 3.2-Å resolution structure of human mTORC2. *Science Advances* **6**(2020).
55. McMahon, S.B., Van Buskirk, H.A., Dugan, K.A., Copeland, T.D. & Cole, M.D. The novel ATM-related protein TRRAP is an essential cofactor for the c-Myc and E2F oncoproteins. *Cell* **94**, 363-74 (1998).
56. Helmlinger, D. et al. Tra1 has specific regulatory roles, rather than global functions, within the SAGA co-activator complex. *EMBO J* **30**, 2843-52 (2011).
57. Murr, R., Vaissiere, T., Sawan, C., Shukla, V. & Herceg, Z. Orchestration of chromatin-based processes: mind the TRRAP. *Oncogene* **26**, 5358-72 (2007).
58. Karousis, E.D. & Muhlemann, O. Nonsense-Mediated mRNA Decay Begins Where Translation Ends. *Cold Spring Harb Perspect Biol* **11**(2019).
59. Kurosaki, T. & Maquat, L.E. Nonsense-mediated mRNA decay in humans at a glance. *J Cell Sci* **129**, 461-7 (2016).
60. Yamashita, A., Ohnishi, T., Kashima, I., Taya, Y. & Ohno, S. Human SMG-1, a novel phosphatidylinositol 3-kinase-related protein kinase, associates with components of the mRNA surveillance complex and is involved in the regulation of nonsense-mediated mRNA decay. *Genes Dev* **15**, 2215-28 (2001).

61. Denning, G., Jamieson, L., Maquat, L.E., Thompson, E.A. & Fields, A.P. Cloning of a novel phosphatidylinositol kinase-related kinase: characterization of the human SMG-1 RNA surveillance protein. *J Biol Chem* **276**, 22709-14 (2001).
62. Isken, O. et al. Upf1 phosphorylation triggers translational repression during nonsense-mediated mRNA decay. *Cell* **133**, 314-27 (2008).
63. Gat, Y. et al. InsP(6) binding to PIKK kinases revealed by the cryo-EM structure of an SMG1-SMG8-SMG9 complex. *Nature Structural & Molecular Biology* **26**, 1089-+ (2019).
64. Langer, L.M., Gat, Y., Bonneau, F. & Conti, E. Structure of substrate-bound SMG1-8-9 kinase complex reveals molecular basis for phosphorylation specificity. *Elife* **9**(2020).
65. Zhu, L., Li, L., Qi, Y., Yu, Z. & Xu, Y. Cryo-EM structure of SMG1-SMG8-SMG9 complex. *Cell Res* **29**, 1027-1034 (2019).
66. Loewith, R. et al. Two TOR complexes, only one of which is rapamycin sensitive, have distinct roles in cell growth control. *Mol Cell* **10**, 457-68 (2002).
67. Kim, D.H. et al. GbetaL, a positive regulator of the rapamycin-sensitive pathway required for the nutrient-sensitive interaction between raptor and mTOR. *Mol Cell* **11**, 895-904 (2003).
68. Wullschleger, S., Loewith, R., Oppliger, W. & Hall, M.N. Molecular organization of target of rapamycin complex 2. *J Biol Chem* **280**, 30697-704 (2005).
69. Guertin, D.A. et al. Ablation in mice of the mTORC components raptor, rictor, or mLST8 reveals that mTORC2 is required for signaling to Akt-FOXO and PKCalpha, but not S6K1. *Dev Cell* **11**, 859-71 (2006).
70. Hwang, Y. et al. Disruption of the Scaffolding Function of mLST8 Selectively Inhibits mTORC2 Assembly and Function and Suppresses mTORC2-Dependent Tumor Growth In Vivo. *Cancer Res* **79**, 3178-3184 (2019).
71. Hara, K. et al. Raptor, a binding partner of target of rapamycin (TOR), mediates TOR action. *Cell* **110**, 177-89 (2002).
72. Kim, D.H. et al. mTOR interacts with raptor to form a nutrient-sensitive complex that signals to the cell growth machinery. *Cell* **110**, 163-75 (2002).
73. Nojima, H. et al. The mammalian target of rapamycin (mTOR) partner, raptor, binds the mTOR substrates, p70 S6 kinase and 4E-BP1, through their TOR signaling (TOS) motif (vol 278, pg 15461, 2003). *Journal of Biological Chemistry* **278**, 26302-26302 (2003).
74. Tee, A.R. & Proud, C.G. Caspase cleavage of initiation factor 4E-binding protein 1 yields a dominant inhibitor of cap-dependent translation and reveals a novel regulatory motif. *Molecular and Cellular Biology* **22**, 1674-1683 (2002).

75. Schalm, S.S., Fingar, D. & Blenis, J. Identification of a conserved motif required for mTOR signaling. *Molecular Biology of the Cell* **13**, 152a-152a (2002).
76. Wang, L., Harris, T.E., Roth, R.A. & Lawrence, J.C., Jr. PRAS40 regulates mTORC1 kinase activity by functioning as a direct inhibitor of substrate binding. *J Biol Chem* **282**, 20036-44 (2007).
77. Sancak, Y. et al. PRAS40 is an insulin-regulated inhibitor of the mTORC1 protein kinase. *Mol Cell* **25**, 903-15 (2007).
78. Thedieck, K. et al. PRAS40 and PRR5-like protein are new mTOR interactors that regulate apoptosis. *PLoS One* **2**, e1217 (2007).
79. Sarbassov, D.D. et al. Rictor, a novel binding partner of mTOR, defines a rapamycin-insensitive and raptor-independent pathway that regulates the cytoskeleton. *Curr Biol* **14**, 1296-302 (2004).
80. Frias, M.A. et al. mSin1 is necessary for Akt/PKB phosphorylation, and its isoforms define three distinct mTORC2s. *Curr Biol* **16**, 1865-70 (2006).
81. Yang, Q., Inoki, K., Ikenoue, T. & Guan, K.L. Identification of Sin1 as an essential TORC2 component required for complex formation and kinase activity. *Genes Dev* **20**, 2820-32 (2006).
82. Jacinto, E. et al. SIN1/MIP1 maintains rictor-mTOR complex integrity and regulates Akt phosphorylation and substrate specificity. *Cell* **127**, 125-37 (2006).
83. Pearce, L.R. et al. Identification of Protor as a novel Rictor-binding component of mTOR complex-2. *Biochem J* **405**, 513-22 (2007).
84. Sarbassov, D.D. et al. Prolonged rapamycin treatment inhibits mTORC2 assembly and Akt/PKB. *Mol Cell* **22**, 159-68 (2006).
85. Choo, A.Y., Yoon, S.O., Kim, S.G., Roux, P.P. & Blenis, J. Rapamycin differentially inhibits S6Ks and 4E-BP1 to mediate cell-type-specific repression of mRNA translation. *Proceedings of the National Academy of Sciences of the United States of America* **105**, 17414-17419 (2008).
86. Kang, S.A. et al. mTORC1 Phosphorylation Sites Encode Their Sensitivity to Starvation and Rapamycin. *Science* **341**, 364-+ (2013).
87. Thoreen, C.C. et al. An ATP-competitive mammalian target of rapamycin inhibitor reveals rapamycin-resistant functions of mTORC1. *J Biol Chem* **284**, 8023-32 (2009).
88. Sancak, Y. et al. The Rag GTPases bind raptor and mediate amino acid signaling to mTORC1. *Science* **320**, 1496-1501 (2008).
89. Sancak, Y. et al. Ragulator-Rag Complex Targets mTORC1 to the Lysosomal Surface and Is Necessary for Its Activation by Amino Acids. *Cell* **141**, 290-303 (2010).

90. Kim, E., Goraksha-Hicks, P., Li, L., Neufeld, T.P. & Guan, K.L. Regulation of TORC1 by Rag GTPases in nutrient response. *Nature Cell Biology* **10**, 935-945 (2008).
91. Rogala, K.B. et al. Structural basis for the docking of mTORC1 on the lysosomal surface. *Science* **366**, 468-475 (2019).
92. Bar-Peled, L. et al. A Tumor Suppressor Complex with GAP Activity for the Rag GTPases That Signal Amino Acid Sufficiency to mTORC1. *Science* **340**, 1100-1106 (2013).
93. Wolfson, R.L. et al. KICSTOR recruits GATOR1 to the lysosome and is necessary for nutrients to regulate mTORC1. *Nature* **543**, 438-+ (2017).
94. Peng, M., Yin, N. & Li, M.O. SZT2 dictates GATOR control of mTORC1 signalling. *Nature* **543**, 433-+ (2017).
95. Chantranupong, L. et al. The Sestrins Interact with GATOR2 to Negatively Regulate the Amino-Acid-Sensing Pathway Upstream of mTORC1. *Cell Reports* **9**, 1-8 (2014).
96. Parmigiani, A. et al. Sestrins Inhibit mTORC1 Kinase Activation through the GATOR Complex. *Cell Reports* **9**, 1281-1291 (2014).
97. Kim, J.S. et al. Sestrin2 inhibits mTORC1 through modulation of GATOR complexes. *Scientific Reports* **5**(2015).
98. Saxton, R.A. et al. Structural basis for leucine sensing by the Sestrin2-mTORC1 pathway. *Science* **351**, 53-8 (2016).
99. Wolfson, R.L. et al. Sestrin2 is a leucine sensor for the mTORC1 pathway. *Science* **351**, 43-8 (2016).
100. Chen, J. et al. SAR1B senses leucine levels to regulate mTORC1 signalling. *Nature* **596**, 281-+ (2021).
101. Chantranupong, L. et al. The CASTOR Proteins Are Arginine Sensors for the mTORC1 Pathway. *Cell* **165**, 153-164 (2016).
102. Saxton, R.A., Chantranupong, L., Knockenhauer, K.E., Schwartz, T.U. & Sabatini, D.M. Mechanism of arginine sensing by CASTOR1 upstream of mTORC1. *Nature* **536**, 229-33 (2016).
103. Xia, J., Wang, R., Zhang, T. & Ding, J. Structural insight into the arginine-binding specificity of CASTOR1 in amino acid-dependent mTORC1 signaling. *Cell Discov* **2**, 16035 (2016).
104. Gai, Z. et al. Structural mechanism for the arginine sensing and regulation of CASTOR1 in the mTORC1 signaling pathway. *Cell Discov* **2**, 16051 (2016).
105. Zhou, Y.X., Wang, C., Xiao, Q.J. & Guo, L. Crystal structures of arginine sensor CASTOR1 in arginine-bound and ligand free states. *Biochemical and Biophysical Research Communications* **508**, 387-391 (2019).

106. Gu, X. et al. SAMTOR is an S-adenosylmethionine sensor for the mTORC1 pathway. *Science* **358**, 813-818 (2017).
107. Lawrence, R.E. et al. Structural mechanism of a Rag GTPase activation checkpoint by the lysosomal folliculin complex. *Science* **366**, 971-+ (2019).
108. Shen, K. et al. Cryo-EM Structure of the Human FLCN-FNIP2-Rag-Ragulator Complex. *Cell* **179**, 1319-+ (2019).
109. Wang, S.Y. et al. Lysosomal amino acid transporter SLC38A9 signals arginine sufficiency to mTORC1. *Science* **347**, 188-194 (2015).
110. Jung, J., Genau, H.M. & Behrends, C. Amino Acid-Dependent mTORC1 Regulation by the Lysosomal Membrane Protein SLC38A9. *Molecular and Cellular Biology* **35**, 2479-2494 (2015).
111. Rebsamen, M. et al. SLC38A9 is a component of the lysosomal amino acid sensing machinery that controls mTORC1. *Nature* **519**, 477-+ (2015).
112. Lei, H.T., Ma, J.M., Martinez, S.S. & Gonen, T. Crystal structure of arginine-bound lysosomal transporter SLC38A9 in the cytosol-open state. *Nature Structural & Molecular Biology* **25**, 522-+ (2018).
113. Lei, H.T., Mu, X.L., Hattne, J. & Gonen, T. A conformational change in the N terminus of SLC38A9 signals mTORC1 activation. *Structure* **29**, 426-+ (2021).
114. Fromm, S.A., Lawrence, R.E. & Hurley, J.H. Structural mechanism for amino acid-dependent Rag GTPase nucleotide state switching by SLC38A9. *Nature Structural & Molecular Biology* **27**, 1017-+ (2020).
115. Castellano, B.M. et al. CHOLESTEROL SENSING Lysosomal cholesterol activates mTORC1 via an SLC38A9-Niemann-Pick C1 signaling complex. *Science* **355**, 1306-1311 (2017).
116. Duran, R.V. et al. Glutaminolysis Activates Rag-mTORC1 Signaling. *Molecular Cell* **47**, 349-358 (2012).
117. Han, J.M. et al. Leucyl-tRNA Synthetase Is an Intracellular Leucine Sensor for the mTORC1-Signaling Pathway. *Cell* **149**, 410-424 (2012).
118. Long, X., Lin, Y., Ortiz-Vega, S., Yonezawa, K. & Avruch, J. Rheb binds and regulates the mTOR kinase. *Current Biology* **15**, 702-713 (2005).
119. Tee, A.R., Manning, B.D., Roux, P.P., Cantley, L.C. & Blenis, J. Tuberous sclerosis complex gene products, tuberin and hamartin, control mTOR signaling by acting as a GTPase-activating protein complex toward Rheb. *Current Biology* **13**, 1259-1268 (2003).
120. Zhang, Y. et al. Rheb is a direct target of the tuberous sclerosis tumour suppressor proteins. *Nature Cell Biology* **5**, 578-581 (2003).

121. Garami, A. et al. Insulin activation of Rheb, a mediator of mTOR/S6K/4E-BP signaling, is inhibited by TSC1 and 2. *Molecular Cell* **11**, 1457-1466 (2003).
122. Traut, T.W. Physiological Concentrations of Purines and Pyrimidines. *Molecular and Cellular Biochemistry* **140**, 1-22 (1994).
123. Gao, X.S. et al. Tsc tumour suppressor proteins antagonize amino-acid-TOR signalling. *Nature Cell Biology* **4**, 699-704 (2002).
124. Tee, A.R. et al. Tuberous sclerosis complex-1 and -2 gene products function together to inhibit mammalian target of rapamycin (mTOR)-mediated downstream signaling. *Proceedings of the National Academy of Sciences of the United States of America* **99**, 13571-13576 (2002).
125. Manning, B.D., Tee, A.R., Logsdon, M.N., Blenis, J. & Cantley, L.C. Identification of the tuberous sclerosis complex-2 tumor suppressor gene product tuberin as a target of the phosphoinositide 3-Kinase/Akt pathway. *Molecular Cell* **10**, 151-162 (2002).
126. Inoki, K., Li, Y., Zhu, T.Q., Wu, J. & Guan, K.L. TSC2 is phosphorylated and inhibited by Akt and suppresses mTOR signalling. *Nature Cell Biology* **4**, 648-657 (2002).
127. Menon, S. et al. Spatial Control of the TSC Complex Integrates Insulin and Nutrient Regulation of mTORC1 at the Lysosome. *Cell* **156**, 771-785 (2014).
128. Roux, P.P., Ballif, B.A., Anjum, R., Gygi, S.P. & Blenis, J. Tumor-promoting phorbol esters and activated Ras inactivate the tuberous sclerosis tumor suppressor complex via p90 ribosomal S6 kinase. *Proceedings of the National Academy of Sciences of the United States of America* **101**, 13489-13494 (2004).
129. Ma, L., Chen, Z.B., Erdjument-Bromage, H., Tempst, P. & Pandolfi, P.P. Phosphorylation and functional inactivation of TSC2 by Erk: Implications for tuberous sclerosis and cancer pathogenesis. *Cell* **121**, 179-193 (2005).
130. Vander Haar, E., Lee, S., Bandhakavi, S., Griffin, T.J. & Kim, D.H. Insulin signalling to mTOR mediated by the Akt/PKB substrate PRAS40. *Nature Cell Biology* **9**, 316-U126 (2007).
131. Li, T. et al. RNF167 activates mTORC1 and promotes tumorigenesis by targeting CASTOR1 for ubiquitination and degradation. *Nat Commun* **12**, 1055 (2021).
132. Inoki, K., Zhu, T.Q. & Guan, K.L. TSC2 mediates cellular energy response to control cell growth and survival. *Cell* **115**, 577-590 (2003).
133. Gwinn, D.M. et al. AMPK phosphorylation of raptor mediates a metabolic checkpoint. *Molecular Cell* **30**, 214-226 (2008).
134. Brugarolas, J. et al. Regulation of mTOR function in response to hypoxia by REDD1 and the TSC1/TSC2 tumor suppressor complex. *Genes & Development* **18**, 2893-2904 (2004).

135. Reiling, J.H. & Hafen, E. The hypoxia-induced paralogs scylla and charybdis inhibit growth by down-regulating S6K activity upstream of TSC in Drosophila. *Genes & Development* **18**, 2879-2892 (2004).
136. DeYoung, M.P., Horak, P., Sofer, A., Sgroi, D. & Ellisen, L.W. Hypoxia regulates TSC1/2-mTOR signaling and tumor suppression through REDD1-mediated 14-3-3 shuttling. *Genes & Development* **22**, 239-251 (2008).
137. Saveljeva, S. et al. Endoplasmic reticulum stress-mediated induction of SESTRIN 2 potentiates cell survival. *Oncotarget* **7**, 12254-12266 (2016).
138. Budanov, A.V. & Karin, M. p53 Target Genes Sestrin1 and Sestrin2 Connect Genotoxic Stress and mTOR Signaling (vol 134, pg 451, 2008). *Cell* **136**, 378-378 (2009).
139. Buttgereit, F. & Brand, M.D. A Hierarchy of Atp-Consuming Processes in Mammalian-Cells. *Biochemical Journal* **312**, 163-167 (1995).
140. Fletcher, C.M. et al. 4E binding proteins inhibit the translation factor eIF4E without folded structure. *Biochemistry* **37**, 9-15 (1998).
141. Brunn, G.J. et al. Phosphorylation of the translational repressor PHAS-I by the mammalian target of rapamycin. *Science* **277**, 99-101 (1997).
142. Gingras, A.C. et al. Regulation of 4E-BP1 phosphorylation: a novel two-step mechanism. *Genes & Development* **13**, 1422-1437 (1999).
143. Hara, K. et al. Regulation of eIF-4E BP1 phosphorylation by mTOR. *Journal of Biological Chemistry* **272**, 26457-26463 (1997).
144. Böhm, R. et al. The dynamic mechanism of 4E-BP1 recognition and phosphorylation by mTORC1. *Mol Cell* (2021).
145. Burnett, P.E., Barrow, R.K., Cohen, N.A., Snyder, S.H. & Sabatini, D.M. RAFT1 phosphorylation of the translational regulators p70 S6 kinase and 4E-BP1. *Proc Natl Acad Sci U S A* **95**, 1432-7 (1998).
146. Pullen, N. et al. Phosphorylation and activation of p70(s6k) by PDK1. *Science* **279**, 707-710 (1998).
147. Ruvinsky, I. et al. Ribosomal protein S6 phosphorylation is a determinant of cell size and glucose homeostasis. *Genes & Development* **19**, 2199-2211 (2005).
148. Chauvin, C. et al. Ribosomal protein S6 kinase activity controls the ribosome biogenesis transcriptional program. *Oncogene* **33**, 474-483 (2014).
149. Hannan, K.M. et al. mTOR-Dependent regulation of ribosomal gene transcription requires S6K1 and is mediated by phosphorylation of the carboxy-terminal activation domain of the nucleolar transcription factor UBF. *Molecular and Cellular Biology* **23**, 8862-8877 (2003).

150. Michels, A.A. et al. mTORC1 directly phosphorylates and regulates human MAF1. *Mol Cell Biol* **30**, 3749-57 (2010).
151. Shor, B. et al. Requirement of the mTOR Kinase for the Regulation of Maf1 Phosphorylation and Control of RNA Polymerase III-dependent Transcription in Cancer Cells. *Journal of Biological Chemistry* **285**, 15380-15392 (2010).
152. Mayer, C., Zhao, J., Yuan, X.J. & Grummt, I. mTOR-dependent activation of the transcription factor TIMA links rRNA synthesis to nutrient availability. *Genes & Development* **18**, 423-434 (2004).
153. Shimano, H. & Sato, R. SREBP-regulated lipid metabolism: convergent physiology - divergent pathophysiology. *Nature Reviews Endocrinology* **13**, 710-730 (2017).
154. Brown, M.S. & Goldstein, J.L. The SREBP pathway: Regulation of cholesterol metabolism by proteolysis of a membrane-bound transcription factor. *Cell* **89**, 331-340 (1997).
155. Peterson, T.R. et al. mTOR Complex 1 Regulates Lipin 1 Localization to Control the SREBP Pathway. *Cell* **146**, 408-420 (2011).
156. Grygiel-Gorniak, B. Peroxisome proliferator-activated receptors and their ligands: nutritional and clinical implications - a review. *Nutrition Journal* **13**(2014).
157. Kim, J.E. & Chen, J. Regulation of peroxisome proliferator-activated receptor-gamma activity by mammalian target of rapamycin and amino acids in adipogenesis. *Diabetes* **53**, 2748-2756 (2004).
158. Lane, A.N. & Fan, T.W.M. Regulation of mammalian nucleotide metabolism and biosynthesis. *Nucleic Acids Research* **43**, 2466-2485 (2015).
159. Ben-Sahra, I., Hoxhaj, G., Ricoult, S.J.H., Asara, J.M. & Manning, B.D. mTORC1 induces purine synthesis through control of the mitochondrial tetrahydrofolate cycle. *Science* **351**, 728-733 (2016).
160. Ben-Sahra, I., Howell, J.J., Asara, J.M. & Manning, B.D. Stimulation of de Novo Pyrimidine Synthesis by Growth Signaling Through mTOR and S6K1. *Science* **339**, 1323-1328 (2013).
161. Robitaille, A.M. et al. Quantitative Phosphoproteomics Reveal mTORC1 Activates de Novo Pyrimidine Synthesis. *Science* **339**, 1320-1323 (2013).
162. He, C.C. & Klionsky, D.J. Regulation Mechanisms and Signaling Pathways of Autophagy. *Annual Review of Genetics* **43**, 67-93 (2009).
163. Kim, J., Kundu, M., Viollet, B. & Guan, K.L. AMPK and mTOR regulate autophagy through direct phosphorylation of Ulk1. *Nat Cell Biol* **13**, 132-41 (2011).

164. Martina, J.A., Chen, Y., Gucek, M. & Puertollano, R. MTORC1 functions as a transcriptional regulator of autophagy by preventing nuclear transport of TFEB. *Autophagy* **8**, 903-914 (2012).
165. Mori, S. et al. The mTOR Pathway Controls Cell Proliferation by Regulating the FoxO3a Transcription Factor via SGK1 Kinase. *Plos One* **9**(2014).
166. Brunet, A. et al. Akt promotes cell survival by phosphorylating and inhibiting a forkhead transcription factor. *Cell* **96**, 857-868 (1999).
167. Jacinto, E. et al. Mammalian TOR complex 2 controls the actin cytoskeleton and is rapamycin insensitive. *Nat Cell Biol* **6**, 1122-8 (2004).
168. Chen, C.Y., Chen, J.Y., He, L.N. & Stiles, B.L. PTEN: Tumor Suppressor and Metabolic Regulator. *Frontiers in Endocrinology* **9**(2018).
169. Liu, P.D. et al. PtdIns(3,4,5)P-3-Dependent Activation of the mTORC2 Kinase Complex. *Cancer Discovery* **5**, 1194-1209 (2015).
170. Betz, C. et al. mTOR complex 2-Akt signaling at mitochondria-associated endoplasmic reticulum membranes (MAM) regulates mitochondrial physiology. *Proceedings of the National Academy of Sciences of the United States of America* **110**, 12526-12534 (2013).
171. Ebner, M., Sinkovics, B., Szczygiel, M., Ribeiro, D.W. & Yudushkin, I. Localization of mTORC2 activity inside cells. *Journal of Cell Biology* **216**, 343-353 (2017).
172. Oh, W.J. et al. mTORC2 can associate with ribosomes to promote cotranslational phosphorylation and stability of nascent Akt polypeptide. *EMBO J* **29**, 3939-51 (2010).
173. Sato, T., Nakashima, A., Guo, L. & Tamanoi, F. Specific activation of mTORC1 by Rheb G-protein in vitro involves enhanced recruitment of its substrate protein. *J Biol Chem* **284**, 12783-91 (2009).
174. Locke, M.N. & Thorner, J. Rab5 GTPases are required for optimal TORC2 function. *J Cell Biol* **218**, 961-976 (2019).
175. Joly, M.M. et al. Two distinct mTORC2-dependent pathways converge on Rac1 to drive breast cancer metastasis. *Breast Cancer Research* **19**(2017).
176. Senoo, H. et al. Phosphorylated Rho-GDP directly activates mTORC2 kinase towards AKT through dimerization with Ras-GTP to regulate cell migration. *Nature Cell Biology* **21**, 867-+ (2019).
177. Kovalski, J.R. et al. The Functional Proximal Proteome of Oncogenic Ras Includes mTORC2. *Molecular Cell* **73**, 830-+ (2019).
178. Um, S.H. et al. Absence of S6K1 protects against age- and diet-induced obesity while enhancing insulin sensitivity (vol 431, pg 200, 2004). *Nature* **431**, 485-485 (2004).

179. Yang, H. et al. mTOR kinase structure, mechanism and regulation. *Nature* **497**, 217-23 (2013).
180. Aylett, C.H. et al. Architecture of human mTOR complex 1. *Science* **351**, 48-52 (2016).
181. Baretic, D., Berndt, A., Ohashi, Y., Johnson, C.M. & Williams, R.L. Tor forms a dimer through an N-terminal helical solenoid with a complex topology. *Nat Commun* **7**, 11016 (2016).
182. Peterson, T.R. et al. DEPTOR Is an mTOR Inhibitor Frequently Overexpressed in Multiple Myeloma Cells and Required for Their Survival. *Cell* **137**, 873-886 (2009).
183. Caron, A., Briscoe, D.M., Richard, D. & Laplante, M. Deptor at the Nexus of Cancer, Metabolism, and Immunity. *Physiological Reviews* **98**, 1765-1803 (2018).
184. Hernandez-Negrete, I. et al. P-Rex1 links mammalian target of rapamycin signaling to Rac activation and cell migration. *Journal of Biological Chemistry* **282**, 23708-23715 (2007).
185. Consonni, S.V., Maurice, M.M. & Bos, J.L. DEP domains: structurally similar but functionally different. *Nature Reviews Molecular Cell Biology* **15**, 357-362 (2014).
186. Schultz, J., Milpetz, F., Bork, P. & Ponting, C.P. SMART, a simple modular architecture research tool: Identification of signaling domains. *Proceedings of the National Academy of Sciences of the United States of America* **95**, 5857-5864 (1998).
187. Liu, X. & Fuentes, E.J. Emerging Themes in PDZ Domain Signaling: Structure, Function, and Inhibition. *International Review of Cell and Molecular Biology, Vol 343* **343**, 129-218 (2019).
188. Duan, S.S. et al. mTOR Generates an Auto-Amplification Loop by Triggering the beta TrCP- and CK1 alpha-Dependent Degradation of DEPTOR. *Molecular Cell* **44**, 317-324 (2011).
189. Gao, D.M. et al. mTOR Drives Its Own Activation via SCF beta TrCP-Dependent Degradation of the mTOR Inhibitor DEPTOR. *Molecular Cell* **44**, 290-303 (2011).
190. Zhao, Y.C., Xiong, X.F. & Sun, Y. DEPTOR, an mTOR Inhibitor, Is a Physiological Substrate of SCF beta TrCP E3 Ubiquitin Ligase and Regulates Survival and Autophagy. *Molecular Cell* **44**, 304-316 (2011).
191. Zhao, L.L. et al. OTUB1 protein suppresses mTOR complex 1 (mTORC1) activity by deubiquitinating the mTORC1 inhibitor DEPTOR. *Journal of Biological Chemistry* **293**, 4883-4892 (2018).
192. Simonetta, K.R. et al. Prospective discovery of small molecule enhancers of an E3 ligase-substrate interaction. *Nature Communications* **10**(2019).
193. Schweitzer, A. et al. Structure of the human 26S proteasome at a resolution of 3.9 angstrom. *Proceedings of the National Academy of Sciences of the United States of America* **113**, 7816-7821 (2016).

194. Fang, Y.M. et al. PLD1 regulates mTOR signaling and mediates Cdc42 activation of S6K1. *Current Biology* **13**, 2037-2044 (2003).
195. Fang, Y.M., Vilella-Bach, M., Bachmann, R., Flanigan, A. & Chen, J. Phosphatidic acid-mediated mitogenic activation of mTOR signaling. *Science* **294**, 1942-1945 (2001).
196. Yoon, M.S. et al. Rapid Mitogenic Regulation of the mTORC1 Inhibitor, DEPTOR, by Phosphatidic Acid. *Molecular Cell* **58**, 549-556 (2015).
197. Song, H.I. & Yoon, M.S. PLD1 regulates adipogenic differentiation through mTOR - IRS-1 phosphorylation at serine 636/639. *Scientific Reports* **6**(2016).
198. Das, F. et al. Transforming Growth Factor beta Integrates Smad 3 to Mechanistic Target of Rapamycin Complexes to Arrest Deptor Abundance for Glomerular Mesangial Cell Hypertrophy. *Journal of Biological Chemistry* **288**, 7756-7768 (2013).
199. Ji, Y.M. et al. DEPTOR suppresses the progression of esophageal squamous cell carcinoma and predicts poor prognosis. *Oncotarget* **7**, 14188-14198 (2016).
200. Li, H. et al. DEPTOR has growth suppression activity against pancreatic cancer cells. *Oncotarget* **5**, 12811-12819 (2014).
201. Zhou, X.F. et al. Reciprocal Negative Regulation between EGFR and DEPTOR Plays an Important Role in the Progression of Lung Adenocarcinoma. *Molecular Cancer Research* **14**, 448-457 (2016).
202. Ohshima, K. et al. Argininosuccinate Synthase 1-Deficiency Enhances the Cell Sensitivity to Arginine through Decreased DEPTOR Expression in Endometrial Cancer. *Scientific Reports* **7**(2017).
203. Parvani, J.G. et al. Deptor Enhances Triple-Negative Breast Cancer Metastasis and Chemoresistance through Coupling to Survivin Expression. *Neoplasia* **17**, 317-328 (2015).
204. Hu, B.W. et al. Downregulation of DEPTOR inhibits the proliferation, migration, and survival of osteosarcoma through PI3K/Akt/mTOR pathway. *Oncotargets and Therapy* **10**, 4379-4391 (2017).
205. Caron, A. et al. Mediobasal hypothalamic overexpression of DEPTOR protects against high-fat diet-induced obesity. *Molecular Metabolism* **5**, 102-112 (2016).
206. Laplante, M. et al. DEPTOR Cell-Autonomously Promotes Adipogenesis, and Its Expression Is Associated with Obesity. *Cell Metabolism* **16**, 202-212 (2012).
207. Caron, A. et al. Loss of hepatic DEPTOR alters the metabolic transition to fasting. *Molecular Metabolism* **6**, 447-458 (2017).
208. Wang, Y.F. et al. Has the prevalence of overweight, obesity and central obesity levelled off in the United States? Trends, patterns, disparities, and future projections for the obesity epidemic. *International Journal of Epidemiology* **49**, 810-823 (2020).

209. Djalalinia, S., Qorbani, M., Peykari, N. & Kelishadi, R. Health impacts of obesity. *Pakistan Journal of Medical Sciences* **31**, 239-242 (2015).
210. Berger, J. & Moller, D.E. The mechanisms of action of PPARs. *Annual Review of Medicine* **53**, 409-435 (2002).
211. Liu, G.Y. & Sabatini, D.M. mTOR at the nexus of nutrition, growth, ageing and disease. *Nature Reviews Molecular Cell Biology* **21**, 183-203 (2020).
212. Loewith, R. & Hall, M.N. Target of Rapamycin (TOR) in Nutrient Signaling and Growth Control. *Genetics* **189**, 1177-1201 (2011).
213. Weng, Z., Shen, X., Zheng, J., Liang, H. & Liu, Y. Structural basis of DEPTOR to recognize phosphatidic acid using its tandem DEP domains. *Journal of Molecular Biology*, 166989 (2021).
214. Catena, V. & Fanciulli, M. Deptor: not only a mTOR inhibitor. *J Exp Clin Cancer Res* **36**, 12 (2017).
215. Wedel, J. et al. DEPTOR modulates activation responses in CD4(+) T cells and enhances immunoregulation following transplantation. *American Journal of Transplantation* **19**, 77-88 (2019).
216. Wedel, J., Bruneau, S., Liu, K.F., Laplante, M. & Briscoe, D.M. DEPTOR modulates alloimmunity by increasing regulatory T cell function and stabilizing Foxp3 expression. *Transplantation* **100**, S221-S221 (2016).
217. Anandapadamanaban, M. et al. Architecture of human Rag GTPase heterodimers and their complex with mTORC1. *Science* **366**, 203-210 (2019).
218. Lee, H.-J. & Zheng, J.J. PDZ domains and their binding partners: structure, specificity, and modification. *Cell Communication and Signaling* **8**, 8 (2010).
219. Ota, T. et al. Complete sequencing and characterization of 21,243 full-length human cDNAs. *Nature Genetics* **36**, 40-45 (2004).
220. Grabiner, B.C. et al. A Diverse Array of Cancer-Associated MTOR Mutations Are Hyperactivating and Can Predict Rapamycin Sensitivity. *Cancer Discovery* **4**, 554-563 (2014).
221. Sato, T., Nakashima, A., Guo, L., Coffman, K. & Tamanoi, F. Single amino-acid changes that confer constitutive activation of mTOR are discovered in human cancer. *Oncogene* **29**, 2746-52 (2010).
222. Xu, J. et al. Mechanistically distinct cancer-associated mTOR activation clusters predict sensitivity to rapamycin. *J Clin Invest* **126**, 3526-40 (2016).
223. Tatebe, H. et al. Substrate specificity of TOR complex 2 is determined by a ubiquitin-fold domain of the Sin1 subunit. *Elife* **6**(2017).

224. Benavides-Serrato, A. et al. Specific blockade of Rictor-mTOR association inhibits mTORC2 activity and is cytotoxic in glioblastoma. *Plos One* **12**(2017).
225. Benjamin, D., Colombi, M., Moroni, C. & Hall, M.N. Rapamycin passes the torch: a new generation of mTOR inhibitors. *Nature Reviews Drug Discovery* **10**, 868-880 (2011).
226. Wang, Q. et al. The mTOR inhibitor manassantin B reveals a crucial role of mTORC2 signaling in Epstein-Barr virus reactivation. *Journal of Biological Chemistry* **295**, 7431-7441 (2020).
227. Guenzle, J. et al. Pharmacological Inhibition of mTORC2 Reduces Migration and Metastasis in Melanoma. *International Journal of Molecular Sciences* **22**(2021).
228. Heimhalt, M. et al. Bipartite binding and partial inhibition links DEPTOR and mTOR in a mutually antagonistic embrace. *Elife* **10**(2021).
229. Takahara, T., Amemiya, Y., Sugiyama, R., Maki, M. & Shibata, H. Amino acid-dependent control of mTORC1 signaling: a variety of regulatory modes. *Journal of Biomedical Science* **27**(2020).
230. Fitzgerald, D.J. et al. Protein complex expression by using multigene baculoviral vectors. *Nature Methods* **3**, 1021-1032 (2006).
231. Evans, P.R. & Murshudov, G.N. How good are my data and what is the resolution? *Acta Crystallographica Section D-Biological Crystallography* **69**, 1204-1214 (2013).
232. White, M.A. et al. Structural Analyses of a Constitutively Active Mutant of Exchange Protein Directly Activated by cAMP. *Plos One* **7**(2012).
233. Mccoy, A.J. et al. Phaser crystallographic software. *Journal of Applied Crystallography* **40**, 658-674 (2007).
234. Emsley, P. & Cowtan, K. Coot: model-building tools for molecular graphics. *Acta Crystallographica Section D-Structural Biology* **60**, 2126-2132 (2004).
235. Adams, P.D. et al. PHENIX: building new software for automated crystallographic structure determination. *Acta Crystallographica Section D-Structural Biology* **58**, 1948-1954 (2002).
236. Williams, C.J. et al. MolProbity: More and better reference data for improved all-atom structure validation. *Protein Science* **27**, 293-315 (2018).
237. Svergun, D., Barberato, C. & Koch, M.H.J. CRYSOL - A program to evaluate x-ray solution scattering of biological macromolecules from atomic coordinates. *Journal of Applied Crystallography* **28**, 768-773 (1995).
238. Manalastas-Cantos, K. et al. ATSAS 3.0: expanded functionality and new tools for small-angle scattering data analysis. *Journal of Applied Crystallography* **54**, 343-355 (2021).
239. Mastronarde, D.N. Automated electron microscope tomography using robust prediction of specimen movements. *Journal of Structural Biology* **152**, 36-51 (2005).

240. Punjani, A., Rubinstein, J.L., Fleet, D.J. & Brubaker, M.A. cryoSPARC: algorithms for rapid unsupervised cryo-EM structure determination. *Nature Methods* **14**, 290-+ (2017).
241. Zivanov, J. et al. New tools for automated high-resolution cryo-EM structure determination in RELION-3. *Elife* **7**(2018).
242. Zheng, S.Q. et al. MotionCor2: anisotropic correction of beam-induced motion for improved cryo-electron microscopy. *Nature Methods* **14**, 331-332 (2017).
243. Rohou, A. & Grigorieff, N. CTFFIND4: Fast and accurate defocus estimation from electron micrographs. *Journal of Structural Biology* **192**, 216-221 (2015).
244. Zivanov, J., Nakane, T. & Scheres, S.H.W. Estimation of high-order aberrations and anisotropic magnification from cryo-EM data sets in RELION-3.1. *Iucrj* **7**, 253-267 (2020).
245. Punjani, A., Zhang, H.W. & Fleet, D.J. Non-uniform refinement: adaptive regularization improves single-particle cryo-EM reconstruction. *Nature Methods* **17**, 1214-+ (2020).
246. Punjani, A. & Fleet, D.J. 3D variability analysis: Resolving continuous flexibility and discrete heterogeneity from single particle cryo-EM. *J Struct Biol* **213**, 107702 (2021).
247. Yang, J.Y. et al. Improved protein structure prediction using predicted interresidue orientations. *Proceedings of the National Academy of Sciences of the United States of America* **117**, 1496-1503 (2020).
248. Afonine, P.V. et al. Real-space refinement in PHENIX for cryo-EM and crystallography. *Acta Crystallographica Section D-Structural Biology* **74**, 531-544 (2018).
249. Krissinel, E. & Henrick, K. Inference of macromolecular assemblies from crystalline state. *Journal of Molecular Biology* **372**, 774-797 (2007).
250. Madeira, F. et al. The EMBL-EBI search and sequence analysis tools APIs in 2019. *Nucleic Acids Research* **47**, W636-W641 (2019).
251. Pei, J.M. & Grishin, N.V. AL2CO: calculation of positional conservation in a protein sequence alignment. *Bioinformatics* **17**, 700-712 (2001).
252. Pettersen, E.F. et al. UCSF ChimeraX: Structure visualization for researchers, educators, and developers. *Protein Science* **30**, 70-82 (2021).
253. Schrodinger, LLC. The PyMOL Molecular Graphics System, Version 1.8. (2015).
254. Schmelzle, T. & Hall, M.N. TOR, a central controller of cell growth. *Cell* **103**, 253-62 (2000).
255. Hunter, T. The genesis of tyrosine phosphorylation. *Cold Spring Harb Perspect Biol* **6**, a020644 (2014).
256. Wullschleger, S., Loewith, R. & Hall, M.N. TOR signaling in growth and metabolism. *Cell* **124**, 471-84 (2006).
257. Saxton, R.A. & Sabatini, D.M. mTOR Signaling in Growth, Metabolism, and Disease. *Cell* **169**, 361-371 (2017).

258. Chao, L.H. & Avruch, J. Cryo-EM insight into the structure of MTOR complex 1 and its interactions with Rheb and substrates. *F1000Res* **8**(2019).
259. Karuppasamy, M. et al. Cryo-EM structure of Saccharomyces cerevisiae target of rapamycin complex 2. *Nat Commun* **8**, 1729 (2017).
260. Berchtold, D. & Walther, T.C. TORC2 plasma membrane localization is essential for cell viability and restricted to a distinct domain. *Mol Biol Cell* **20**, 1565-75 (2009).
261. Liu, P. et al. PtdIns(3,4,5)P3-Dependent Activation of the mTORC2 Kinase Complex. *Cancer Discov* **5**, 1194-209 (2015).
262. Condon, K.J. & Sabatini, D.M. Nutrient regulation of mTORC1 at a glance. *J Cell Sci* **132**(2019).
263. Tsun, Z.Y. et al. The folliculin tumor suppressor is a GAP for the RagC/D GTPases that signal amino acid levels to mTORC1. *Mol Cell* **52**, 495-505 (2013).
264. Petit, C.S., Roczniak-Ferguson, A. & Ferguson, S.M. Recruitment of folliculin to lysosomes supports the amino acid-dependent activation of Rag GTPases. *J Cell Biol* **202**, 1107-22 (2013).
265. Anthony, J.C. et al. Leucine stimulates translation initiation in skeletal muscle of postabsorptive rats via a rapamycin-sensitive pathway. *J Nutr* **130**, 2413-9 (2000).
266. Chen, J. et al. SAR1B senses leucine levels to regulate mTORC1 signalling. *Nature* **596**, 281-284 (2021).
267. Dibble, C.C. et al. TBC1D7 is a third subunit of the TSC1-TSC2 complex upstream of mTORC1. *Mol Cell* **47**, 535-46 (2012).
268. Huang, J. & Manning, B.D. The TSC1-TSC2 complex: a molecular switchboard controlling cell growth. *Biochem J* **412**, 179-90 (2008).
269. Dibble, C.C. & Manning, B.D. Signal integration by mTORC1 coordinates nutrient input with biosynthetic output. *Nat Cell Biol* **15**, 555-64 (2013).
270. Steinberg, G.R. & Carling, D. AMP-activated protein kinase: the current landscape for drug development. *Nat Rev Drug Discov* **18**, 527-551 (2019).
271. Van Nostrand, J.L. et al. AMPK regulation of Raptor and TSC2 mediate metformin effects on transcriptional control of anabolism and inflammation. *Genes Dev* **34**, 1330-1344 (2020).
272. Gonzalez, A., Hall, M.N., Lin, S.C. & Hardie, D.G. AMPK and TOR: The Yin and Yang of Cellular Nutrient Sensing and Growth Control. *Cell Metabolism* **31**, 472-492 (2020).
273. Ling, N.X.Y. et al. mTORC1 directly inhibits AMPK to promote cell proliferation under nutrient stress. *Nat Metab* **2**, 41-49 (2020).

274. Needham, E.J. et al. Personalized phosphoproteomics identifies functional signaling. *Nat Biotechnol* (2021).
275. Kazyken, D. et al. AMPK directly activates mTORC2 to promote cell survival during acute energetic stress. *Sci Signal* **12**(2019).
276. Zinzalla, V., Stracka, D., Oppliger, W. & Hall, M.N. Activation of mTORC2 by association with the ribosome. *Cell* **144**, 757-68 (2011).
277. Yang, G., Murashige, D.S., Humphrey, S.J. & James, D.E. A Positive Feedback Loop between Akt and mTORC2 via SIN1 Phosphorylation. *Cell Rep* **12**, 937-43 (2015).
278. Harrington, L.S. et al. The TSC1-2 tumor suppressor controls insulin-PI3K signaling via regulation of IRS proteins. *J Cell Biol* **166**, 213-23 (2004).
279. Shah, O.J., Wang, Z. & Hunter, T. Inappropriate activation of the TSC/Rheb/mTOR/S6K cassette induces IRS1/2 depletion, insulin resistance, and cell survival deficiencies. *Curr Biol* **14**, 1650-6 (2004).
280. Um, S.H. et al. Absence of S6K1 protects against age- and diet-induced obesity while enhancing insulin sensitivity. *Nature* **431**, 200-5 (2004).
281. Dibble, C.C., Asara, J.M. & Manning, B.D. Characterization of Rictor phosphorylation sites reveals direct regulation of mTOR complex 2 by S6K1. *Mol Cell Biol* **29**, 5657-70 (2009).
282. Julien, L.A., Carriere, A., Moreau, J. & Roux, P.P. mTORC1-activated S6K1 phosphorylates Rictor on threonine 1135 and regulates mTORC2 signaling. *Mol Cell Biol* **30**, 908-21 (2010).
283. Liu, P. et al. Sin1 phosphorylation impairs mTORC2 complex integrity and inhibits downstream Akt signalling to suppress tumorigenesis. *Nat Cell Biol* **15**, 1340-50 (2013).
284. Walchli, M. et al. Regulation of human mTOR complexes by DEPTOR. *Elife* **10**(2021).
285. Kovacina, K.S. et al. Identification of a proline-rich Akt substrate as a 14-3-3 binding partner. *J Biol Chem* **278**, 10189-94 (2003).
286. Oshiro, N. et al. The proline-rich Akt substrate of 40 kDa (PRAS40) is a physiological substrate of mammalian target of rapamycin complex 1. *J Biol Chem* **282**, 20329-39 (2007).
287. Wang, L., Harris, T.E. & Lawrence, J.C., Jr. Regulation of proline-rich Akt substrate of 40 kDa (PRAS40) function by mammalian target of rapamycin complex 1 (mTORC1)-mediated phosphorylation. *J Biol Chem* **283**, 15619-27 (2008).
288. Magnuson, B., Ekim, B. & Fingar, D.C. Regulation and function of ribosomal protein S6 kinase (S6K) within mTOR signalling networks. *Biochem J* **441**, 1-21 (2012).
289. Tavares, M.R. et al. The S6K protein family in health and disease. *Life Sci* **131**, 1-10 (2015).

290. Alessi, D.R., Kozlowski, M.T., Weng, Q.P., Morrice, N. & Avruch, J. 3-Phosphoinositide-dependent protein kinase 1 (PDK1) phosphorylates and activates the p70 S6 kinase in vivo and in vitro. *Curr Biol* **8**, 69-81 (1998).
291. Weng, Q.P. et al. Regulation of the p70 S6 kinase by phosphorylation in vivo. Analysis using site-specific anti-phosphopeptide antibodies. *J Biol Chem* **273**, 16621-9 (1998).
292. Keshwani, M.M., von Daake, S., Newton, A.C., Harris, T.K. & Taylor, S.S. Hydrophobic motif phosphorylation is not required for activation loop phosphorylation of p70 ribosomal protein S6 kinase 1 (S6K1). *J Biol Chem* **286**, 23552-8 (2011).
293. Ferrari, S., Bannwarth, W., Morley, S.J., Totty, N.F. & Thomas, G. Activation of p70s6k is associated with phosphorylation of four clustered sites displaying Ser/Thr-Pro motifs. *Proc Natl Acad Sci U S A* **89**, 7282-6 (1992).
294. Mukhopadhyay, N.K. et al. An array of insulin-activated, proline-directed serine/threonine protein kinases phosphorylate the p70 S6 kinase. *J Biol Chem* **267**, 3325-35 (1992).
295. Saitoh, M. et al. Regulation of an activated S6 kinase 1 variant reveals a novel mammalian target of rapamycin phosphorylation site. *J Biol Chem* **277**, 20104-12 (2002).
296. Beretta, L., Gingras, A.C., Svitkin, Y.V., Hall, M.N. & Sonenberg, N. Rapamycin blocks the phosphorylation of 4E-BP1 and inhibits cap-dependent initiation of translation. *EMBO J* **15**, 658-64 (1996).
297. von Manteuffel, S.R., Gingras, A.C., Ming, X.F., Sonenberg, N. & Thomas, G. 4E-BP1 phosphorylation is mediated by the FRAP-p70s6k pathway and is independent of mitogen-activated protein kinase. *Proc Natl Acad Sci U S A* **93**, 4076-80 (1996).
298. Poulin, F., Gingras, A.C., Olsen, H., Chevalier, S. & Sonenberg, N. 4E-BP3, a new member of the eukaryotic initiation factor 4E-binding protein family. *J Biol Chem* **273**, 14002-7 (1998).
299. Pause, A. et al. Insulin-dependent stimulation of protein synthesis by phosphorylation of a regulator of 5'-cap function. *Nature* **371**, 762-7 (1994).
300. Lin, T.A. et al. PHAS-I as a link between mitogen-activated protein kinase and translation initiation. *Science* **266**, 653-6 (1994).
301. Mader, S., Lee, H., Pause, A. & Sonenberg, N. The translation initiation factor eIF-4E binds to a common motif shared by the translation factor eIF-4 gamma and the translational repressors 4E-binding proteins. *Mol Cell Biol* **15**, 4990-7 (1995).
302. Heesom, K.J. & Denton, R.M. Dissociation of the eukaryotic initiation factor-4E/4E-BP1 complex involves phosphorylation of 4E-BP1 by an mTOR-associated kinase. *FEBS Lett* **457**, 489-93 (1999).

303. Mothe-Satney, I., Yang, D., Fadden, P., Haystead, T.A. & Lawrence, J.C., Jr. Multiple mechanisms control phosphorylation of PHAS-I in five (S/T)P sites that govern translational repression. *Mol Cell Biol* **20**, 3558-67 (2000).
304. Gingras, A.C. et al. Hierarchical phosphorylation of the translation inhibitor 4E-BP1. *Genes Dev* **15**, 2852-64 (2001).
305. Bah, A. et al. Folding of an intrinsically disordered protein by phosphorylation as a regulatory switch. *Nature* **519**, 106-9 (2015).
306. Dawson, J.E. et al. Non-cooperative 4E-BP2 folding with exchange between eIF4E-binding and binding-incompatible states tunes cap-dependent translation inhibition. *Nat Commun* **11**, 3146 (2020).
307. Shang, L. et al. Nutrient starvation elicits an acute autophagic response mediated by Ulk1 dephosphorylation and its subsequent dissociation from AMPK. *Proc Natl Acad Sci U S A* **108**, 4788-93 (2011).
308. Puente, C., Hendrickson, R.C. & Jiang, X. Nutrient-regulated Phosphorylation of ATG13 Inhibits Starvation-induced Autophagy. *J Biol Chem* **291**, 6026-6035 (2016).
309. King, K.E., Losier, T.T. & Russell, R.C. Regulation of Autophagy Enzymes by Nutrient Signaling. *Trends Biochem Sci* (2021).
310. Dunlop, E.A., Hunt, D.K., Acosta-Jaquez, H.A., Fingar, D.C. & Tee, A.R. ULK1 inhibits mTORC1 signaling, promotes multisite Raptor phosphorylation and hinders substrate binding. *Autophagy* **7**, 737-47 (2011).
311. Settembre, C. et al. TFEB links autophagy to lysosomal biogenesis. *Science* **332**, 1429-33 (2011).
312. Settembre, C. et al. TFEB controls cellular lipid metabolism through a starvation-induced autoregulatory loop. *Nat Cell Biol* **15**, 647-58 (2013).
313. Ramirez Reyes, J.M.J., Cuesta, R. & Pause, A. Folliculin: A Regulator of Transcription Through AMPK and mTOR Signaling Pathways. *Front Cell Dev Biol* **9**, 667311 (2021).
314. Roczniak-Ferguson, A. et al. The transcription factor TFEB links mTORC1 signaling to transcriptional control of lysosome homeostasis. *Sci Signal* **5**, ra42 (2012).
315. Settembre, C. et al. A lysosome-to-nucleus signalling mechanism senses and regulates the lysosome via mTOR and TFEB. *EMBO J* **31**, 1095-108 (2012).
316. Martina, J.A. et al. The nutrient-responsive transcription factor TFE3 promotes autophagy, lysosomal biogenesis, and clearance of cellular debris. *Sci Signal* **7**, ra9 (2014).
317. Martina, J.A. & Puertollano, R. Rag GTPases mediate amino acid-dependent recruitment of TFEB and MITF to lysosomes. *J Cell Biol* **200**, 475-91 (2013).

318. Napolitano, G. et al. A substrate-specific mTORC1 pathway underlies Birt-Hogg-Dube syndrome. *Nature* **585**, 597-602 (2020).
319. Vega-Rubin-de-Celis, S., Pena-Llopis, S., Konda, M. & Brugarolas, J. Multistep regulation of TFEB by MTORC1. *Autophagy* **13**, 464-472 (2017).
320. Sha, Y., Rao, L., Settembre, C., Ballabio, A. & Eissa, N.T. STUB1 regulates TFEB-induced autophagy-lysosome pathway. *EMBO J* **36**, 2544-2552 (2017).
321. Su, B. & Jacinto, E. Mammalian TOR signaling to the AGC kinases. *Crit Rev Biochem Mol Biol* **46**, 527-47 (2011).
322. Williams, M.R. et al. The role of 3-phosphoinositide-dependent protein kinase 1 in activating AGC kinases defined in embryonic stem cells. *Curr Biol* **10**, 439-48 (2000).
323. James, S.R. et al. Specific binding of the Akt-1 protein kinase to phosphatidylinositol 3,4,5-trisphosphate without subsequent activation. *Biochem J* **315 (Pt 3)**, 709-13 (1996).
324. Alessi, D.R. et al. Characterization of a 3-phosphoinositide-dependent protein kinase which phosphorylates and activates protein kinase Balpha. *Curr Biol* **7**, 261-9 (1997).
325. Calleja, V., Laguerre, M., Parker, P.J. & Larijani, B. Role of a novel PH-kinase domain interface in PKB/Akt regulation: structural mechanism for allosteric inhibition. *PLoS Biol* **7**, e17 (2009).
326. Truebestein, L. et al. Structure of autoinhibited Akt1 reveals mechanism of PIP3-mediated activation. *Proc Natl Acad Sci U S A* **118**(2021).
327. Bornancin, F. & Parker, P.J. Phosphorylation of threonine 638 critically controls the dephosphorylation and inactivation of protein kinase Calpha. *Curr Biol* **6**, 1114-23 (1996).
328. Hauge, C. et al. Mechanism for activation of the growth factor-activated AGC kinases by turn motif phosphorylation. *EMBO J* **26**, 2251-61 (2007).
329. Facchinetti, V. et al. The mammalian target of rapamycin complex 2 controls folding and stability of Akt and protein kinase C. *EMBO J* **27**, 1932-43 (2008).
330. Ikenoue, T., Inoki, K., Yang, Q., Zhou, X. & Guan, K.L. Essential function of TORC2 in PKC and Akt turn motif phosphorylation, maturation and signalling. *EMBO J* **27**, 1919-31 (2008).
331. Stokoe, D. et al. Dual role of phosphatidylinositol-3,4,5-trisphosphate in the activation of protein kinase B. *Science* **277**, 567-70 (1997).
332. Kobayashi, T. & Cohen, P. Activation of serum- and glucocorticoid-regulated protein kinase by agonists that activate phosphatidylinositide 3-kinase is mediated by 3-phosphoinositide-dependent protein kinase-1 (PDK1) and PDK2. *Biochem J* **339 (Pt 2)**, 319-28 (1999).

333. Garcia-Martinez, J.M. & Alessi, D.R. mTOR complex 2 (mTORC2) controls hydrophobic motif phosphorylation and activation of serum- and glucocorticoid-induced protein kinase 1 (SGK1). *Biochem J* **416**, 375-85 (2008).
334. Chen, W. et al. Regulation of a third conserved phosphorylation site in SGK1. *J Biol Chem* **284**, 3453-60 (2009).
335. Liu, P. et al. Cell-cycle-regulated activation of Akt kinase by phosphorylation at its carboxyl terminus. *Nature* **508**, 541-5 (2014).
336. Baffi, T.R. et al. mTORC2 controls the activity of PKC and Akt by phosphorylating a conserved TOR interaction motif. *Sci Signal* **14**(2021).
337. Dunlop, E.A. & Tee, A.R. mTOR and autophagy: a dynamic relationship governed by nutrients and energy. *Semin Cell Dev Biol* **36**, 121-9 (2014).
338. Dossou, A.S. & Basu, A. The Emerging Roles of mTORC1 in Macromanaging Autophagy. *Cancers (Basel)* **11**(2019).
339. Peterson, R.T., Beal, P.A., Comb, M.J. & Schreiber, S.L. FKBP12-rapamycin-associated protein (FRAP) autophosphorylates at serine 2481 under translationally repressive conditions. *J Biol Chem* **275**, 7416-23 (2000).
340. Copp, J., Manning, G. & Hunter, T. TORC-specific phosphorylation of mammalian target of rapamycin (mTOR): phospho-Ser2481 is a marker for intact mTOR signaling complex 2. *Cancer Res* **69**, 1821-7 (2009).
341. Soliman, G.A. et al. mTOR Ser-2481 autophosphorylation monitors mTORC-specific catalytic activity and clarifies rapamycin mechanism of action. *J Biol Chem* **285**, 7866-79 (2010).
342. Yin, Y. et al. mTORC2 promotes type I insulin-like growth factor receptor and insulin receptor activation through the tyrosine kinase activity of mTOR. *Cell Res* **26**, 46-65 (2016).
343. Sturgill, T.W. & Hall, M.N. Activating mutations in TOR are in similar structures as oncogenic mutations in PI3KCalpha. *ACS Chem Biol* **4**, 999-1015 (2009).
344. Warren, C. & Pavletich, N.P. Structure of the human ATM kinase and mechanism of Nbs1 binding. *bioRxiv*, 2021.10.17.464701 (2021).
345. Hsu, P.P. et al. The mTOR-Regulated Phosphoproteome Reveals a Mechanism of mTORC1-Mediated Inhibition of Growth Factor Signaling. *Science* **332**, 1317-1322 (2011).
346. Tzatsos, A. Raptor binds the SAIN (Shc and IRS-1 NPXY binding) domain of insulin receptor substrate-1 (IRS-1) and regulates the phosphorylation of IRS-1 at Ser-636/639 by mTOR. *J Biol Chem* **284**, 22525-34 (2009).
347. Majeed, S.T. et al. mTORC1 induces eukaryotic translation initiation factor 4E interaction with TOS-S6 kinase 1 and its activation. *Cell Cycle* **20**, 839-854 (2021).

348. Tao, Z., Barker, J., Shi, S.D., Gehring, M. & Sun, S. Steady-state kinetic and inhibition studies of the mammalian target of rapamycin (mTOR) kinase domain and mTOR complexes. *Biochemistry* **49**, 8488-98 (2010).
349. Crooks, G.E., Hon, G., Chandonia, J.M. & Brenner, S.E. WebLogo: a sequence logo generator. *Genome Res* **14**, 1188-90 (2004).
350. Schwarz, J.J. et al. Functional Proteomics Identifies Acinus L as a Direct Insulin- and Amino Acid-Dependent Mammalian Target of Rapamycin Complex 1 (mTORC1) Substrate. *Mol Cell Proteomics* **14**, 2042-55 (2015).
351. Nazio, F. et al. mTOR inhibits autophagy by controlling ULK1 ubiquitylation, self-association and function through AMBRA1 and TRAF6. *Nat Cell Biol* **15**, 406-16 (2013).
352. Ren, Q.N. et al. Phosphorylation of Androgen Receptor by mTORC1 Promotes Liver Steatosis and Tumorigenesis. *Hepatology* (2021).
353. Geraghty, K.M. et al. Regulation of multisite phosphorylation and 14-3-3 binding of AS160 in response to IGF-1, EGF, PMA and AICAR. *Biochem J* **407**, 231-41 (2007).
354. Yuan, H.X., Russell, R.C. & Guan, K.L. Regulation of PIK3C3/VPS34 complexes by MTOR in nutrient stress-induced autophagy. *Autophagy* **9**, 1983-95 (2013).
355. Ando, R. et al. The Transcription Factor Bach2 Is Phosphorylated at Multiple Sites in Murine B Cells but a Single Site Prevents Its Nuclear Localization. *J Biol Chem* **291**, 1826-1840 (2016).
356. Choi, J.H. et al. The FKBP12-rapamycin-associated protein (FRAP) is a CLIP-170 kinase. *EMBO Rep* **3**, 988-94 (2002).
357. Han, J. et al. The CREB coactivator CRTC2 controls hepatic lipid metabolism by regulating SREBP1. *Nature* **524**, 243-6 (2015).
358. Koren, I., Reem, E. & Kimchi, A. DAP1, a novel substrate of mTOR, negatively regulates autophagy. *Curr Biol* **20**, 1093-8 (2010).
359. Duan, S. et al. mTOR generates an auto-amplification loop by triggering the betaTrCP- and CK1alpha-dependent degradation of DEPTOR. *Mol Cell* **44**, 317-24 (2011).
360. Gao, D. et al. mTOR drives its own activation via SCF(betaTrCP)-dependent degradation of the mTOR inhibitor DEPTOR. *Mol Cell* **44**, 290-303 (2011).
361. Wang, X. et al. Eukaryotic elongation factor 2 kinase activity is controlled by multiple inputs from oncogenic signaling. *Mol Cell Biol* **34**, 4088-103 (2014).
362. Gandin, V. et al. mTORC1 and CK2 coordinate ternary and eIF4F complex assembly. *Nat Commun* **7**, 11127 (2016).
363. Batool, A. et al. Eukaryotic initiation factor 4E is a novel effector of mTORC1 signaling pathway in cross talk with Mnk1. *Mol Cell Biochem* **465**, 13-26 (2020).

364. Alayev, A. et al. mTORC1 directly phosphorylates and activates ERalpha upon estrogen stimulation. *Oncogene* **35**, 3535-43 (2016).
365. Nuchel, J. et al. An mTORC1-GRASP55 signaling axis controls unconventional secretion to reshape the extracellular proteome upon stress. *Mol Cell* **81**, 3275-3293 e12 (2021).
366. Yu, Y.H. et al. Phosphoproteomic Analysis Identifies Grb10 as an mTORC1 Substrate That Negatively Regulates Insulin Signaling. *Science* **332**, 1322-1326 (2011).
367. Chou, S.D., Prince, T., Gong, J. & Calderwood, S.K. mTOR is essential for the proteotoxic stress response, HSF1 activation and heat shock protein synthesis. *PLoS One* **7**, e39679 (2012).
368. Dai, N. et al. mTOR phosphorylates IMP2 to promote IGF2 mRNA translation by internal ribosomal entry. *Genes Dev* **25**, 1159-72 (2011).
369. Yoneyama, Y. et al. Serine Phosphorylation by mTORC1 Promotes IRS-1 Degradation through SCFbeta-TRCP E3 Ubiquitin Ligase. *iScience* **5**, 1-18 (2018).
370. Tzatsos, A. & Kandror, K.V. Nutrients suppress phosphatidylinositol 3-kinase/Akt signaling via raptor-dependent mTOR-mediated insulin receptor substrate 1 phosphorylation. *Mol Cell Biol* **26**, 63-76 (2006).
371. La, P., Yang, G. & Dennery, P.A. Mammalian target of rapamycin complex 1 (mTORC1)-mediated phosphorylation stabilizes ISCU protein: implications for iron metabolism. *J Biol Chem* **288**, 12901-9 (2013).
372. Viscarra, J.A., Wang, Y., Nguyen, H.P., Choi, Y.G. & Sul, H.S. Histone demethylase JMJD1C is phosphorylated by mTOR to activate de novo lipogenesis. *Nat Commun* **11**, 796 (2020).
373. Rauwel, B. et al. Release of human cytomegalovirus from latency by a KAP1/TRIM28 phosphorylation switch. *Elife* **4**(2015).
374. Hong, S. et al. LARP1 functions as a molecular switch for mTORC1-mediated translation of an essential class of mRNAs. *Elife* **6**(2017).
375. Jia, J.J. et al. mTORC1 promotes TOP mRNA translation through site-specific phosphorylation of LARP1. *Nucleic Acids Res* **49**, 3461-3489 (2021).
376. Li, T. et al. PKM2 coordinates glycolysis with mitochondrial fusion and oxidative phosphorylation. *Protein Cell* **10**, 583-594 (2019).
377. Cho, J.H. et al. Deubiquitinase OTUD5 is a positive regulator of mTORC1 and mTORC2 signaling pathways. *Cell Death Differ* **28**, 900-914 (2021).
378. Ma, X. et al. MTORC1-mediated NRBF2 phosphorylation functions as a switch for the class III PtdIns3K and autophagy. *Autophagy* **13**, 592-607 (2017).

379. Wan, W. et al. mTORC1 Phosphorylates Acetyltransferase p300 to Regulate Autophagy and Lipogenesis. *Mol Cell* **68**, 323-335 e6 (2017).
380. Jung, S.H. et al. mTOR kinase leads to PTEN-loss-induced cellular senescence by phosphorylating p53. *Oncogene* **38**, 1639-1650 (2019).
381. Ichimura, Y. et al. Phosphorylation of p62 activates the Keap1-Nrf2 pathway during selective autophagy. *Mol Cell* **51**, 618-31 (2013).
382. Cheng, X. et al. Pacer Is a Mediator of mTORC1 and GSK3-TIP60 Signaling in Regulation of Autophagosome Maturation and Lipid Metabolism. *Mol Cell* **73**, 788-802 e7 (2019).
383. Kikani, C.K. et al. Activation of PASK by mTORC1 is required for the onset of the terminal differentiation program. *Proc Natl Acad Sci U S A* **116**, 10382-10391 (2019).
384. Mackey, A.M., Sarkes, D.A., Bettencourt, I., Asara, J.M. & Rameh, L.E. PIP4kgamma is a substrate for mTORC1 that maintains basal mTORC1 signaling during starvation. *Sci Signal* **7**, ra104 (2014).
385. Yang, G. et al. RagC phosphorylation autoregulates mTOR complex 1. *EMBO J* **38**(2019).
386. Wang, L., Lawrence, J.C., Jr., Sturgill, T.W. & Harris, T.E. Mammalian target of rapamycin complex 1 (mTORC1) activity is associated with phosphorylation of raptor by mTOR. *J Biol Chem* **284**, 14693-7 (2009).
387. Foster, K.G. et al. Regulation of mTOR complex 1 (mTORC1) by raptor Ser863 and multisite phosphorylation. *J Biol Chem* **285**, 80-94 (2010).
388. Raman, N., Nayak, A. & Muller, S. mTOR signaling regulates nucleolar targeting of the SUMO-specific isopeptidase SENP3. *Mol Cell Biol* **34**, 4474-84 (2014).
389. Back, J.H. et al. Cancer cell survival following DNA damage-mediated premature senescence is regulated by mammalian target of rapamycin (mTOR)-dependent Inhibition of sirtuin 1. *J Biol Chem* **286**, 19100-8 (2011).
390. Tsang, C.K. et al. SOD1 Phosphorylation by mTORC1 Couples Nutrient Sensing and Redox Regulation. *Mol Cell* **70**, 502-515 e8 (2018).
391. Yokogami, K., Wakisaka, S., Avruch, J. & Reeves, S.A. Serine phosphorylation and maximal activation of STAT3 during CNTF signaling is mediated by the rapamycin target mTOR. *Curr Biol* **10**, 47-50 (2000).
392. Dodd, K.M., Yang, J., Shen, M.H., Sampson, J.R. & Tee, A.R. mTORC1 drives HIF-1alpha and VEGF-A signalling via multiple mechanisms involving 4E-BP1, S6K1 and STAT3. *Oncogene* **34**, 2239-50 (2015).
393. Tang, Z. et al. Mammalian target of rapamycin (mTor) mediates tau protein dyshomeostasis: implication for Alzheimer disease. *J Biol Chem* **288**, 15556-70 (2013).

394. Onyenwoke, R.U. et al. The mucolipidosis IV Ca2+ channel TRPML1 (MCOLN1) is regulated by the TOR kinase. *Biochem J* **470**, 331-42 (2015).
395. Lu, X.Y. et al. Feeding induces cholesterol biosynthesis via the mTORC1-USP20-HMGCR axis. *Nature* **588**, 479-484 (2020).
396. Kim, Y.M. et al. mTORC1 phosphorylates UVRAG to negatively regulate autophagosome and endosome maturation. *Mol Cell* **57**, 207-18 (2015).
397. Munson, M.J. et al. mTOR activates the VPS34-UVRAG complex to regulate autolysosomal tubulation and cell survival. *EMBO J* **34**, 2272-90 (2015).
398. Huang, H. et al. mTOR-mediated phosphorylation of VAMP8 and SCFD1 regulates autophagosome maturation. *Nat Commun* **12**, 6622 (2021).
399. Wan, W. et al. mTORC1-Regulated and HUWE1-Mediated WIPI2 Degradation Controls Autophagy Flux. *Mol Cell* **72**, 303-315 e6 (2018).
400. Hoxhaj, G. et al. The E3 ubiquitin ligase ZNRF2 is a substrate of mTORC1 and regulates its activation by amino acids. *Elife* **5**(2016).
401. Chen, Y. et al. mTOR complex-2 stimulates acetyl-CoA and de novo lipogenesis through ATP citrate lyase in HER2/PIK3CA-hyperactive breast cancer. *Oncotarget* **7**, 25224-40 (2016).
402. Artinian, N. et al. Phosphorylation of the Hippo Pathway Component AMOTL2 by the mTORC2 Kinase Promotes YAP Signaling, Resulting in Enhanced Glioblastoma Growth and Invasiveness. *J Biol Chem* **290**, 19387-401 (2015).
403. Benavides-Serrato, A. et al. mTORC2 modulates feedback regulation of p38 MAPK activity via DUSP10/MKP5 to confer differential responses to PP242 in glioblastoma. *Genes Cancer* **5**, 393-406 (2014).
404. Kim, S.J. et al. mTOR complex 2 regulates proper turnover of insulin receptor substrate-1 via the ubiquitin ligase subunit Fbw8. *Mol Cell* **48**, 875-87 (2012).
405. Chantaravisoot, N., Wongkongkathep, P., Loo, J.A., Mischel, P.S. & Tamanoi, F. Significance of filamin A in mTORC2 function in glioblastoma. *Mol Cancer* **14**, 127 (2015).
406. Moloughney, J.G. et al. mTORC2 modulates the amplitude and duration of GFAT1 Ser-243 phosphorylation to maintain flux through the hexosamine pathway during starvation. *J Biol Chem* **293**, 16464-16478 (2018).
407. Dai, N., Christiansen, J., Nielsen, F.C. & Avruch, J. mTOR complex 2 phosphorylates IMP1 cotranslationally to promote IGF2 production and the proliferation of mouse embryonic fibroblasts. *Genes Dev* **27**, 301-12 (2013).
408. Sciarretta, S. et al. mTORC2 regulates cardiac response to stress by inhibiting MST1. *Cell Rep* **11**, 125-36 (2015).

409. Sengupta, S. et al. Regulation of OSR1 and the sodium, potassium, two chloride cotransporter by convergent signals. *Proc Natl Acad Sci U S A* **110**, 18826-31 (2013).
410. Gu, Y. et al. mTORC2 Regulates Amino Acid Metabolism in Cancer by Phosphorylation of the Cystine-Glutamate Antiporter xCT. *Mol Cell* **67**, 128-138 e7 (2017).
411. Holmes, B. et al. mTORC2-mediated direct phosphorylation regulates YAP activity promoting glioblastoma growth and invasive characteristics. *Neoplasia* **23**, 951-965 (2021).
412. Sarbassov, D.D., Guertin, D.A., Ali, S.M. & Sabatini, D.M. Phosphorylation and regulation of Akt/PKB by the rictor-mTOR complex. *Science* **307**, 1098-101 (2005).
413. Gan, X. et al. PRR5L degradation promotes mTORC2-mediated PKC-delta phosphorylation and cell migration downstream of Galpha12. *Nat Cell Biol* **14**, 686-96 (2012).
414. Li, X. & Gao, T. mTORC2 phosphorylates protein kinase Czeta to regulate its stability and activity. *EMBO Rep* **15**, 191-8 (2014).
415. Yang, C.S. et al. The protein kinase C super-family member PKN is regulated by mTOR and influences differentiation during prostate cancer progression. *Prostate* **77**, 1452-1467 (2017).
416. Yen, C.H. et al. Functional Characterization of Glycine N-Methyltransferase and Its Interactive Protein DEPDC6/DEPTOR in Hepatocellular Carcinoma. *Molecular Medicine* **18**, 286-296 (2012).
417. DebRoy, S. et al. A Novel Tumor Suppressor Function of Glycine N-Methyltransferase Is Independent of Its Catalytic Activity but Requires Nuclear Localization. *Plos One* **8**(2013).
418. Heinzman, Z., Schmidt, C., Sliwinski, M.K. & Goonesekere, N.C.W. The Case for GNMT as a Biomarker and a Therapeutic Target in Pancreatic Cancer. *Pharmaceuticals* **14**(2021).
419. Weng, Z.F., Shen, X.X., Zheng, J.F., Liang, H.H. & Liu, Y.F. Structural Basis of DEPTOR to Recognize Phosphatidic Acid Using its Tandem DEP Domains. *Journal of Molecular Biology* **433**(2021).
420. Imseng, S., Aylett, C.H.S. & Maier, T. Architecture and activation of phosphatidylinositol 3-kinase related kinases. *Current Opinion in Structural Biology* **49**, 177-189 (2018).
421. Zhang, X.F. et al. Structures of the human spliceosomes before and after release of the ligated exon. *Cell Research* **29**, 274-285 (2019).
422. Rego, A.T. & da Fonseca, P.C.A. Characterization of Fully Recombinant Human 20S and 20S-PA200 Proteasome Complexes. *Molecular Cell* **76**, 138-+ (2019).
423. Shi, Y.J. et al. Cytotoxic Properties of DEPTOR-mTOR Inhibitor in Multiple Myeloma Cells. *Cancer Research* **76**, 5822-5831 (2016).

424. Le, J. et al. Structure-activity relationship study of small molecule inhibitors of the DEPTOR-mTOR interaction. *Bioorganic & Medicinal Chemistry Letters* **27**, 4714-4724 (2017).
425. Rodrik-Outmezguine, V.S. et al. Overcoming mTOR resistance mutations with a new-generation mTOR inhibitor. *Nature* **534**, 272-+ (2016).
426. Betz, C. & Hall, M.N. Where is mTOR and what is it doing there? *Journal of Cell Biology* **203**, 563-574 (2013).
427. Ekman, D., Bjorklund, A.K., Frey-Skott, J. & Elofsson, A. Multi-domain proteins in the three kingdoms of life: Orphan domains and other unassigned regions. *Journal of Molecular Biology* **348**, 231-243 (2005).
428. Vogel, C., Bashton, M., Kerrison, N.D., Chothia, C. & Teichmann, S.A. Structure, function and evolution of multidomain proteins. *Current Opinion in Structural Biology* **14**, 208-216 (2004).